Earth-Science Reviews 256 (2024) 104880

Contents lists available at ScienceDirect

Earth-Science Reviews

journal homepage: www.elsevier.com/locate/earscirev

New perspectives on offshore groundwater exploration through integrated sequence-stratigraphy and source-to-sink analysis: Insights from the late Quaternary succession of the western Central Adriatic system, Italy

B. Campo [a,*], C. Pellegrini [b], I. Sammartino [b], F. Trincardi [c], A. Amorosi [a]

[a] Department of Biological, Geological and Environmental Sciences (BiGeA), University of Bologna, Piazza di Porta San Donato 1, 40126 Bologna, Italy
[b] National Research Council (CNR), Institute of Marine Science (ISMAR), Via Gobetti 101, 40129 Bologna, Italy
[c] National Research Council (CNR), Department of Earth System Sciences and Environmental Technologies (DSSTTA), Piazzale Aldo Moro 7, 00185 Rome, Italy

ARTICLE INFO

Keywords:
Sequence stratigraphy
Source-to-sink analysis
Quaternary
Offshore groundwater exploration
Sediment volume
Onshore-offshore correlation

ABSTRACT

Sequence stratigraphic concepts have a variety of applications well beyond hydrocarbon exploration. Through coastal plain-to-shelf stratigraphic correlation of Last Glacial Maximum deposits from the Central Adriatic area, we tested a source-to-sink approach for exploring offshore groundwater reserves stored within the lowstand systems tract. Above an erosional unconformity (sequence boundary) formed at the Marine Isotope Stage 3–2 transition in response to sea-level fall, lowstand fluvial gravel-sand bodies, up to 20 m thick, can be tracked continuously downstream, from the coastal-plain paleovalleys to the shelf, 30 km away from the modern shoreline. The LST is overlain by a mud-dominated wedge (TST + HST) made up of alluvial, estuarine and delta plain deposits in lateral transition to thick shallow-marine and prodelta clay successions.

Using three catchment-to-shelf transects, 35–70 km long, we document the separation between potential reservoir/aquifer units (LST), primarily made of coarse-grained (porous) deposits, and the overlying, laterally continuous seal (TST + HST), which mainly includes fine-grained (low permeability) estuarine to marine sediments. Thickness maps of reservoir/aquifer and seal units provide a three-dimensional view of the stratigraphic architecture and of accumulation patterns at the systems tract scale. Lowstand fluvial deposits spread across a 5600 km^2 wide area of the western Central Adriatic shelf, with average thickness of about 10 m. North of the Meso-Adriatic Deep (MAD), two major depocenters, up to 60 m thick, reflect the local highest fluvial sediment load that correlates, further offshore, to the lowstand Po Delta. West of the MAD, LST deposits, up to 25 m thick, were nourished by Apennine rivers. In the southern area, lowstand deposits are <10 m thick. The LST is overlain across the entire western Central Adriatic shelf by an up to 80 m-thick succession of TST + HST fine-grained deposits.

A first assessment of sediment volumes provides a value of 130 km^3 for TST + HST and 57.2 km^3 for LST. Sediment provenance analysis delineates the contribution to the shelf of individual detrital sources (Apennine rivers from the west, Po River from the north), offering a powerful tool in quantifying sediment fluxes (about 52 km^3 from the Apennines catchments and 5 km^3 from the lowstand Po system).

As a whole, the application of sequence stratigraphic concepts led, for the first time, to the identification of a potential groundwater reservoir stored beneath the western Central Adriatic shelf. This LST aquifer possibly contains about 13.85 km^3 of groundwater (the salinity of which is unknown), and is vertically confined by a thick, low-permeability unit (i.e., TST + HST) that might have prevented salt-water intrusion into the underlying aquifer. The documented stratigraphic continuity likely makes this offshore aquifer an actively recharging system, with important implications for possible future sustainable exploitation.

* Corresponding author.
E-mail address: bruno.campo@unibo.it (B. Campo).

https://doi.org/10.1016/j.earscirev.2024.104880
Received 10 July 2023; Received in revised form 17 July 2024; Accepted 22 July 2024
Available online 25 July 2024

1. Introduction

In siliciclastic systems, conventional hydrocarbon and groundwater reserves are generally stored within sand-prone reservoirs (Ainsworth, 2010; Beauboeuf and Friedman, 2000; Neal et al., 2016; Shanley and McCabe, 1993) that are part of a broader sedimentary basin fill. For this reason, the principal goal of predevelopment basin studies is an estimation of (i) distribution and lateral extent of sandy facies, (ii) sand bodies geometries, and (iii) their connectivity, to evaluate the production potential of prospective basins (Jervey, 1988).

Sequence stratigraphy (Mitchum, 1977; Payton, 1977; Posamentier and Vail, 1988; Posamentier et al., 1988; Vail et al., 1977a, 1977b, 1984; Van Wagoner et al., 1988, 1990) and the source-to-sink approach (Gawthorpe et al., 1994, 1997; Goodbred, 2003; Meade, 1972, 1982; Reading and Richards, 1994; Schumm, 1977) developed since the late 70s to understand how sediments are partitioned and preserved in different basins, and to make predictions in areas of limited data coverage (Helland-Hansen et al., 2016). Despite initial discussions, criticisms and contrasting approaches (Galloway, 1989; Hunt and Tucker, 1992; Helland-Hansen and Martinsen, 1996; Miall, 1986, 1992a; Schlager, 1993), the sequence stratigraphic subdivision of stratigraphic successions into genetic units separated by laterally extensive erosion or flooding surfaces (Catuneanu et al., 2009) prevailed, especially in the oil industry (Payton, 1977; Posamentier and Weimer, 1993; Weimer and Posamentier, 1993). Mapping of seismic units bounded by laterally extensive surfaces led to a genetic view of the sedimentary record, and sequence stratigraphy became a powerful tool to predict the distribution of porous, coarse-grained sedimentary bodies and of sealing/source rock units within the framework of relative sea-level variations (Embry and Johannessen, 2017; Zecchin and Catuneanu, 2013). However, although changes in lithology and stacking patterns within basin fills generally reflect source area dynamics (Ballato and Strecker, 2014; Deramond et al., 1993; Galloway et al., 1993), sequence stratigraphic analysis focused mostly on the "temporary sink".

Sedimentary fills represent the product of short periods of erosion and deposition superimposed on longer-term allogenic controlling mechanisms (Sømme et al., 2009) that involve the entire source-to-sink transect (Allen, 2008). Sediment supply, one of the two fundamental parameters linked to the deposition of sequences (sensu Vail et al., 1977a), is mainly controlled by relief, climate, substrate lithology and catchment area (Syvitski and Milliman, 2007). Catchment analysis may provide valuable information about sediment supply that, along with accommodation, is a primary controlling factor of the stacking patterns and stratigraphic architecture of basin fills (Muto and Steel, 1997). Sequence stratigraphy and source-to-sink approach complement each other, especially when sediment provenance analysis is utilized to provide source-area-conditioned premises for reservoir characterization (Vincent et al., 2014) or to produce realistic subsurface models of stratigraphic architecture (Amorosi et al., 2020).

Aiming at a better understanding of the basin fill, both sequence stratigraphy and the source-to-sink approach evolved significantly in the last two decades. Following improvements in seismic acquisition and the integration of data from wells and outcrops, sequence stratigraphy is applied to ever smaller (i.e., "sub-seismic") scales of observation and high-resolution sequence stratigraphy developed (Catuneanu, 2019; Zecchin and Catuneanu, 2013). On the other hand, source-to-sink analysis evolved into a quantitative approach for the numerical extraction of sediment flux data (Milliman and Syvitski, 1992; Payenberg et al., 2024). To make predictions on morphological parameters of ancient source-to-sink systems in the subsurface, scaling relationships from modern systems were developed (Blum et al., 2013; Sømme et al., 2009). Application of high-resolution sequence stratigraphic concepts in a source-to-sink framework can shed new lights on the active role of factors shaping the stratigraphic architecture of clastic depositional systems, to determine more reliable predictions during subsurface exploration operations (Amorosi et al., 2016a; Blum and Womack, 2009; Catuneanu et al., 2009; Shepherd et al., 2023).

The perfect field to test this integrated basin analysis methodology is represented by the exploration of offshore freshened groundwater (OFG) reservoirs. By definition, OFG has a total dissolved solids concentration below that of seawater and is preferentially stored within siliciclastic aquifers located in continental shelves worldwide (Micallef et al., 2021). Its emplacement is mostly linked to periods of sea-level lowstand (Post et al., 2013; Sheng et al., 2024), when modern shelf sectors experienced widespread subaerial exposure and widespread valley incision, because of sea-level lowering (Anderson et al., 2004; Blum and Aslan, 2006; Blum and Törnqvist, 2000; Blum et al., 2013; Burger et al., 2001; Lericolais et al., 2001; Wang et al., 2019; Wellner and Bartek, 2003). The growing interest on OFG exploration is due to the increased demand of low-salinity water, especially in coastal zones, where OFG could represent an alternative source (Bakken et al., 2012; Zamrsky et al., 2022) as potential potable water or raw water source for desalination (Sheng et al., 2023), considering the effects of climate change and the over-exploitation of coastal aquifers (Custodio, 2002; UN-Water, 2020; Zamrsky et al., 2024).

OFG resources have not been exploited yet, at least directly, because of several "knowledge gaps" (Micallef et al., 2021) and lack of quantification of their potential.

The discovery of OFG along continental shelves occurred mostly by chance during hydrocarbon production or deep-sea drilling operations (Hathaway et al., 1976, 1979; Lofi et al., 2013; Micallef et al., 2020; Mountain et al., 2009; van Geldern et al., 2013), and the majority of OFG studies primarily rely upon measurements of seafloor bulk resistivity to infer the presence of potential OFG reserves beneath the seafloor (Attias et al., 2020, 2021; Evans, 2007; Gustafson et al., 2019; Evans and Lizarralde, 2011; Haroon et al., 2018, 2021; Müller et al., 2011; Mulligan et al., 2007; Russoniello et al., 2013). Recently, based on hydrogeology, geophysical reflections, porewater geochemistry, and paleo-hydrogeological models, Sheng et al. (2023) documented an OFG body in the Pearl River Estuary (China) and adjacent continental shelf. However, despite the recognized importance of geology and facies architecture as a key factor controlling permeability distribution, flow, and volume of OFG (Micallef et al., 2021), none of these studies relies on robust, high-resolution stratigraphic reconstructions. As a consequence, little attention has generally been paid to the stratigraphic framework for the first identification and characterization of potential aquifer/aquitard units. Geological factors exert a major control on the continuity or connectivity of permeable and/or confining strata, and the overall aquifer heterogeneity (and anisotropy in hydraulic conductivity) is the result of spatial facies distribution and geological processes (Maliva, 2016) that influence offshore hydrogeology (Houben et al., 2018; Li et al., 2016; Michael et al., 2016; Paldor et al., 2020; Sheng et al., 2024; Thomas et al., 2023; Zamrsky et al., 2020). As observed by Bertoni et al. (2020), sequence stratigraphic studies ignored OFG reserves, whereas seismic stratigraphy (Vail et al., 1977a, 1977b) was adopted only by a few works dealing with offshore groundwater analysis (Micallef et al., 2020; Thomas et al., 2019; Varma and Michael, 2012). These studies suggest that large- (i.e., seismic-) scale mapping of potential offshore aquifer units can be obtained using seismic data mostly from the oil industry. However, large scale-mapping cannot provide the suitable resolution to fill some of the "key knowledge gaps" (Micallef et al., 2021), such as: (i) the poor understanding of the distribution, extent and size of OFG bodies; (ii) the scarce knowledge of the control exerted by the geological environment on the spatial distribution (and flow) of OFG; and (iii) the link between continental margin evolution during multiple sea-level cycles and its influence on the emplacement and dynamics of OFG. Furthermore, it is likely that only actively recharging systems may be sustainable in terms of OFG exploitation, "whereas relict bodies are progressively salinizing under modern sea level conditions" (Micallef et al., 2021). On the other hand, high-resolution seismic profiles and borehole logs can be helpful to reconstruct the spatial distribution of potential aquifer bodies, such as paleochannels in large river

delta systems (Sheng et al., 2023). This is why a high-resolution sequence stratigraphic approach may prove extremely helpful to fill all these gaps, and source-to-sink analysis could allow the identification of potential sustainable OFG systems to be sustainably exploited.

Because of the amount of data available and the stratal continuity from alluvial plain to upper slope deposits, the Po Plain-Adriatic source-to-sink system, framed within the Alpine-Apennine foreland basin (Fig. 1a), represents an ideal area to develop and test such an integrated methodology aiming at the exploration of OFG reservoirs in relatively shallow water (< 100 m depth). Its late Quaternary succession (since the Last Glacial Maximum) has been intensively investigated in the last 20 years, as tens of high-resolution sequence stratigraphic studies have been carried out, both in the onshore sector (Amorosi et al., 1999, 2016b, 2023; Bruno et al., 2017, 2019; Campo et al., 2017, 2022; De Santis and Caldara, 2016; De Santis et al., 2020a, 2020b; Longhitano et al., 2016; Ricci Lucchi et al., 2006; Scarponi and Kowalewski, 2004; Scarponi et al., 2013; Stefani and Vincenzi, 2005) and offshore (Cattaneo and Trincardi, 1999; Maselli et al., 2011; Pellegrini et al., 2024; Piva et al., 2008a, 2008b; Oldfield et al., 2003; Ridente and Trincardi, 2002, 2005, 2006; Ridente et al., 2008, 2009; Scarponi et al., 2022; Trincardi and Correggiari, 2000; Trincardi et al., 1996). The Apennine-Adriatic system is characterized by high and laterally variable levels of subsidence, siliciclastic sedimentation, and sediment supply rates under rapid, high-magnitude relative sea-level changes. Based on a chronologically well-constrained stratigraphy, Amorosi et al. (2016a) supplied a thorough paleoenvironmental reconstruction from the fluvial realm (Po Plain) to the deep-marine basin (Mid Adriatic Depression or MAD, Fig. 1), along with a first assessment of sediment volumes stored in each systems tract. More recently, Amorosi et al. (2022) built a model for provenance and sediment flux from the catchments to the final sinks, based upon bulk-sediment geochemistry.

Through high-resolution stratigraphic correlation along three selected catchment-to-shelf transects in the western Central Adriatic system (i.e., Italian side, Fig. 1b), this study, aims at developing a solid stratigraphic methodology for the exploration of OFG reservoirs stored in continental shelves.

Beneath the western Central Adriatic coastal plains, amalgamated fluvial gravel-to-sand bodies that accumulated since the Last Glacial Maximum (LGM, 26.5 to 19 kyr BP: Clark et al., 2009) under lowstand conditions (Fig. 2) represent the most exploited aquifers, and are generally sealed by post-LGM mud-prone strata (Desiderio et al., 2003, 2007; Molinari et al., 2007; Nanni and Vivalda, 2005; Regione Emilia-Romagna, ENI-AGIP, 1998). On the other hand, with the exception of the LGM Po Delta (Gamberi et al., 2020; Pellegrini et al., 2017a, 2017b, 2018), lowstand deposits are poorly documented offshore (Trincardi et al., 1994), and physical correlation with their onshore counterparts, critical to document continuity of coastal aquifers beneath the Adriatic shelf, has never been attempted. Specific goals of this study are: (i) the reconstruction of high-resolution stratigraphic architecture of late Quaternary strata (last 30 kyr), along three selected catchment-to-shelf transects, with a specific focus on the lowstand systems tract (LST); (ii) the creation of thickness maps of LST, as well as of transgressive systems

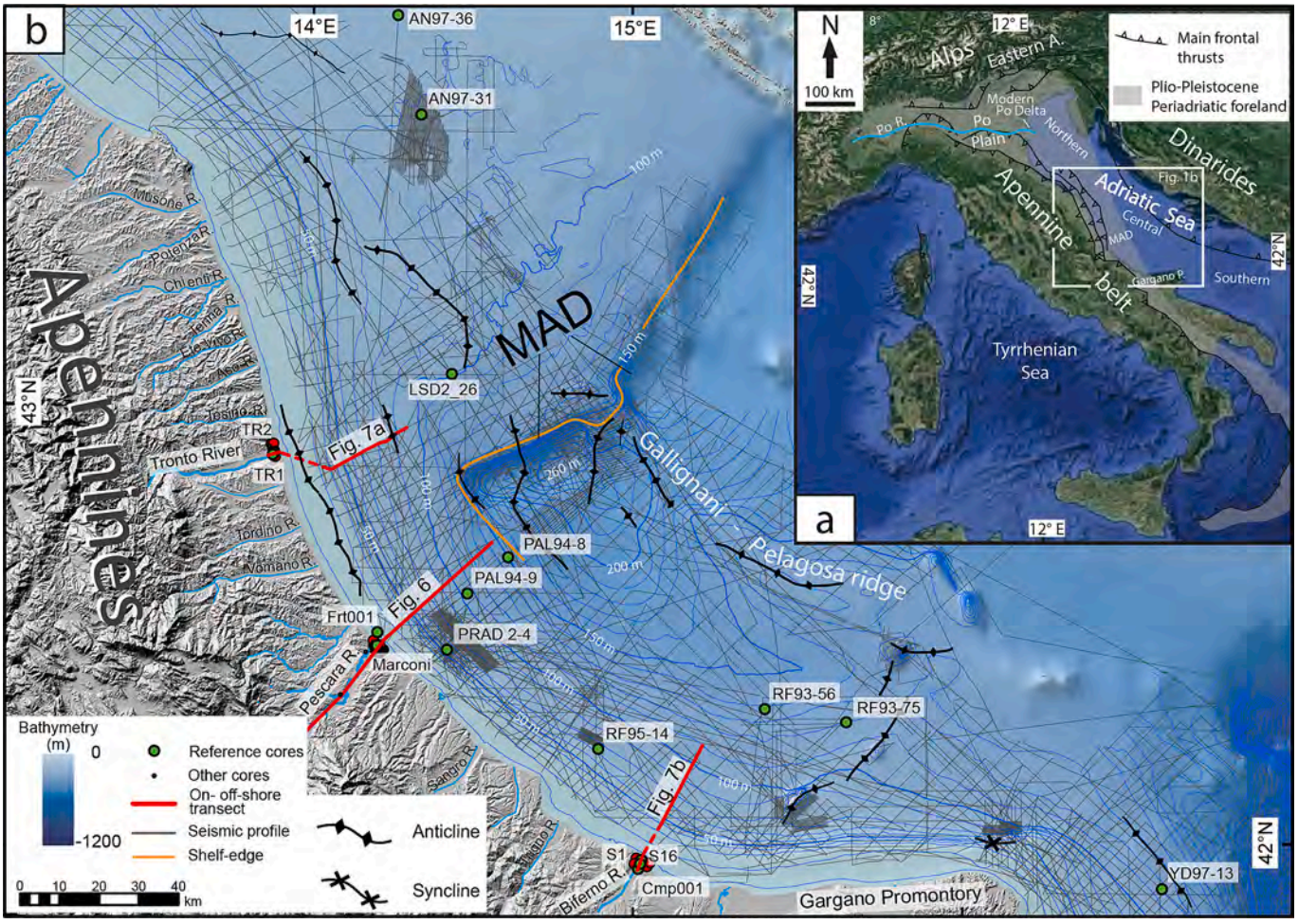

Fig. 1. Location of the study area a) with indication of the major structural features of the Northern and Central Adriatic basin and areal extent of the Plio-Pleistocene Periadriatic foreland (modified from Carruba et al., 2006). b) The study area, with main geological features, selected transects (in red) and the dataset (geophysical and sediment core data) used in this study. (For interpretation of the references to colour in this figure legend, the reader is referred to the web version of this article.)

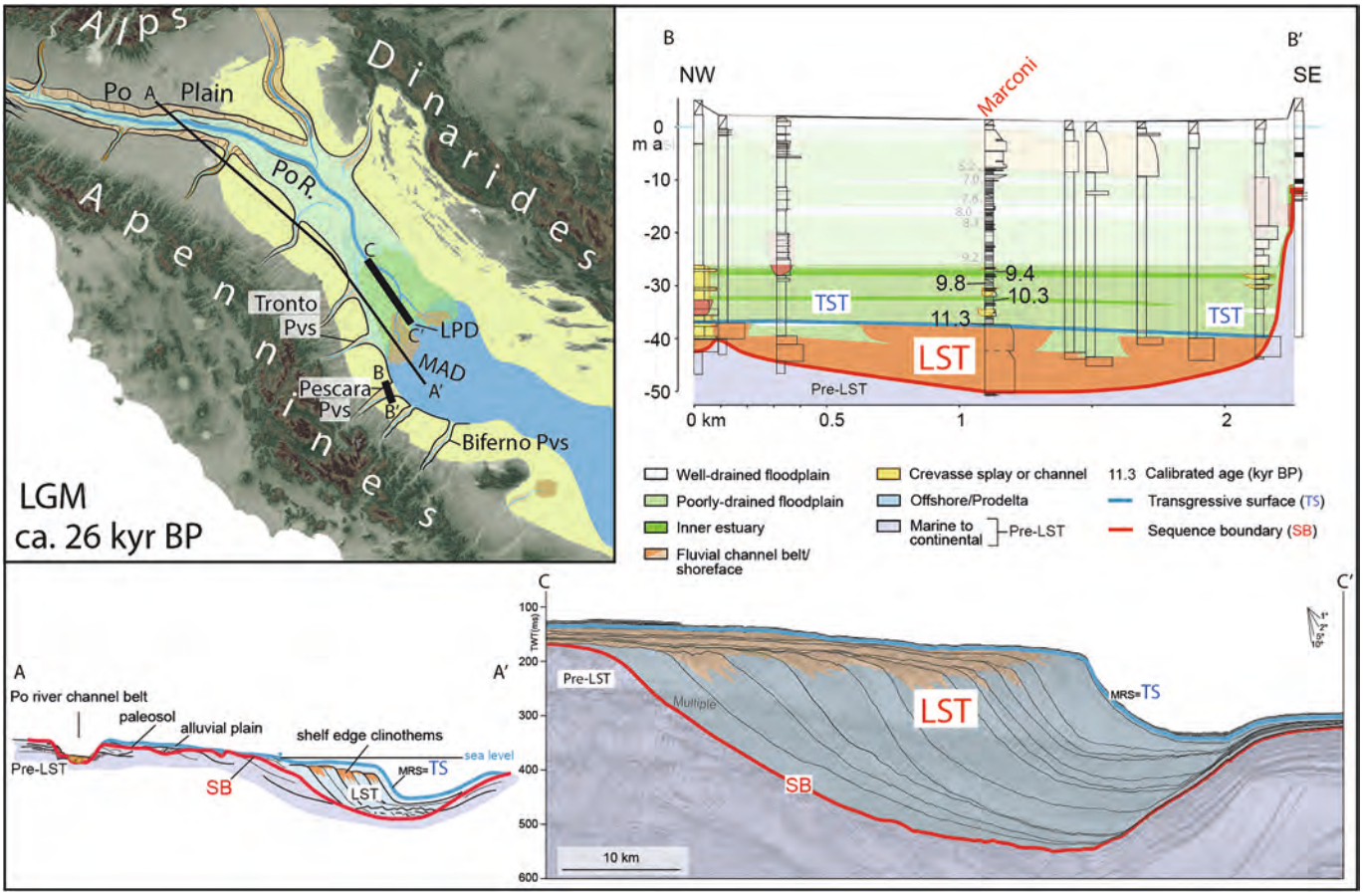

Fig. 2. Palaeogeography of the Northern and Central Adriatic basin during the Last Glacial Maximum (LGM, about 26 cal kyr BP). Transect A-A' represents the stratigraphic architecture of the Po-Adriatic system at lowstand times (modified from Amorosi et al., 2016a). Stratigraphic profiles B-B′ and C-C′ show the pre-LGM and LGM (i.e., pre-LST and LST) stratigraphic architecture in different sectors of the Adriatic (modified from Campo et al., 2022 and Pellegrini et al., 2018). LST: Lowstand systems tact; TST: transgressive systems tract; LPD: Lowstand Po Delta; MAD: Mid-Adriatic Depression; Pvs: paleovalley system.

tract (TST) plus highstand systems tract (HST) at the scale of the entire western Central Adriatic shelf, using high-resolution seismic data calibrated with sediment cores; (iii) the identification of lowstand sand pathways from the source areas through the shelf; (iv) a first assessment of sediment volumes at the systems tract scale, considering LST as a potential reservoir unit, and the overlying TST + HST as a sealing unit; (v) to test the effectiveness of sediment-bulk geochemistry for the identification and characterization of potential reservoirs; (vi) to examine LST deposits as strategic aquifer units.

2. Geological framework of the western Adriatic Basin

2.1. Structural geology

The Adriatic basin, encased between the Apennines, Alps and Dinarides mountain chains, is part of an elongated Plio-Pleistocene foreland domain (Fig. 1a). Its formation reflects tectonic subsidence caused by the eastward rollback of the Apennine subduction hinge (Royden et al., 1987) and deposition of thick syn-orogenic clastic sequences (Doglioni, 1993). Because of the high subsidence rates, the most external thrust fronts of the Alps and Apennines were buried beneath the Po Plain (Burrato et al., 2003) and the Central Adriatic (Rossi et al., 2015). Recent seismic activity recorded in correspondence to these external thrust fronts makes this area seismically active (Caputo et al., 2012). The ongoing structural activity has determined the progressive evolution into a wedge-shaped basin with the deepest depocenters adjacent to the thrust front, where the Plio-Quaternary basin fill is locally up to 8000 m thick (Carminati et al., 2003; Picotti and Pazzaglia, 2008; Ridente et al., 2008). The basin fill shows an overall regressive trend, from deep marine to alluvial deposits (Cantalamessa et al., 1986; Ori et al., 1986; Ricci Lucchi et al., 1982).

High subsidence rates characterize the most subsiding areas of the Po Plain (1 mm/yr; Burrato et al., 2003) and of the Adriatic Sea (0.3 mm/yr; Maselli et al., 2010). Increased accommodation favoured the accumulation and exceptional preservation of thick forced regressive deposits both onshore (Amorosi et al., 2004) and offshore (Ridente and Trincardi, 2002; Trincardi and Correggiari, 2000).

2.2. Morphology and catchment areas

The modern Adriatic Sea is a narrow epicontinental basin, elongated about 800 km in the NW-SE direction and about 200 km across (Fig. 1a). Based on seafloor morphology, the Adriatic Sea can be subdivided into three different sectors. The Northern Adriatic is characterized by a shallow and gently dipping (0.02°) continental shelf extending to about 350 km in a NW-SE direction toward the Mid-Adriatic Depression (MAD; Fig. 1). This latter is a remnant basin (Pellegrini et al., 2018; Trincardi et al., 1994), with maximum depth of 260 m, confined to the north by the lowstand Po River Delta (Cattaneo and Trincardi, 1999) and to the south by the Gallignani-Pellegrosa ridge (Fig. 1). Repeated phases of sea-level fall and subsequent lowstand since the Middle Pleistocene caused the progressive filling of the MAD from the NW, because of the sediment supplied by prograding Po River delta systems (Ciabatti et al., 1987; Dalla Valle et al., 2013), favouring the development of the modern North Adriatic shelf (Zecchin et al., 2017). The Central Adriatic has a narrow continental shelf, parallel to the Apennine front, with maximum

basinward extent of 50 km, and seafloor dipping between 0.3° and 0.7° (Cattaneo et al., 2007). Basinwards, this narrow shelf is confined by morphological highs reflecting deformation along the Apennine thrust-belt front. The Southern Adriatic, with a complex slope morphology due to the interaction between mass transport processes and deep-water circulation (Pellegrini et al., 2016; Ridente et al., 2007; Rovere et al., 2019), is the deepest sector, with maximum depth of about 1200 m.

The main clastic sources to the Adriatic Sea are located north of the Gargano Promontory along the western (i.e., Italian) Adriatic side, with major entry points from the Alps and the rapidly uplifting Apennines (Fig. 1). Catchment areas of the western Adriatic system include the drainage basins of eastern Alpine rivers, the Po River and Apennine rivers (Cattaneo et al., 2003, 2007). The cumulative drainage area of Apennine rivers is less than half of the Po River catchment, which is the largest, extending for 74,500 km^2.

Despite significantly smaller catchment areas, the Apennine rivers deliver about 32.2 × 10^6 t/yr of suspended sediment against 15 × 10^6 t/yr from the Po River, whereas the eastern Alpine rivers mostly feed the Northern Adriatic with 3 × 10^6 t/yr of suspended load (Cattaneo et al., 2003). Because of a cyclonic circulation, the sediment yielded during the last 7.0 kyr BP accumulated along the western side of the Adriatic forming a continuous, mud-prone sedimentary body parallel to the coast (Fig. 3).

Along the Central Adriatic, small coastal plains, about 1.5 km in width, are locally interrupted by rocky cliffs (Parlagreco et al., 2011). These coastal plains represent the distal portions of narrow and generally steep fluvial valleys (Fig. 1b) incised by the Apennine rivers also under a tectonic control (Della Seta et al., 2008). The piedmont area is

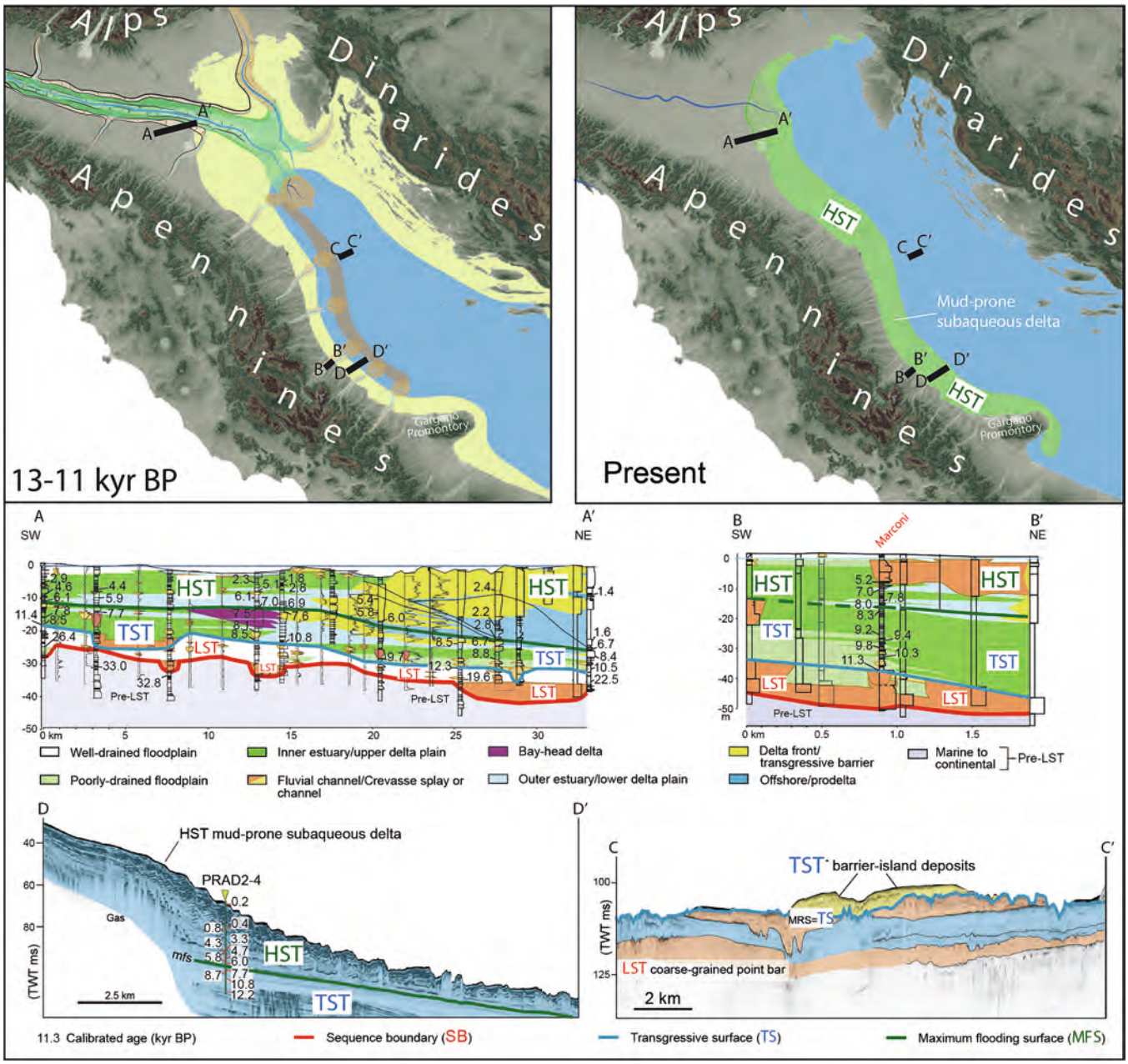

Fig. 3. Palaeogeography of the Northern and Central Adriatic basin during the Late Pleistocene-Holocene transition (about 13–11 cal. kyr BP) and at Present, with stratigraphic profiles (modified from Amorosi et al., 2016a, 2017b; Campo et al., 2022) depicting the stratigraphic architecture of the last 14.4 kyr (i.e., TST + HST) in different Adriatic sectors. Radiocarbon ages of core PRAD2–4 (cross-section D-D′) are from Vigliotti et al. (2008). LST: Lowstand systems tact; TST: transgressive systems tract; HST: highstand systems tract.

characterized by alluvial fans and fluvial terraces of Quaternary age (Fanucci et al., 1996; Farabollini, 1999), the formation of which was linked to alternating phases of fluvial aggradation and erosion driven by climatic oscillations and regional uplift (Della Seta et al., 2008).

Fluvial terrace chronology relies upon stratigraphic correlation and radiocarbon dating. Four orders of terraces have been identified, from the oldest, T1, of Middle Pleistocene age (Nesci et al., 1990), to the youngest, T4, of Holocene age (Elmi et al., 2003). Lower terrace deposits generally host the most important water resources along the Adriatic coast (Desiderio et al., 2007).

2.3. Onshore-offshore sequence stratigraphy of late Quaternary western Adriatic deposits

In this study, for the offshore sector, we adopt the original definition of depositional-sequence boundary of Mitchum (1977), and apply the principal criteria of Vail et al. (1977a, 1977b) to identify the sequence boundary (SB) through reflection or strata terminations. For a better correlation with the river's catchments (i.e., onshore) and the recognition of a depositional-sequence boundary associated with the proximity of terrigenous input, particular attention was dedicated to the identification of coastal onlap at the basin scale (Pellegrini et al., 2018). Onshore, following the classic models (Aitken and Flint, 1996; Gibling and Bird, 1994; Gibling and Wightman, 1994; McCarthy and Guy Plint, 1998; McCarthy et al., 1999; Plint et al., 2001; Van Wagoner et al., 1990), the SB was recognized at the base of the fluvial valley fills and in the associated pedogenized interfluves. Beyond correlations with local or global cycle charts, the overall interpretation of the SB relies upon geometries and stratal stacking patterns from seismic data (offshore), and facies relationships from cores (onshore), as suggested by several authors (Catuneanu et al., 2009; Posamentier and Allen, 1999; Van Wagoner, 1995; Van Wagoner et al., 1987, 1990). In a S2S perspective, from the river catchments to the Adriatic shelf, the SB corresponds to the type 1 sequence boundary of Van Wagoner et al. (1988).

2.3.1. Pre-lowstand systems tract deposits (Pre-LST)

Below the basal and fluvial portion of the paleovalley fills (i.e., LST) along the western Central Adriatic coastal plains (Fig. 2), previous deposits generally consist of older and mud-dominated strata, from the Early Pleistocene shelf Mutignano silty clays (Catanzariti et al., 2009; Di Martino et al., 2023) to Middle/Upper-Pleistocene continental and coastal deposits (Amorosi et al., 2016b; Ricci Lucchi et al., 2006). Considering the catchment-to-shelf scale of this work as well as their different ages, stacking patterns and facies associations, these deposits have been generically defined as pre-LST deposits (Fig. 2).

On the Adriatic shelf, pre-LST strata include only mud-prone and marine deposits dated between 370 and 31.8 kyr BP showing progradational geometries as the underlying HST, but with progressively steeper oblique-tangential clinoforms, sharp downlap terminations and, where present, a thin distal drape (Piva et al., 2008a; Ridente and Trincardi, 2002; Ridente and Trincardi, 2005; Trincardi and Correggiari, 2000). An erosional surface (SB) tops these deposits on the shelf, south of the MAD (Cattaneo and Trincardi, 1999).

2.3.2. Lowstand Systems Tract (LST)

At the onset of the Last Glacial Maximum (about 26 cal kyr BP; Clark et al., 2009), corresponding to the transition from the Marine Isotope Stage (MIS) 3 and MIS 2 (ca. 30 kyr BP - Lisiecki and Raymo, 2005), extensive glaciers capped the Alps (Florineth and Schlüchter, 1998; Ivy-Ochs et al., 2022; Monegato et al., 2007) and sea level dropped to about 135 m below its present level (Lambeck et al., 2014). At that time, the Po River flowed into the MAD cutting through the almost entirely subaerially exposed Northern Adriatic shelf, which experienced fully alluvial conditions (Fig. 2). The Po River catchment reached about 190,000 km^2, i.e., more than double its modern extent (Amorosi et al., 2016a), with a trunk channel acting as a collector of tributaries from the Alps, the Apennines and the Dinarides (Fig. 2). The LGM Po River catchment incorporated most of the Alpine and Apennine rivers, as well as a few minor rivers draining the western Dinaric front (Pellegrini et al., 2017a, 2017b). In the Po Plain, an extensive, weakly-developed paleosol formed on the interfluves because of widespread fluvial incision and is interpreted as the sequence boundary (Morelli et al., 2017; Bruno et al., 2022). This horizon can be traced off the interfluves into a highly diachronous erosional surface at the base of lowstand channel-belt sand bodies (cross-section A-A' in Fig. 2 and Amorosi et al., 2017a). South to the modern Po Delta, the Po-channel belt consists of amalgamated fluvial bodies (Amorosi et al., 2016a) with a composite thickness locally exceeding 30 m, and up to 20 km in width (cross-section A-A' in Fig. 2). High lateral continuity and multi-storey architecture, with a high degree of amalgamation and channel connectivity are consistent with the continuous creation of accommodation due to tectonic subsidence, lateral erosion, and increased sediment supply under lowstand conditions causing sediment load and undergoing sediment compaction. Along the western Adriatic coastal plains, the MIS 3/2 sea-level lowering caused incision of Apennine rivers into older marine to continental strata (Calderoni et al., 2010; Catanzariti et al., 2009; Curzi et al., 2017 - pre-LST deposits of Fig. 2), with formation of a set of coeval paleovalley systems (PVSs in Fig. 2 and De Santis and Caldara, 2016; Longhitano et al., 2016; Ricci Lucchi et al., 2006 among others), and their subsequent widening due to lateral migration and fluvial deposition under lowstand conditions (Blum et al., 2013). All PVSs are floored by amalgamated fluvial gravel bodies, 10–15 m-thick and generally <2 km wide (cross-section B-B′ in Fig. 2), dated to the Late Pleistocene (< 30 cal kyr BP). Based on chronological data and on their overall aggradational stacking pattern, these fluvial successions have been interpreted as LST deposits (Fig. 2), consistent with classic models (Gibling et al., 2011; Zaitlin et al., 1994).

On the Northern Adriatic shelf, despite identification of large erosional features of fluvial origin up to 20 m deep and several kilometres wide (Ferretti et al., 1986; Ronchi et al., 2018; Rovere et al., 2020), the age of LST deposits is not well established (Amadori et al., 2020; Correggiari et al., 1996b; Moscon et al., 2015; Trincardi et al., 1994). Under lowstand (glacial) conditions, in the western shelf sector, most of the sediment was intercepted by the lowstand Po River flowing into the MAD (Kettner and Syvitski, 2008; Pellegrini et al., 2018; Fig. 2). Similarly, a widespread erosional surface (i.e., SB) characterized the Central Adriatic shelf, whereas lowstand deposition took place mostly at the shelf-edge and no comparable ("Po-like") channel belts were identified (Trincardi et al., 1996). As documented by several studies (Trincardi and Correggiari, 2000; Trincardi et al., 1994, 2004a), sediment delivered by the lowstand Po River started progressively to fill the MAD. Between 31.8 and 14.4 cal kyr BP, the lowstand Po Delta system formed a 350 m-thick and mud-dominated sedimentary wedge prograding for over 40 km into the MAD (cross-section C-C′ in Fig. 2 – Pellegrini et al., 2018). On the outer shelf, this wedge is characterized by sandy clinoforms of deltaic and barrier deposits that remained connected to the alluvial plain (Gamberi et al., 2020).

As a whole, from the paleovalley systems to the shelf edge, the SB corresponds to an erosional unconformity of fluvial origin linked to the last significant sea-level drop at the onset of the LGM (MIS3/2 transition - Amorosi et al., 2016a), and showing significant erosional truncation of the underlying older and mud-prone strata (transects A-A' and C-C′ in Fig. 2). Basinward, at the base of the lowstand wedge, the SB corresponds to a correlative conformity.

2.3.3. Transgressive Systems Tract (TST)

The post-glacial stepwise sea-level rise, between about 18 and 7 cal kyr BP (Lambeck et al., 2014), generated TST deposits from the western Adriatic that are generally characterized by a sharp (seismic and sedimentary) facies contrast with underlying LST strata. Onshore, the transgressive surface (TS) clearly marks the transition between fully alluvial lowstand facies associations and overlying, mud-prone and

organic-rich estuarine deposits (cross-sections A-A' and B-B′ in Fig. 3). A distinct pollen signature is also diagnostic of the TS, which marks the transition between glacial (LST) and interglacial (TST) successions (Amorosi et al., 2004). Along the western Adriatic coastal plains, the maximum thickness (21 m) of transgressive deposits, younger than 13.1 cal kyr BP (Amorosi et al., 2016b), is recorded within coastal-paleovalleys (cross-section B-B′ in Fig. 3). Onshore, the TST displays a generally deepening-upward trend and an overall retrogradational stacking pattern (cross-sections A-A' and B-B′ in Fig. 3 - De Santis et al., 2020a, 2020b; Longhitano et al., 2016), recording the backstepping of deltaic and barrier-lagoon systems due to the rapid post-MWP 1 A and MWP 1B (ca. 13–11 kyr BP, Fig. 3) sea-level rise (Pellegrini et al., 2015; Storms et al., 2008;).

Offshore, the TS highlights the widespread post-MWPs 1 A and 1B drowning of the shelf (Fig. 3). Recent work (Pellegrini et al., 2017a) on the Po River lowstand wedge (PRLW) identified the TS atop the PRLW, at the transition from a progradational-aggradational (LST) to retrogradational stacking of coastal transgressive deposits on the shelf, and dated this surface to 14.4 cal kyr BP (cross section C-C′ in Fig. 2). On the Northern Adriatic shelf, the TST consists of scattered, backstepping barrier-island systems, <5 m thick (Correggiari et al., 1996a, 1996b and cross-section C-C′ in Fig. 3). On the Central Adriatic shelf, the TST is made of a composite, up to 25 m-thick, fine-grained sediment body including subaqueous progradational units, but with overall retrogradational tendency, and barrier-island and shoreface sands with scattered distribution (cross-section D-D′ of Fig. 3 - Cattaneo and Trincardi, 1999). The peak of transgression and the maximum landward migration of barrier-lagoon systems was achieved around 7.0 cal kyr BP (cross sections A-A', B-B′ and D-D′ in Fig. 3 – Amorosi et al., 2016a; Storms et al., 2008).

2.3.4. *Highstand Systems Tract (HST)*

The maximum flooding surface (MFS) marks the maximum landward migration of the shoreline, which coincides with the transition from retrogradational to progradational depositional geometries (cross sections A-A', B-B′ and D-D′ in Fig. 3). Along the Adriatic coastal region, the MFS is commonly identified within a fossil-rich horizon characterized by an age mixing of up to 2500 years (Scarponi et al., 2013), which suggests stratigraphic condensation between 8.0 and 6.0 cal kyr BP (cross-sections A-A', B-B′ and C-C′ in Fig. 3 and Asioli, 1996; Oldfield et al., 2003; Piva et al., 2008b). Autogenic processes and climate changes are considered the most important controlling factors of highstand architecture (Amorosi et al., 2017b; Cattaneo et al., 2003; Correggiari et al., 2005a, 2005b), which is generally characterized by aggradation of alluvial plains and progradation of delta systems (Amorosi et al., 2019; Cattaneo and Trincardi, 1999; Pellegrini et al., 2021; Stefani and Vincenzi, 2005). Onshore, beneath the modern coastal plain, the MFS can be tracked from shallow-marine deposits updip into lagoonal facies and alluvial deposits (cross-sections A-A' and B-B′ in Fig. 3). Offshore the Po River and the Apennine coast, down to the Gargano Promontory, HST consists of a muddy subaqueous delta (cross-section D-D′ in Fig. 3), about 600 km long (Fig. 3 - Present) and up to 35 m-thick (Cattaneo et al., 2003; Correggiari et al., 2001; Pellegrini et al., 2015) that formed in response to shore-parallel sediment transport with a predominant southern direction. Onshore, HST has maximum thickness of 28 m in the most distal sectors and progressively thins out landwards (cross-sections A-A' and B-B′ in Fig. 3 - Stefani and Vincenzi, 2005). Topset and foreset strata are separated by the subaqueous rollover point, a prominent morphologic feature that can be traced along the subaqueous delta (Cattaneo et al., 2003). The progradation of the offshore delta wedge is still active (e.g. Friedrichs and Scully, 2007; Harris et al., 2008; Pellegrini et al., 2024), and foresets of the clinoform are forming with a predominantly basinward outbuilding, as also documented by EURODELTA and EUROSTRATAFORM projects (Nittrouer et al., 2004; Trincardi et al., 2004a, 2004b).

3. Methods and dataset

Generating and testing a sequence stratigraphic methodology in a source-to-sink framework for the improvement of offshore groundwater exploration is an ambitious task. The large amount of sedimentological data from boreholes on the onshore portion of the system and seismic lines interpretation from the offshore (Fig. 1 for location) make up the core of sequence stratigraphic analysis. However, onshore-offshore correlation is characterized by a high degree of complexity, inherent to the different techniques of acquisition, investigation and interpretation of stratigraphic and sedimentological data in the subaerial versus submarine depositional settings.

3.1. *Onshore-offshore stratigraphic database*

The study area is comprised of coastal plain and adjacent shelf sectors of the western Central Adriatic Sea (Fig. 1b). Onshore, the stratigraphic database includes over 90 continuous cores, up to 60 m long and intercepting the pre-LST substrate (cross-section B-B′ in Figs. 2 and 3) of Early Pleistocene age. Sediment cores were analyzed by combining sedimentological and palaeontological data. Sedimentary facies analysis was accomplished through a multi-proxy approach based on the description of lithology, grain size, accessory components and resistance to penetration measured through a pocket penetrometer.

Even though well logs from hydrocarbon exploration generally provide low-resolution stratigraphic information, two well log descriptions (Frt001 and Cmp001 in Fig. 1b) from ViDEPI Project were useful to improve the stratigraphic database in areas with scarce data cover.

The offshore dataset includes single-channel profiles shot with a 300-J Sparker electromechanic source and a dense grid of CHIRP sub-bottom lines with a 2–7 kHz outgoing signal. All data were digitally recorded after bandpass filtering and gain adjustment. The seismic grid comprises high-resolution seismic profiles, completely covering the study area and measuring about 5600 km^2 (Fig. 1).

Well log Frt001 was used to integrate the seismic dataset with lithologic information in shallow water, off Pescara (Fig. 1b).

High-resolution onshore-offshore correlation was carried out along three catchment-to-shelf transects of the Apennine-Adriatic system (Fig. 1b). These transects were selected as they provide a well-balanced amount of high-resolution stratigraphic data for both the onshore and offshore sectors, and accurately reflect the depositional characteristics of the western Central Adriatic. To delineate genetically related strata and infer stratigraphic architecture, seismic stratigraphic interpretation and seismic-facies analysis were conducted based on the principles of seismic stratigraphy (Mitchum and Van Wagoner, 1991; Mitchum, 1977) and the accommodation-succession method (Neal and Abreu, 2009; Neal et al., 2016). These approaches use reflection terminations as the principal criteria for the recognition of key stratigraphic surfaces, such as the Sequence Boundary (SB) at the base of the western Adriatic LST deposits (Pellegrini et al., 2017a, 2018). An equivalent approach was adopted onshore to identify sequence stratigraphic surfaces, as already shown by Campo et al. (2020).

The software Petrel (Schlumberger) was utilized for geological mapping and for sediment volumes assessment. For mapping, the most reliable interpolation was achieved using the convergent interpolation method. This method is based on a control-point-oriented algorithm that leads to a sequential improvement of the grid resolution by iteratively converging upon the solution. For additional information about this interpolation methodology, the reader is referred to Geach et al. (2014). The volume calculation tool of Petrel was utilized to calculate the decompacted volumes of the targeted i) potential LST aquifer unit, and ii) TST + HST aquitard unit, but only after the mapping of main stratigraphic surfaces was completed. Volumes calculation was accomplished by setting the areal extent (i.e., polygon of the study area of Fig. 1b) along with the upper and/or lower limits (i.e., stratigraphic surfaces) of

each unit. Grid and size position were determined from the selected input data and boundary, with a grid increment of 50 for x-y increments. Besides all these automatic operations, all maps were edited manually by using the Petrel tool "map editing", to include regional trends and the best fitting geological interpretation. A seismic velocity of 1600 m/s, as suggested by sonic logs (Maselli et al., 2010), was adopted to convert two-way travel times (TWTT) into depth units and to calculate the volume of seismic units.

3.2. Bulk sediment geochemistry and sediment provenance

The geochemical dataset includes a total of 137 samples that were analyzed by X-ray fluorescence (XRF) at University of Bologna laboratories. Twenty-four samples that penetrated the LST were collected from 8 Central Adriatic shelf cores (AN97–36, AN97–31, LSD_26, PAL94–8, PAL94–9, RF93–56, RF93–75, YD97–13 in Fig. 1b) and analyzed for sediment provenance. Data from cores PAL94–8 and PAL94–9 have been published by Lucchini et al. (2003). Bulk samples were geochemically analyzed according to the same sample-preparation methods. Samples were oven dried at 50 °C, powdered and homogenized in an agate mortar and analyzed by X-ray fluorescence (XRF) spectrometry using a Panalytical Axios 4000 spectrometer. The matrix correction methods of Franzini et al. (1972), Leoni and Saitta (1976), and Leoni et al. (1982) were followed. The estimated precision and accuracy for trace-element determinations was 5%. For elements with low concentration (<10 ppm), the accuracy was 10%.

For sediment provenance inferences, LST core data from the Adriatic shelf were matched against the known geochemical compositions of the two major fluvial end-members: Po River and Central Apennine rivers. The whole grain size spectrum, from coarse sand to clay, was investigated. Particularly, we used 35 data representative of modern Po River sediment composition and 46 data from 11 modern Central Apennine rivers: from north to south, Aso, Tronto, Vibrata, Salinello, Tordino, Vomano, Piomba, Pescara, Sangro, Sinello, and Trigno (Amorosi et al., 2022). We also used 18 representative data of the lowstand Po channel belt (Amorosi et al., 2022) and 14 unpublished data from the lowstand Pescara channel belt.

We controlled possible effects of size-selective transport on a sedimentological basis, by grouping samples into facies associations (Garzanti et al., 2009; Razum et al., 2021; Weltje, 2004) and we did not adopt size fractionation, as this approach does not ensure source representativeness and typically results in different elemental compositions based on the particle size fraction selected (Laceby et al., 2017). In order to compensate for grain-size variability of geochemical element concentration, we normalized geochemical data of fluvial to shallow-marine facies associations using vanadium as a grain size proxy. The Cr/V plot, in particular, was adopted as a powerful tool for the discrimination of ultramafic (Po River-derived) versus non-ultramafic (Apennine rivers) source-rock composition (Amorosi and Sammartino, 2007).

4. Sedimentary facies associations and seismic facies from the western Central Adriatic area

4.1. Sedimentary facies associations (onshore units)

The depositional facies associations that compose the late Pleistocene-Holocene succession and older strata (i.e., pre-LST) in the western Central Adriatic coastal plain have been described extensively by numerous works (Amorosi et al., 2016b, 2023; Campo et al., 2022; Cantalamessa and Di Celma, 2004; Catanzariti et al., 2009; Curzi et al., 2017; Longhitano et al., 2016; Ricci Lucchi et al., 2006), and will not be reiterated here in detail. Above the pre-LST substrate, fourteen facies associations were grouped into five depositional systems. Substrate and different groups are summarized below, in stratigraphic order, along with their main sedimentological features observed through core analysis (Fig. 4).

4.1.1. Substrate

The substrate of Early to Middle Pleistocene age includes two main depositional facies. The first facies association (Sub 1 of Fig. 4a) is made of massive and bioturbated gray to brownish clays and silty clays (Fig. 4a, 51.4–52 m core depth). Small percentages (< 5%) of very fine sand occur as cm-thick intercalations. Faint horizontal lamination is locally observed. Pocket penetration (Pp) values are generally >5 kg/cm^2. The foraminiferal content typically consists of benthic species (*Bolivina spp, Bulimina marginata, Globobulimina affinis, Globobulimina Pyrula*) indicative of a shelf depositional environment of Early Pleistocene (Calabrian) age.

Below the coastal areas, this facies association is the distal expression of the 'Argille Azzurre' Fm (Amorosi et al., 1998; Channell et al., 1994), and coeval Mutignano Fm (Crescenti and D'amato, 1980) and Montesecco clays (Bracone et al., 2012). These units typically crop out at the Apennine foothills between river valleys (Desiderio et al., 2007; Geological Map of Italy at 1:50,000 scale, 2024a, 2024b, 2024c, 2024d, 2024e, 2024f, 2024g, 2024h, 2024i), and represent the Early Pleistocene substrate. The second facies association (Sub 2 of Fig. 4b) consists of gray silty clays, with cm- to dm intercalations of sand and overall coarsening-upward trend (Fig. 4b, 35.5–34.5 m core depth). Shells and mollusc fragments of marine species (predominant *Corbula gibba* and *Bittium reticulatum*) are abundant and locally associated with vegetal remains. The meiofauna content is abundant and characterized by remarkable species richness typical of a shallow-marine environment subject to moderate fluvial influence. This facies association is predominant within the Middle-Pleistocene "lower valley fill" of the Biferno paleovalley system (Amorosi et al., 2016b), and here is considered part of the substrate (pre-LST). As also shown by Calderoni et al. (2010), Elmi et al. (2003) and Longhitano et al. (2016), beneath the western Central Adriatic coastal plain, the mud-dominated substrate is encountered at highly variable depths.

4.1.2. Alluvial plain deposits

Three major alluvial facies associations are mostly representative of this depositional system. The fluvial-channel facies (FC in Fig. 4), between 2 and 20 m-thick, consists of amalgamated gravel (Fig. 4a) to gravelly sand (Fig. 4b) bodies with fining-upward trends (FU) and erosional lower boundary, locally cutting into the older substrate (Fig. 4a, ca. 51.4 m core depth). Gravels are poorly sorted with calcareous rounded cobbles and pebbles generally embedded in a whitish silty-sandy matrix (Fig. 4a). Fossils or vegetal remains are absent. Lithology, poor sorting, presence of amalgamation surfaces and erosional bases are consistent with deposition in a high-energy (likely braided) fluvial environment (Bridge, 2006; Miall, 1992b). The channel-related facies association includes levee and crevasse deposits that are composed of sand-silt alternations containing roots and silty sand bodies (< 2 m thick). Crevasse splays (Crs in Fig. 4a) exhibit coarsening-upward (CU) trends and gradational lower boundaries (Allen, 1965; Collinson, 1996; Longhitano et al., 2016), whereas crevasse channels (Crc in Fig. 4a) show FU trends and sharp lower boundaries (Fig. 4, core-1 – Farrell, 2001; Burns et al., 2017; Ricci Lucchi et al., 2006). Wood and shell fragments are scarce and include freshwater mollusc remains (*Pisidium* sp. and *Bithynia* opercula). Well-drained floodplain deposits (WDFP in Fig. 4b) consist of rooted and gray to brownish silty clay with yellowish mottles (Fig. 4b). Pedogenic features, such as paleosols, can be observed locally (Amorosi et al., 2016b; Ricci Lucchi et al., 2006), coherently with diffused pedogenic alteration in floodplain deposits (Ghazi and Mountney, 2009; Miall, 2013; Muller et al., 2004). Pocket penetration values are invariably >2 kg/cm^2. The well-drained floodplain facies is generally barren or contains at most a few shells of land molluscs (*Pomatias elegans, P. pygmaeum, Hygromiinae and Cernuella* – Grano and Di Giuseppe, 2021) or scattered benthic and planktic foraminifers (Ricci Lucchi et al., 2006).

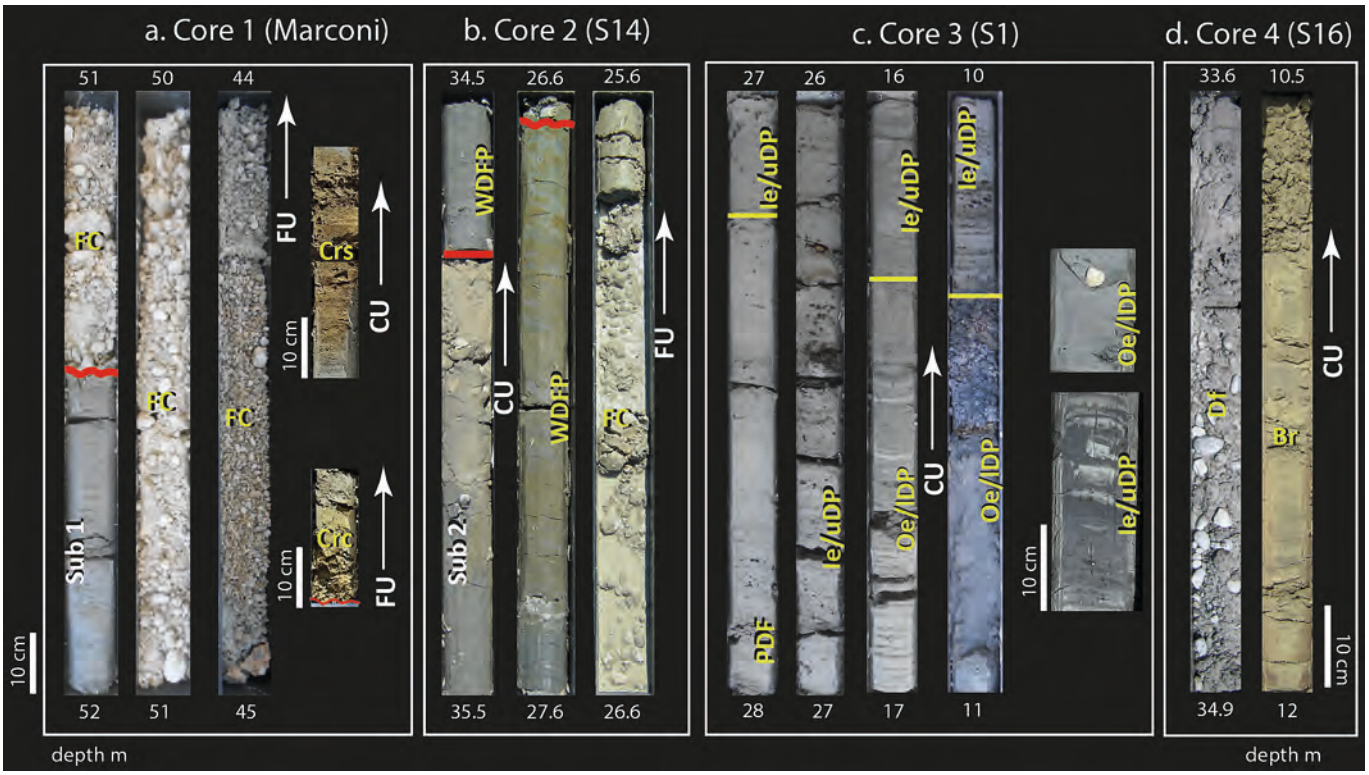

Fig. 4. Representative photographs of the Lower to Middle Pleistocene substrate and main facies associations identified in cores of the western Central Adriatic coastal plain. a) Core 1: Fluvial channel (FC) gravels showing erosional lower boundary (red-wavy line) and fining-upward (FU) trend. Details of crevasse channels (Crc) and crevasse splay (Crs) with FU and coarsening-upward (CU) tendencies, respectively. b) Core 2: well-drained floodplain (WDFP) clays unconformably overlying shallow-marine substrate facies (Sub 2). Fluvial channel gravels with FU tendency and erosional base cutting into an older WDFP deposit. c) Inner estuary/upper delta plain (Ie/uDP) and outer estuary/lower delta plain (Oe/lDP) main characteristics, with details on *Cerastoderma glaucum* shell within Oe muds and high organic-matter content in Ie/uDP clays. d) Delta front (Df) and beach-ridge (Br) deposits with peculiar CU trend. Cores location in Fig. 1b. (For interpretation of the references to colour in this figure legend, the reader is referred to the web version of this article.)

4.1.3. Freshwater, organic-rich inner estuary/upper delta plain deposits

This depositional system includes four main facies associations. The poorly-drained floodplain facies association (PDF in Fig. 4c), commonly <1.5 m thick, is made of massive gray clay and silty clay (Fig. 4c). Pedogenic features are absent and carbonate concretion are rare. Pocket penetration values range between 1.0 and 1.8 kg/cm^2. Only decomposed organic material can be locally observed as mm to cm-thick layers (Fig. 4c). The fossil content includes shell fragments of pulmonate gastropods (*Pomatis elegans*) and a freshwater fauna (*Candona neglecta, Ilyocypris* spp. *and Pseudocandona albicans*). On the contrary, abundant wood fragments and vegetal remains are characteristic of inner estuary (Ie in Fig. 4c) or upper delta plain (uDP in Fig. 4c) deposits. These latter, up to 9 m thick, are composed of very soft (Pp < 1 kg/cm^2), dark to brown clay with diagnostic peat layers at distinct stratigraphic intervals (Fig. 4c). Inner estuary/upper delta plain deposits are dominated by freshwater-hypoaline taxa, such as *Pseudocandona albicans* and *Ilyocypris species* that can be observed in association with rare specimens of euryhaline ostracods (*Cyprideis torosa*) and benthic foraminifers (*Ammonia tepida*). For both poorly-drained and inner estuary/upper delta plain clays, the combination of sedimentological characteristics and meiofauna assemblages suggests low-energy and freshwater to low-brackish depositional environments with variable (poorly-drained) to permanent (Inner estuary/upper delta plain) waterlogging conditions, typical of the inner sector of an estuary (TST) or upper delta plain (HST).

Distributary-channel and related crevasse/levee deposits share several characteristics with their alluvial counterparts, such as lithology, erosional to transitional lower boundaries and grain-size trends. However, distributary-channel bodies are commonly thinner and finer-grained than fluvial-channel deposits.

4.1.4. Brackish water, outer estuary/lower delta plain deposits

This depositional system includes a wide range of brackish environments generally located behind a barrier complex, but it is dominated by the outer estuary facies association/lower delta plain (Oe/lDP in Fig. 4c), up to 2 m thick, composed of very soft (Pp between 0.2 and 1 kg/cm^2) gray clays (Fig. 4c, 17–16.3 m core depth). This facies is characterized by a diagnostic brackish fauna tolerant to sudden changes in salinity and organic matter content. The ostracod assemblage is dominated by *Cyprideis torosa*, whereas euryhaline species, such as *Ammonia tepida* and *Ammonia parkinsoniana,* prevail among foraminifera. Mollusc shell fragments of brackish speciments, such as *Cerastoderma glaucum* (Fig. 4c and Parlagreco et al., 2011) and *A. segmentum,* are generally found within this facies association, which is invariably representative of outer estuary (TST) or lower delta plain (HST) depositional environments. Silt and silty sand can be locally abundant within stratigraphic intervals <1 m thick and showing CU trends that are likely representative of a more distal (outer lagoon) environment (Fig. 4c, 11–10.35 m core depth). Bay deposits can be distinguished from outer-estuary deposits based on microbenthic and meiofauna assemblages, more typical of a shallow-marine environment moderately influenced by riverine discharge such as a bay (Amorosi et al., 2023, their Fig. 5b, c; Catanzariti et al., 2009, their interval 3).

4.1.5. Transgressive Barrier Island/Strandplain/Delta front deposits

This depositional system includes three main facies associations characterized by high sand content. These facies can be distinguished on the basis of grain size, thickness range, facies boundaries and fossil content. The transgressive sand-sheet facies association consists of fine to medium sand and gravel, about 2 m thick, with FU trend and erosional lower boundary. Fossils are mostly reworked, with many

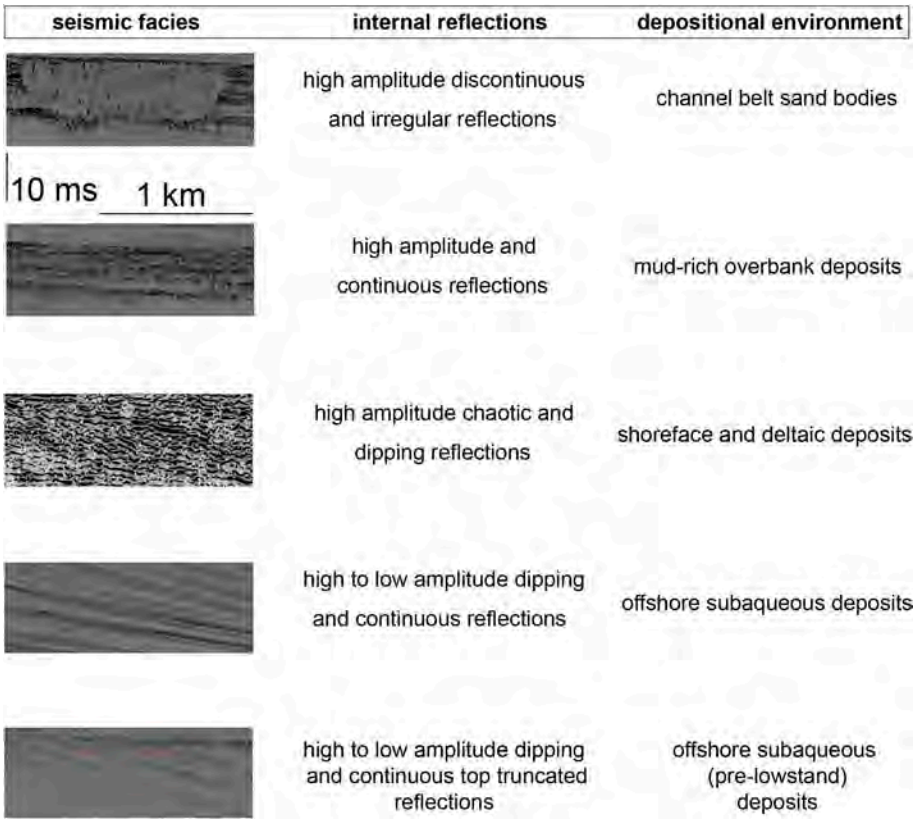

Fig. 5. Seismic facies observed in seismic profiles, with internal configuration and inferred depositional environment. Red arrows highlight toplap terminations. (For interpretation of the references to colour in this figure legend, the reader is referred to the web version of this article.)

bivalve and gastropod shell fragments (Ricci Lucchi et al., 2006; Rossi et al., 2024), and scarce and poorly preserved foraminiferal speciments of *Ammonia* and *Quinqueloculina* (Catanzariti et al., 2009). The upper shoreface/foreshore facies association (i.e., beach ridge; Br in Fig. 4d) is made of yellowish, well-sorted fine to medium sand bodies (Fig. 4d) up to 5 m thick, with sharp or erosive base (Ricci Lucchi et al., 2006). Molluscs shell fragments are common (Parlagreco et al., 2011). The mouth bar facies association (i.e., delta front or Df in Fig. 4d) consists of fine to medium sand with rounded cobbles and pebbles, and gradational lower boundary on the underlying prodelta muds and overall CU tendency (Fig. 4d). Thickness values range between 5 and 14 m. Silty intervals a few cm-to-dm thick can be found within sand packages and plant debris are locally abundant. Within this facies association, no ostracods or foraminifera are commonly preserved and shells fragments are scarce.

All these facies associations accumulated in high-energy nearshore environments as part of back-stepping transgressive shorelines (transgressive barrier deposits) or prograding delta systems (delta front and beach ridge deposits).

4.1.6. Offshore/Prodelta deposits

This mud-dominated depositional system includes two main facies associations. The first one is composed of bioturbated clay deposits, up to 2 m thick. The fossil content shows a highly diversified meiofauna typical of open-marine conditions that, along with lithological characteristics are consistent with a relatively deep (i.e., inner shelf) environment (Rossi and Vaiani, 2008; Rossi and Horton, 2009; Rossi et al., 2024).

The second facies association consist of homogeneous gray clay, up to 12 m thick. Silt intercalations are widespread. Organic matter and vegetal remains can be locally observed. This facies association is dominated by opportunistic foraminifers, ostracods and mollusc species (i.e., *Ammonia tepida, Ammonia parkinsoniana, Nonionella turgida, Turritella communis, Varicorbula gibba*) tolerant to important variations in salinity, turbidity and nutrient flux that are specific to prodelta environments (Asioli, 1996; Barbieri et al., 2019; Oldfield et al., 2003; Piva et al., 2008b; Rossi et al., 2024; Van der Zwaan and Jorissen, 1991).

4.2. Seismic facies and depositional environments (offshore units)

4.2.1. Channel-belt deposits: sand bodies vs overbank muds

The inner-shelf succession shows high amplitude discontinuous and irregular reflections with local small-scale, v-shaped incisions (Fig. 5), reminiscent of amalgamated fluvial channel belts. When calibrated through sediment cores, these seismic facies correspond to sand-silt delta plain deposits (Gamberi et al., 2020). Channel-belt sand bodies have average thickness of 10 m, and are laterally confined by high-amplitude and continuous reflections that suggest the presence of fine-grained overbank deposits (Fig. 5; Pellegrini et al., 2018) diagnostic of distal flood-plain environments (Blum et al., 2013).

4.2.2. Shoreface and deltaic deposits

On the mid-shelf, high amplitude chaotic and dipping reflections highlight preserved subaerial sandy-silty deltaic progradation. Along a dip-oriented profile and offshore the main Apennine river mouths, the seismic facies changes to high amplitude discontinuous and chaotic dipping reflections with local v-shaped incisions (Fig. 5), suggesting the presence of delta-scale sandy-silty deposits characterized by amalgamated distributary channels (Pellegrini et al., 2018). Shoreface and deltaic deposits show macrofossil assemblage consisting of shallow-water taxa (Fig. 5; Gamberi et al., 2020; Scarponi et al., 2022) and display average thickness of 15 m (Fig. 5).

4.2.3. Offshore subaqueous deposits

On the outer shelf, the succession is characterized by high-to-low amplitude, continuous reflections with sigmoidal clinoform configuration (Fig. 5). The geometry of the clinoform varies along the Central Adriatic shelf with gradient values of dipping clinoforms that change from 0.5°-1° and with clinoforms topsets that become steeper and narrower (Fig. 5). Sediment cores retrieved along-dip transects documented the muddy nature of the clinoforms and the presence of ecozones typical of mud belt environments (Cattaneo et al., 2003). The terrestrial organic matter shows a scattered distribution and is mainly confined in hotspots close to river entry points and recording high rates of sediment burial with minimal reworking (Pellegrini et al., 2021). Overall, the offshore subaqueous deposits attain >30 m of thickness and show depocenters elongated parallel to the coast and confined landward, as a result of sediment advection from riverine input (Cattaneo et al., 2007; Frignani et al., 2005; Nittrouer et al., 2004; Palinkas et al., 2005; Pellegrini et al., 2015, 2024; Puig et al., 2007; Sherwood et al., 2015). Locally, older (pre-LST) clinoforms show an overall oblique-tangential configuration with marked toplap and downlap terminations in the foreset and bottomset, respectively (Fig. 5).

5. Onshore-offshore correlation

Despite the noise in the seismic signal due to the presence of biogenic gas in shallow waters (< 20 m; D-D′ cross-section in Fig. 3), the large amount of high-resolution stratigraphic data available allowed onshore-offshore correlations with a high degree of confidence. The stratigraphic panels of Figs. 6 and 7 show the along-dip facies architecture and sequence stratigraphic interpretation of three selected catchment-to-shelf transects representative of the western Central Adriatic along the Pescara (Fig. 6), Tronto and Biferno (Fig. 7) river systems. All transects are parallel to the river valley axes and extend basinwards on the shelf down to about 130 m depth (Fig. 1b for location). As we aim at the identification of potential low-salinity aquifers stored in the shelf likely corresponding to amalgamated fluvial gravel and sand bodies that accumulated under lowstand conditions (Post et al., 2013; Sheng et al., 2023), we mostly focused on the shelfal portion that experienced subaerial exposure during the LGM (i.e., ca. first 120 m b.s.l., Fig. 1b for location).

5.1.1. The Pescara transect

The Pescara transect (Fig. 6), about 70 km long, extends from the river valley (altitude ca. 20 m a.s.l.) to the coastal plain and to the outer shelf down to about 160 m b.s.l. (Fig. 6). Subsurface stratigraphy in the coastal plain relies upon the recent work of Campo et al. (2022), integrated by stratigraphic data from the Abruzzo Geological Survey, and previous information from Desiderio et al. (2007). The offshore reconstruction is based on the integration of well-logs, core, seismic and chronological data from previous studies (Cattaneo et al., 2007; Gamberi et al., 2020; Maselli et al., 2011; Pellegrini et al., 2018).

In the onshore part of the transect, an unconformity surface can be continuously tracked for about 30 km. This surface, marks the abrupt facies shift from Lower Pleistocene marine clays of the Mutignano Formation (i.e., substrate) to significantly younger continental deposits, assigned to the Last Glacial Maximum (29–19 cal kyr BP), and likely formed during the latest stages of sea-level fall (MIS 3/2 transition). For this reason, this surface is interpreted to represent the sequence boundary (SB; Fig. 6). In the upstream sector of the valley (55 to 25 m a.s.l., Fig. 6), amalgamated, lowstand fluvial gravel bodies, up to 20 m

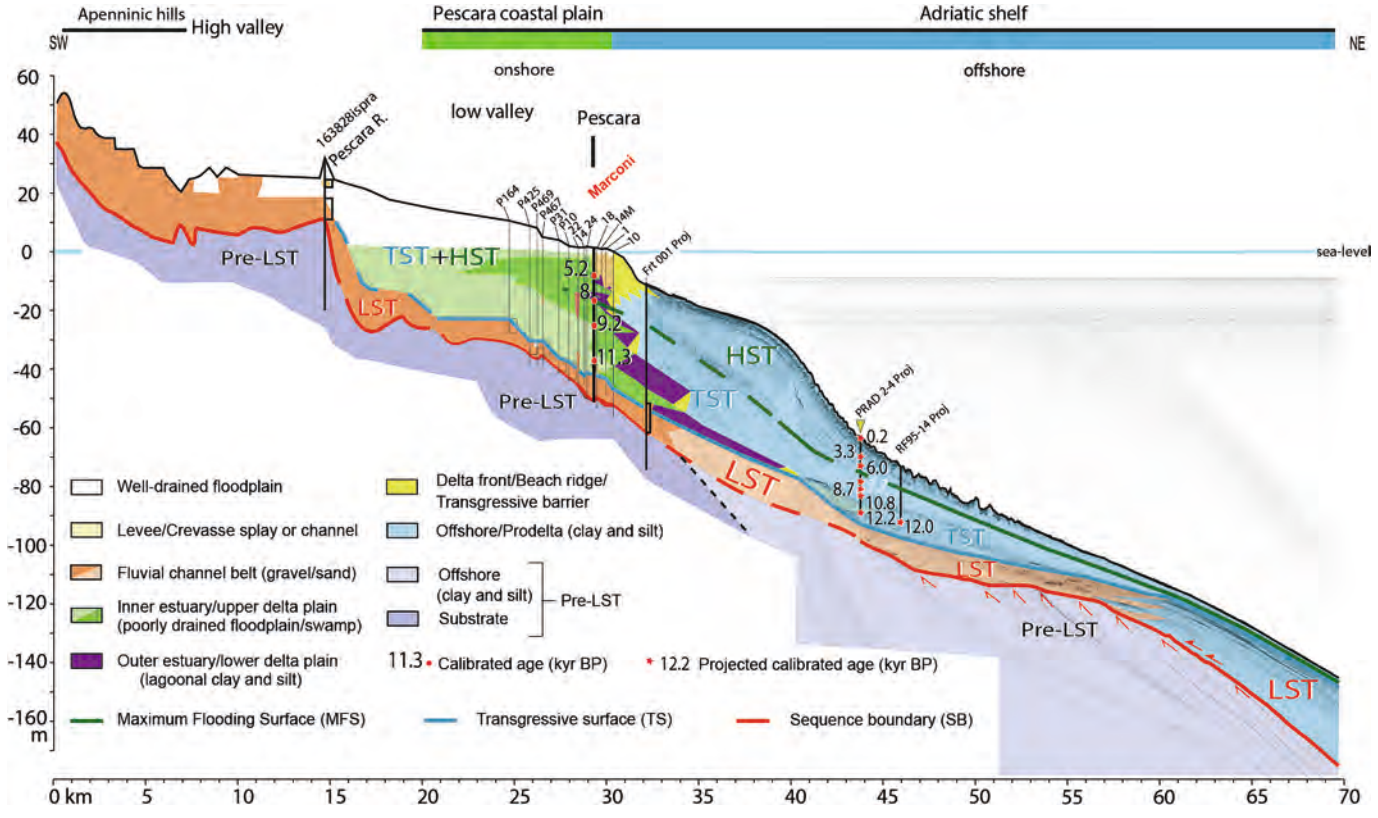

Fig. 6. Stratigraphic panel illustrating onshore-offshore facies architecture from the Pescara River valley to the Central Adriatic shelf, with a focus on the last 30 kyr and sequence stratigraphic interpretation (LST: lowstand systems tract; TST: transgressive systems tract; HST: highstand systems tract). Red arrows mark the erosional truncation and onlap terminations. (For interpretation of the references to colour in this figure legend, the reader is referred to the web version of this article.)

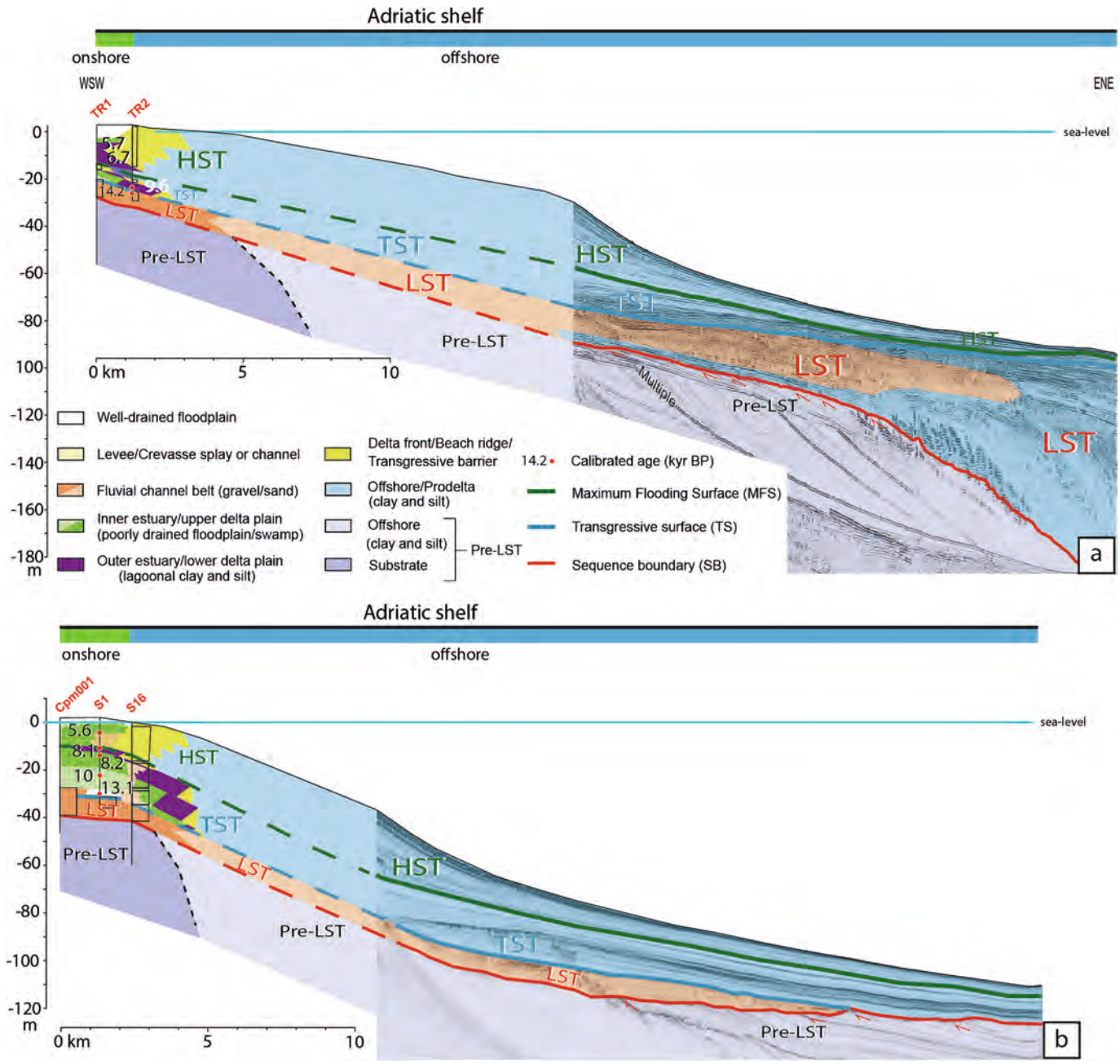

Fig. 7. Stratigraphic panels illustrating the onshore-offshore facies architecture from the a) Tronto and b) Biferno coastal plains to the Central Adriatic shelf, with a focus on the last 30 kyr and sequence stratigraphic interpretation (LST: lowstand systems tract; TST: transgressive systems tract; HST: highstand systems tract). Red arrows mark the erosional truncation. (For interpretation of the references to colour in this figure legend, the reader is referred to the web version of this article.)

thick, crop out above the substrate in proximity of the modern Pescara riverbed (Fig. 6). Seawards, these fluvial gravel deposits exhibit a characteristic aggradational stacking pattern and correspond to the basal portion of the Pescara paleovalley fill: they can be traced in the subsurface at progressively increasing depths where their thickness decreases to 10 m (Fig. 6). Scarcity or lack of associated crevasse, levee or well-drained floodplain deposits at this stratigraphic level suggest repeated episodes of fluvial erosion in a high-energy (braided?) fluvial regime, due to the lateral migration of the river in the narrow valley. Fluvial erosion possibly led to the complete removal of fine-grained sediment that was transferred further seawards into the deep basin (Pellegrini et al., 2017a).

In the offshore sector, the same erosional unconformity recognized from core data can be identified and continuously traced for tens of kms, down to about 160 m b.s.l. (Fig. 6). The SB is highlighted by truncations and toplap terminations of the underlying reflections and by onlap reflections terminations above (Fig. 6). This surface is highlighted by a sharp seismic facies change from highly continuous reflections of the pre-LST, below, to discontinuous and chaotic reflections of the overlying LST (Fig. 6). Whereas the former unit corresponds to the fine-grained offshore deposits of the pre-LST (FSST of Cattaneo and Trincardi, 1999 and Trincardi and Correggiari, 2000), the latter represents the seaward correlative of the lowstand fluvial deposits that floor the Pescara paleovalley onshore. Thickness around 10 m, and lateral continuity of about 30 km of this seismic unit (at ca. 120 b.s.l. - Fig. 6) are also consistent with the characteristics of its onshore counterpart. Basinward, below 120 m b.s.l., this unit is in lateral transition with a seismic facies showing low to high amplitude dipping and continuous reflections and

interpreted as offshore muds (Figs. 6 and 5). This latter unit thickens downdip from about 10 m to 30 m in the most distal part of the transect (Fig. 6). The occurrence of a 10 m-thick fluvial gravel body, between 50 and 60 m b.s.l., about 2 km off the Pescara coast (well log "Frt001"; Fig. 6), strongly supports the stratigraphic correlation between the onshore and offshore sectors. Comparable seismic facies and related coarse grained-fluvial deposits have been reported from the Adriatic shelf north of the MAD, where coastal plain deposits of the Po River lowstand delta accumulated between 31.8 and 14.4 cal kyr BP (Pellegrini et al., 2018).

Along the Pescara coastal plain and the proximal part of the Adriatic shelf, the lowstand fluvial unit is overlain by a laterally continuous, mud-dominated succession (TST + HST) identified through the whole onshore-offshore transect (Fig. 6). This succession, which is up to 40 m thick, progressively thins out basinwards (Fig. 6). Core data from the onshore sector show that this unit consists almost entirely of silt and clay, interpreted as alluvial (well-drained floodplain) to estuarine (poorly-drained floodplain and swamp) facies. These fine-grained deposits are in lateral transition to discontinuous barrier-lagoon systems, shallow-marine, prodelta and mud-belt facies on the shelf (Fig. 6 and Cattaneo and Trincardi, 1999; Cattaneo et al., 2007). Lens-shaped fluvial-channel bodies encased in estuarine muds of latest Pleistocene age are found above the multi-storey lowstand unit (see core Marconi and well log Frt001 in Fig. 6). The vertical transition from amalgamated gravel bodies to finer-grained estuarine deposits with isolated channel bodies marks a major phase of channel abandonment, interpreted as the boundary between the LST and lower TST (i.e., the transgressive surface or TS). This abrupt lithofacies change at the fluvial-estuary transition and the concurrent variation in fluvial-channel geometry suggest evolution of the fluvial system into a meandering alluvial plain, in response to the post-glacial sea-level rise that followed Melt Water Pulse (MWP) 1 A (Maselli et al., 2011; Vacchi et al., 2016; Zecchin et al., 2015). Based on stratigraphic correlation with the Po River lowstand wedge (Gamberi et al., 2020; Pellegrini et al., 2017a, 2018), the TS in offshore position marks the top of the lowstand fluvial body (Fig. 6). The sharp facies change from fluvial to shallow-marine (offshore) muds highlights the sudden drowning of the shelf, and the following backstepping of the shoreline (Figs. 6–7). Early TST estuarine deposits onshore are correlative basinwards with a prominent prograding sedimentary wedge, up to 15 m thick, identified between 80 and 110 m b.s.l. (Fig. 6). This wedge shows seaward dipping internal reflectors and consists mainly of offshore muds containing sharp-based sand layers, as also suggested by high-values of saturation isothermal remanent magnetization (SIRM) in the basal part of core PRAD 2–4 (Vigliotti et al., 2008). For this prograding unit, benthic foraminifera and the mollusc fauna are consistent with a shallow-marine (< 30 m) depositional environment (Maselli et al., 2011) locally subjected to a fluvial (deltaic) influence (Cattaneo and Trincardi, 1999). ^{14}C ages available for the uppermost part of this unit (Fig. 6; Vigliotti et al., 2008) link this interval to a period of overall rapid sea-level rise (i.e., between MWPs 1 A and 1B) and increasing sediment input to the basin, as documented by the correlation with pollen spectra from the deep basin (Asioli et al., 2001; Oldfield et al., 2003).

The early Holocene succession, between about 11.5 and 8.0 cal ky BP, records the final phase of sea-level rise that followed MWP 1B (Bard et al., 1996) and thus represents the late TST. It is dominated, both onshore and offshore, by fine-grained facies (Fig. 6). Beneath the modern Pescara coastal plain (core Marconi, Fig. 6), the late TST is essentially an incised-valley fill about 25 m thick, that records the backstepping of a wave-dominated estuary under eustatic forcing. The upper valley fill exhibits upward increasing marine influence, with the vertical transition from poorly-drained floodplain facies to swamp organic-rich clays (inner estuary) and brackish deposits (outer estuary; Fig. 6). The maximum flooding surface (MFS; Fig. 6) coincides with the maximum landward migration of the barrier-lagoon systems, around 8.0 cal kyr BP (Fig. 6).

Offshore, the late TST consists almost entirely of bioturbated marine mud, as revealed by planktonic foraminiferal assemblages (Maselli et al., 2011). This unit, up to 25 m-thick (Fig. 6) and dated between about 10.8 and 7.0 cal kyr BP, displays acoustically transparent to faintly laminated seismic facies, with low amplitude and high-continuity reflectors (Fig. 6, Cattaneo and Trincardi, 1999). The MFS coincides with a prominent downlap surface (Fig. 6), characterized by an interval of condensed deposition (Amorosi et al., 2016a).

Middle-late Holocene (HST) deposits (post-8.0 cal kyr BP) onshore display a characteristic shallowing-upward trend (Fig. 6) that reflects transition from an estuarine environment to a deltaic depositional system made up of brackish lagoons that were replaced by freshwater swamps, poorly-drained floodplains, and eventually by the modern coastal plain. Offshore, above the downlap surface (Fig. 6), HST displays an aggradational-progradational stacking pattern that reflects the late Holocene progradation of fluvio-deltaic systems (Cattaneo et al., 2007; Correggiari et al., 2005a, 2005b), as revealed by the occurrence of an up to 25 m-thick subaqueous delta prograding onto the shelf (Cattaneo et al., 2003) that correlates with coeval delta plain facies onshore.

5.1.2. *Tronto and Biferno transects*

Two additional transects, exceeding 30 km in length (Fig. 7a, b), were built north and south of Pescara (Tronto and Biferno river systems, respectively) to reconstruct the catchment-to-shelf facies architecture along the western Central Adriatic area. To avoid redundant concepts and descriptions, only the main similarities and differences between the two systems will be highlighted here. For both systems, the lower data coverage compared to the Pescara transect prevented from reconstructing stratigraphy in the proximal part of the valleys, as well as in very shallow shelf areas (10 km from the shoreline; Fig. 1b, for location).

Similar to the Pescara transect, Late Pleistocene amalgamated fluvial gravel bodies unconformably overlie significantly older muddy strata (Fig. 7a, b). In the Tronto system, the bedrock corresponds to Early Pleistocene outer-shelf muds (Fig. 7a; Catanzariti et al., 2009; Curzi et al., 2017), whereas in the Biferno coastal plain, the substrate (Fig. 7b) consists mostly of Middle-Pleistocene shallow-marine mud or pedogenized floodplain clay (i.e., substrate). The erosional unconformity that floors the Biferno paleovalley records the SB at the MIS 3/2 transition (Amorosi et al., 2016b). Offshore, SB can be traced beneath the shelf into the coeval "ESb surface", an unconformity dated at 31.8 cal kyr BP (Pellegrini et al., 2017b - Fig. 7a, b). Offshore the Tronto river mouth, the SB shows truncation and toplap terminations of the underlying reflections, and onlap reflection terminations above (Fig. 7a).

Aggradationally-stacked LST fluvial bodies onshore are correlative with offshore seismic units chronologically constrained between 31.8 and 14.4 cal kyr BP with progradational to aggradational stacking pattern (Pellegrini et al., 2018), showing high-amplitude discontinuous reflections (Fig. 7a) and low-amplitude chaotic strata (Fig. 7b). These seismic features are characteristic of coarse-grained fluvial deposits (Fig. 5 and Pellegrini et al., 2018; Gamberi et al., 2020). For this reason, lowstand units in the shelf area are tentatively interpreted as the distal portion of the fluvial-channel belts hosted at the base of the Apennine paleovalleys. Along the Tronto transect the lowstand fluvio-deltaic unit thickens considerably offshore, up to 20 m (Fig. 7a). The prograding lowstand deltaic unit pinches out about 30 km offshore the modern shoreline, at the transition with lowstand fine-grained subaqueous muds between 100 m and 120 m b.s.l. (Fig. 7a). In contrast, in the Biferno transect, the laterally continuous (about 26 km) fluvial body is about 8 m thick, and wedges out basinwards around 120 m b.s.l. (Fig. 7b). Inherited morphology appears to be the key controlling driver of such an unusual geometry, though most likely also tectonic activity played an important role (Ridente and Trincardi, 2006).

Above the lowstand fluvial unit, the stratigraphic architecture records an overall upward increase of marine influence (TST), with significant similarities among Tronto, Biferno (Fig. 7a, b) and the Pescara areas (Fig. 6) in terms of lithology, facies architecture, stacking patterns,

chronology and thickness distribution. In the onshore sectors, the abrupt facies change from amalgamated fluvial bodies to overlying mud-prone successions with isolated fluvial-channel bodies coincides with the transgressive surface (TS). This latter is slightly diachronous, being invariably younger (Fig. 7a, b) than 14.4 cal kyr BP in offshore position, within the MAD basin (Pellegrini et al., 2018). The Biferno and Tronto paleovalley fills, despite their markedly different thicknesses (about 21 and 6 m, respectively) show a similar transition from alluvial to estuarine strata of early Holocene age. Well-drained floodplain clays are progressively replaced by inner-estuary (poorly drained and freshwater swamp) facies associations and then outer-estuary to barrier-beach deposits (Fig. 7a, b). In the study areas, seismic reflections suggest homogeneous prodelta muds thinning out basinwards (Fig. 7a, b).

The age of the MFS in the Biferno coastal plain is consistent with the age (about 8.0 cal kyr BP) documented for the Pescara transect (Figs. 6 and 7b). A decreasing marine influence typifies middle-late Holocene HST deposits in the onshore sectors, where shallow-marine and lagoonal clays are overlain by fluvio-deltaic deposits of the modern coastal plain (Fig. 7a, b). Offshore, two prograding sedimentary wedges, up to 30 m-thick and made up of prodelta muds, cap both sedimentary successions (Fig. 7a, b).

Overall, TST and HST form an up to 42 m-thick sedimentary wedge mostly composed of fine-grained deposits that thin out basinwards (Figs. 6 and 7).

5.2. Systems tract thickness maps

Stratigraphic panels in Figs. 6 and 7 are well representative of the late Quaternary facies architecture in the western Central Adriatic, from river catchments to the shelf, and document the lateral transition from fluvial to marine environments (between 100 m and 140 m b.s.l.) during the LGM sea level lowstand. These three transects, however, cannot depict the entire three-dimensional complexity of the stratigraphic succession. To provide an overview of spatial facies distribution and accumulation patterns at the systems tract scale, highlighting source-to-sink dynamics and changes in sediment pathways, fluvial coarse-grained deposits (LST) and overlying fine-grained units (TST + HST) were mapped across a 5600 km^2 wide area of the western Central Adriatic shelf (Figs. 8–9 and Fig. 1b). Although lowstand depocenters are thickest in slope and basin sectors (up to 350 m in the MAD, Pellegrini et al., 2018), these areas have been intentionally excluded from the maps because of their typical fine-grained lithology (Cattaneo and Trincardi, 1999; Pellegrini et al., 2018) and inherently high salt-water content that is incompatible with OFG reserves (Sheng et al., 2023). Mapping operations relied upon published and unpublished data from several tens of high-resolution chirp and sparker profiles available for the whole Central Adriatic shelf (Fig. 1b).

5.2.1. LST thickness map

Fig. 8 shows the total thickness of LST deposits in the western Central Adriatic shelf, between 0 and about 110 m b.s.l. (Fig. 1b for location). As a whole, LST is thickest in the northern sector, close to the MAD basin (Fig. 8). North of the MAD, two main depocenters with overall NW-SE orientation display maximum thickness of about 60 m (Fig. 8) and can most likely be ascribed to the lowstand Po Delta system (Pellegrini et al., 2018). The main depocenter, in the easternmost sector (Fig. 8), is probably linked to the main river channel, whereas a secondary depocenter to the west records the influence of a minor distributary channel (Pellegrini et al., 2018). West of the MAD, the LST thins gradually toward the modern coastline, from about 25 m to 20 m offshore (Fig. 8).

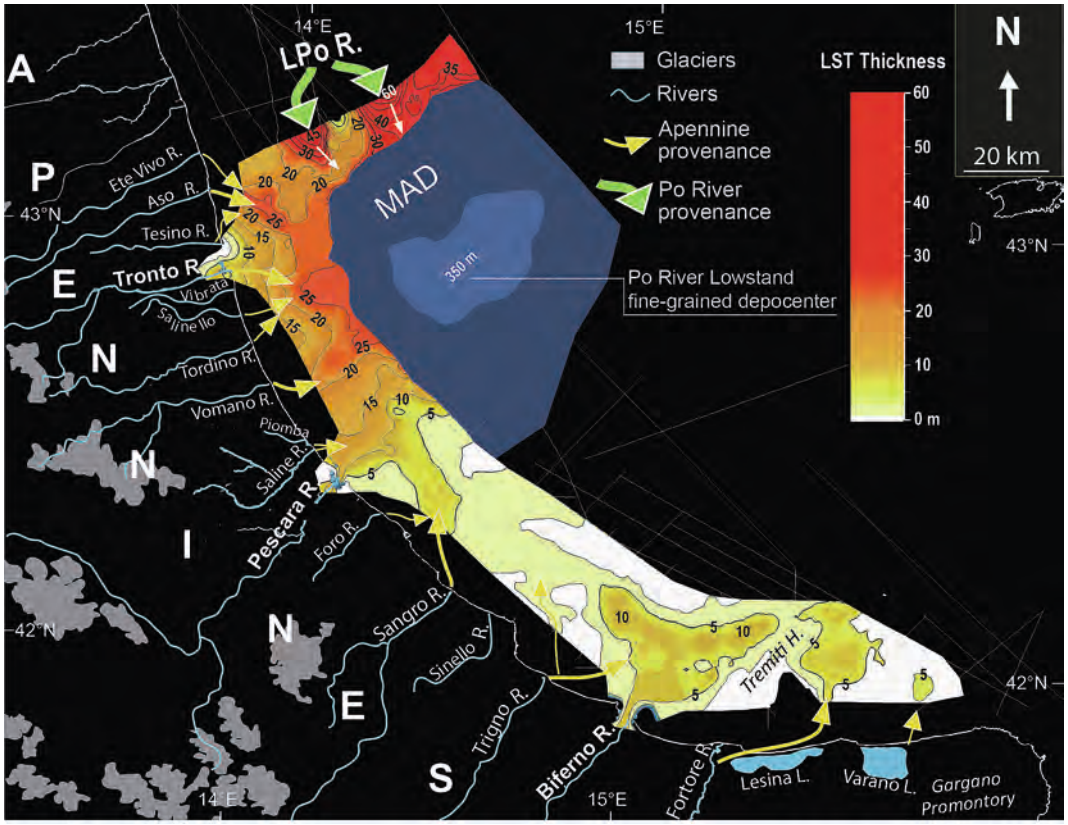

Fig. 8. Net thickness map (in meters) of lowstand systems tract (LST), from the Tronto, Pescara and Biferno coastal plains to the basinward limit of the LGM fluvial systems, across the western Central Adriatic shelf. Orange arrows: Apenninic catchment sediment provenance; green arrows: Po catchment sediment provenance; white arrows: orientation of the two main Po depocenters. Apennine glacier extent (after Giraudi, 2017). (For interpretation of the references to colour in this figure legend, the reader is referred to the web version of this article.)

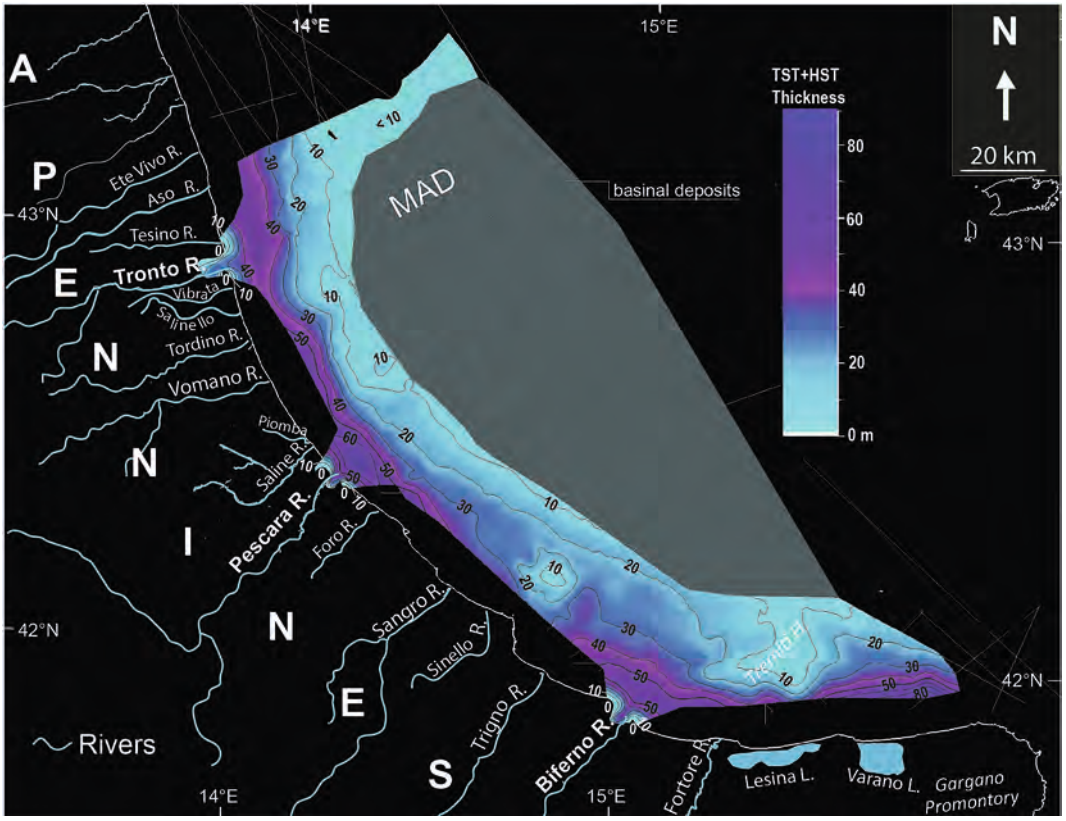

Fig. 9. Cumulative net thickness map (in meters) of transgressive systems tract (TST) and highstand systems tract (HST), from the Tronto, Pescara and Biferno coastal plains to basinward limit of the lowstand fluvial systems, across the western Central Adriatic shelf.

Sediment packages further thin out upstream, where LST sediment distribution is characterized by a clear ramification pattern in coincidence with Apennine river valleys (Fig. 8). This configuration suggests continuous progradation and aggradation of lowstand river systems triggered by glacio-eustatic forcing, with increased sediment delivery at fluvial mouths. The main depocenters, up to 25 m-thick, show overall W-E direction, and likely were generated by the Vomano and Tronto rivers (Fig. 8). Distally, these two depocenters coalesce and display a distribution slightly elongated in a NW-SE direction (Fig. 8), suggesting possible sediment redistribution along the LGM shoreline by marine processes. A third, prominent sedimentary entry point, elongated in NW-SE direction, coincides with the confluence of three minor river systems (Ete Vivo, Aso and Tesino), north of Tronto River (Fig. 8).

Southwards, the Pescara River mouth represents another important sediment entry point (Fig. 8). A narrow stripe of LST deposits, exceeding 10 m in thickness, spreads out from the Pescara paleovalley system, to possibly intercept additional sediment delivered by the Saline and Piomba rivers (Fig. 8). South of the Pescara River, the confluence of the Foro and Sangro river systems produced a 5–10 m thick LST deposit (Fig. 8). Its S—N elongated pattern is coherent with a northward flow direction for these rivers and their possible mixing with other systems before reaching the MAD (Fig. 8). In the southernmost sector, LST is generally 5–10 m thick (Fig. 8). Lower thickness values (< 5 m) are recorded between the two main depocenters, north of the Gargano Promontory, around the Tremiti High (Fig. 8; Cattaneo and Trincardi, 1999; Correggiari et al., 1992; Maselli et al., 2011). This morphological feature of tectonic origin strongly affected lowstand sediment accumulation in this area. Because of the Tremiti High morphological barrier, the Fortore River probably flowed in a NE direction across the shelf, north of the modern Lesina and Varano lakes, and nourished the easternmost LST depocenter (Fig. 8). Stratigraphic data from the Lesina cored succession, east of the modern Fortore delta plain, strongly support this interpretation (Longhitano et al., 2016; Ricci Lucchi et al., 2006). Additional material might have been supplied by a secondary river network draining the Gargano Promontory (Fig. 8). West of the Tremiti High, the largest depocenter of the southern area is filled by a fan-shaped sedimentary body that thins out downdip, with average thickness of 10 m (Fig. 8). Biferno River, one of the largest rivers in this area along with Fortore River, likely acted as the major sediment entry point to the shelf for this laterally extensive lowstand deposit. North of Biferno River, Trigno River supplied a considerable amount of coarse-grained material (Fig. 8). The shelf-scale spreading of LST fluvial deposits (Fig. 8) could be due to the abrupt topographic break between the low-gradient shelf and the high-gradient river valleys, accompanied by a high sediment flux from the Apennine catchments. Therefore, on the modern shelf, an intricate network of interconnected fluvial channels systems formed because of the merging of several Apennine river systems, similar to coeval braid plains documented worldwide (Blum et al., 2000; Kasse et al., 1995; Kozarski, 1991; Leigh et al., 2004; Panda et al., 2022; Saucier, 1994).

The greater thickness recorded in the northern sector compared to the southern area could reflect increased erosional activity by glaciers that covered the highest peaks of the Central Apennines during the LGM (Fig. 8; Giraudi, 2017). Post-glacial melting of Central Apennine glaciers likely caused further erosion, which enhanced sediment accumulation in the valleys and on the shelf. On the other hand, glaciers were absent in the southern sector of the Apenninic chain. In addition, the calcareous lithotype of the Gargano Promontory and associated karstic phenomena may have hindered the production and subsequent delivery of siliciclastic sediments to the shelf.

5.2.2. *TST + HST thickness map*

Fig. 9 displays the cumulative thickness of TST and HST from the three selected river catchments (Tronto, Pescara, and Biferno) to the

distal segments of the western Central Adriatic shelf. Mud-prone, marine and prodelta facies associations represent transgressive and highstand strata on the shelf, with maximum thickness exceeding 80 m close to the modern coastline (Fig. 9). Transgressive and highstand marine muds are thinner (< 10 m) at basinward locations (Fig. 9). In the onshore sector, paleovalley systems include the thickest TSTs, with cumulative TST + HST thickness of about 40 m for the Pescara River, and about 30 m for the Biferno and the Tronto rivers (Fig. 9). Far from the axes of the coastal paleovalleys, above the interfluves, the thickness of TST + HST is invariably lower than 10 m (Fig. 9).

The overall sediment distribution of TST + HST (Fig. 9) differs substantially from the LST configuration (Fig. 8): for example, north and west of the MAD basin, thickness is <10 m (Fig. 9). In the south, like for LST, the thinnest (< 10 m) portion coincides with the Tremiti High (compare Figs. 8 and 9).

Spatial thickness variations of TST and HST deposits are consistent with the stratal geometries and stacking patterns documented in Figs. 6 and 7. Particularly, vertically-stacked retrogradational (TST) and aggradational-progradational (HST) successions (Figs. 6 and 7) result in higher sediment supply to the proximal parts of the system (Fig. 9). Whereas transgressive sedimentation on the western Adriatic shelf was mostly influenced by the stepwise post-glacial sea-level rise, with sediment entry points (i.e., fluvial mouths) progressively being drowned and moved landwards (Storms et al., 2008), HST sediment accumulation is mainly ascribed to progradation of deltaic systems under a prevailing autogenic control (Amorosi et al., 2017b). The accumulation of the laterally continuous and shore-parallel late Holocene (HST) subaqueous delta (Correggiari et al., 2001; Cattaneo et al., 2003) accounts for the greatest thickness of TST + HST close to the shoreline (Fig. 9). This subaqueous delta formed in response to the prevailing coast-parallel sediment transport from the main sediment entry point in the north (Po Delta) and the sequestering of sediment delivered from a multitude of western Apennine rivers (Cattaneo et al., 2003, 2007). As a whole, lowstand, coarse-grained fluvial deposits (Fig. 8) are invariably buried beneath thick, fine-grained TST and HST muds across the entire shelf (Fig. 9).

6. Sediment budget

6.1. Approach

In the Adriatic Sea, a few studies (Brommer, 2009; Brommer et al., 2009; Weltje and Brommer, 2011) have focused on sediment budget analysis of prodelta deposits. Mass-accumulation rates were derived by means of stochastic simulations, through combined analysis of seismic data, porosity profiles and radiocarbon dating. An estimation of sediment volumes based on sequence-stratigraphic concepts and basin-scale correlation was attempted by Amorosi et al. (2016a), who provided sediment volumes stored in each systems tract over the entire Po-Adriatic Basin, with a decreasing level of uncertainty from the LST to the HST. Despite inevitable approximations, this sequence stratigraphic approach clearly documented how the main sediment storage areas shifted through time across different segments of the source-to-sink system (alluvial plain, coastal area, continental shelf, and the deep MAD basin). To further develop an integrated S2S and sequence stratigraphic approach for OFG exploration at the continental shelf scale, we estimated sediment volumes of the major lithofacies associations (gravel/sand versus mud), based on the spatial facies distribution and accumulation patterns of Figs. 8 and 9. Being aware that lateral facies variability is intrinsic to all sedimentary successions because of their depositional dynamics (Bridge, 2006; Cattaneo and Steel, 2003; Helland-Hansen and Gjelberg, 1994; Miall, 1988; Pellegrini et al., 2024; Zecchin, 2007), we focused on the bipartition between potential reservoir/aquifer units (LST) made up primarily of coarse-grained (porous) fluvial deposits, and the seal (TST + HST), which includes predominantly fine-grained (poorly permeable) estuarine to marine sediments.

The shelf is an area of complex sediment mixing from distinct sources, especially in multi-source supplied systems, such as the Western Adriatic Sea. As incorrect assessment of source areas may generate unrealistic estimates of sediment routes, and consequently flux, we stress in this section the potential of sediment provenance analysis based upon bulk-sediment geochemistry as a powerful tool for reconstructing sediment pathways, and thus contribute to sediment budget modelling (Amorosi et al., 2022).

6.2. Systems tract volumes and sediment budget partitioning on the western Central Adriatic shelf

We estimated decompacted sediment volumes, at the systems tracts scale (LST vs TST + HST), stored in the catchment-to-shelf sector analyzed in this study, and shown in the same area (about 5600 km^2) illustrated in the maps of Figs. 8 and 9. LST is characterized by a total volume of 57.2 km^3, consisting mainly of gravel and sand fluvial-channel belt bodies, as shown by sedimentological and geophysical data coupled with stratigraphic correlation and mapping (Figs. 6, 7 and 8). Considering the areal extent of the lowstand Po channel belt and its average sediment volume of 50 km^3 (Amorosi et al., 2016a), rough volumetric contribution to the LST total volume in the western Central Adriatic shelf (Fig. 8) possibly do not exceed 5 km^3. This implies that the largest part of LST (approximately 52 km^3) has been supplied to the investigated catchment-shelf sector (Fig. 8) by Apennine river catchments. The western Apennines alone delivered sediment volumes comparable to those of the lowstand Po River between 31.8 and 14.4 cal kyr BP. Dividing the sediment volume of presumed Apennine provenance (i.e., 52 km^3) by the duration of the LST yields a sediment accumulation rate of 2.88 km^3/kyr from Apennine sources. Similarly, the accumulation rate assessed for the Po channel belt is 4.16 km^3/kyr. This value suggests that the larger catchment of the Po River during the lowstand was able alone to supply more sediment than the sum of the other smaller Apennine rivers (Fig. 8). It should be noted, however, that many tributaries to the lowstand Po River north of the MAD basin were indeed from the Apennines (Amorosi et al., 2016a; Pellegrini et al., 2017a). Sediment patterns (Fig. 8) and volume calculations for LST in this sector of the Central Adriatic shelf are consistent with the models sketched by Sømme et al. (2009; their Fig. 9). These authors showed that during lowstand periods rivers tend to merge into larger river systems, resulting in increased sediment flux (Mulder and Syvitski, 1996). Since river catchments and the slope are generally connected, the largest sediment volumes (particularly, fine-grained sediment) are directly transported to the deep basin, as shown for the Adriatic slope and MAD basin by Pellegrini et al. (2018) with about 475 km^3. Although the assessed volume of 57.2 km^3 for the catchment-shelf portion (Fig. 8) represents only 12% of its equivalent basinal counterpart, it consists mainly of coarse-grained deposits, and thus may constitute a potential reservoir. The cumulative sediment volume for the mud-dominated TST and HST is 130 km^3. This value is representative of the last 14.4 kyr, suggesting an average sedimentation rate of 9.28 km^3/kyr for the investigated catchments-to-shelf area, averaging out also the intervals of reduced deposition at the time of the MFS and other minor flooding surfaces. Basin-scale calculations (Amorosi et al., 2016a) indicated sediment volumes of about 185 km^3 (TST) and 140 km^3 (HST) for the continental shelf. Considering the cumulative TST + HST value of 325 km^3 in 18,000 years, the average sedimentation rate is 18 km^3/kyr. This higher value could reflect a broader area, extending to the entire North Adriatic shelf. This latter is characterized by an almost flat shelf morphology compared to the Central Adriatic (Cattaneo et al., 2007) and includes transgressive barrier island systems (Correggiari et al., 1996b; Storms et al., 2008), small-scale incised valleys (Ronchi et al., 2018) and the modern Po Delta system (Correggiari et al., 2005a, 2005b), the most important entry point for sediments into the Adriatic Sea (Cattaneo et al., 2003).

The sedimentation rate assessed for the transgressive and highstand units in the western Central Adriatic shelf (9.28 km^3/kyr) is about three

times larger than the value obtained for lowstand fluvial deposits of Apennine provenance (2.88 km^3/kyr). This value, along with sediment patterns in Fig. 9 (TST + HST) is also consistent with the model proposed by Sømme et al. (2009) for periods of sea-level rise or highstand, when catchments and slope are disconnected. During these periods, larger amount of sediment, mostly fine-grained, can be stored in the shelf rather than in the deeper slope and basin settings (Fig. 9), as effectively documented by Amorosi et al. (2016a). They assessed a total sediment volume of about 325 km^3 for the Adriatic continental shelf against about 40 km^3 for the MAD basin during the last transgression and following highstand.

6.3. *Unravelling sediment mixing in the western Central Adriatic Sea by bulk-sediment geochemistry*

The reconstruction of the sediment routing system through seismic stratigraphic analysis (Figs. 8 and 9) is largely supported by sediment provenance characterization of eight Adriatic shelf cores (Fig. 1b), which allowed tracing detrital signatures and transport pathways in a consistent manner through the western Central Adriatic shelf. In the Cr/V diagram of Fig. 10, modern fluvial samples from the Po River (light gray dots) and Central Apennine rivers (dark gray dots) form two distinct, straight lines that reflect sediment supply from two separate source areas, here used as compositional end-members for the Po-Adriatic system. High Cr values have been typically interpreted to reflect erosion of Cr-rich ultramafic rocks exposed in the Po River catchment (Amorosi and Sammartino, 2007). Whereas, relatively lower Cr concentrations are invariably recorded where sediment supply is from ophiolite-free, Apennine sources. The positive correlation between Cr and V across both provenance domains reflects particular element concentrations within progressively finer sediment fractions. The highly contrasting (ultramafic versus non-ultramafic) geochemical signature of the Po and Central Apennine rivers catchments is clearly reflected in the trace-element composition of lowstand, channel-belt sand bodies from the Po and Pescara paleovalleys onshore (Fig. 10). These LST deposits, consistent with their modern counterparts, show relatively high (Po River) and negligible (Central Apennines) Cr values, respectively. The remarkably lower V content of lowstand deposits compared to modern fluvial-channel bodies reflects typically coarser grain sediment of the LST channel belts.

On the Adriatic shelf, the relatively low Cr values observed within lowstand deposits from the central (PAL94–8, PAL94–9) and southern (RF93–56, RF93–75, YD97–13) parts of the study area, and their remarkable overlap in composition with Central Apennine river samples, suggest that conspicuous detrital input to the shelf was supplied during the Last Glacial Maximum from transversal (Apennine) sources, as shown in Fig. 8. On the other hand, a mixed, Apennine-Po River composition is apparent for core samples from the northern part of the study area (AN97–36, AN97–31). Finally, one Cr-rich sample from core LSD_26 (close to the MAD) documents strong compositional affinity with ultramafic-rich detritus, revealing a possible longitudinal dispersion, with Po River as the major feeding source to the MAD (Lucchini et al., 2003; Pellegrini et al., 2018; Pigorini, 1968; Weltje and Brommer, 2011).

7. New frontiers for sequence stratigraphy and S2S analysis: offshore freshened groundwater exploration

Despite the growing interest worldwide upon offshore freshened groundwater (OFG), exploration research still lacks a robust stratigraphic methodology aiming at the identification and characterization of siliciclastic OFG reservoirs. Major knowledge gaps on OFG include estimates of reservoir geometry and size, as well as understanding the control exerted by the geological environment on OFG spatial distribution (Micallef et al., 2021). Potential OFG in shelf areas worldwide has been typically identified in siliciclastic aquifers within 55 km from the coast, in water depths <100 m (Micallef et al., 2021; Sheng et al., 2023). These characteristics make the western Central Adriatic shelf (Fig. 1b) a suitable location to test an exploration methodology based on integrated sequence stratigraphy and S2S analysis.

In this study, the high-resolution sequence stratigraphic reconstruction of post-LGM facies architecture along three catchment-to-shelf transects (Figs. 6 and 7), coupled with detailed mapping of LST (Fig. 8) and TST + HST (Fig. 9) thickness, forms the basis for the identification of a potential, regionally extensive groundwater reservoir beneath the western Central Adriatic shelf, corresponding to lowstand fluvial unit

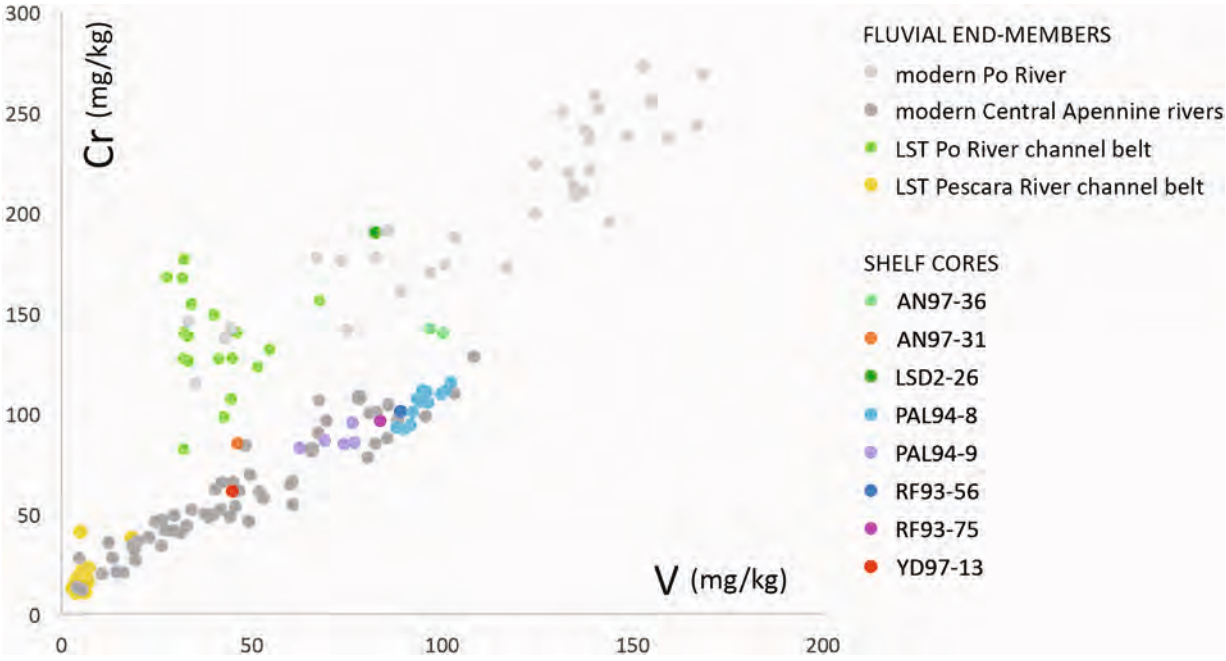

Fig. 10. Scatterplot of Cr versus V from LST core samples of the western Central Adriatic area (in colour) and their comparison to modern fluvial sediment composition (in gray). Po River and Central Apennine river sediments are used as compositional end-members.

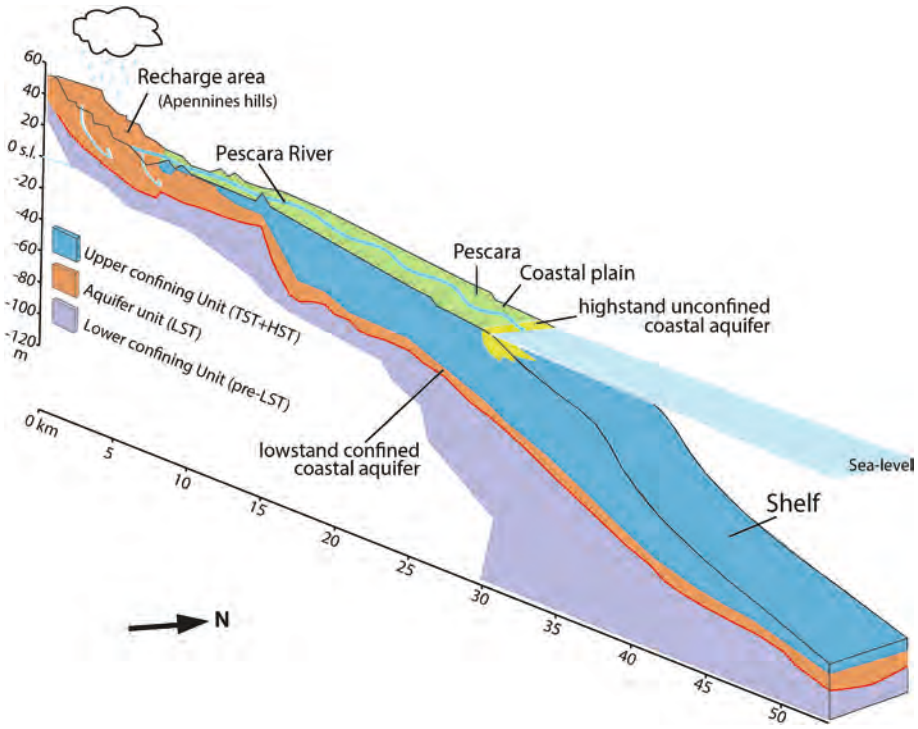

Fig. 11. Three-dimensional view of the LST aquifer and its confining (fine-grained) units along the onshore-offshore Pescara transect (Fig. 1b for location).

(Fig. 11).

In the subsurface of the western Adriatic coastal plains, lowstand deposits stored in incised-valley fills represent the most widespread and most exploited confined aquifers (Cavallina et al., 2022; Desiderio et al., 2003, 2007; Molinari et al., 2007; Nanni and Vivalda, 2005; Palmucci et al., 2016; Regione Emilia-Romagna, ENI-AGIP, 1998). However, their offshore extent has never been documented. In this work, onshore-offshore correlation based on high-resolution sequence-stratigraphic analysis, allowed to document, for the first time, the basinward continuity of a confined coastal aquifer system (LST) beneath the modern western Central Adriatic shelf (Figs. 8 and 11). This lowstand aquifer lies tens of meters in the subsurface and is sealed by thick, mud-prone TST and HST beds (Figs. 9 and 11). Despite intrinsic lateral facies variability and heterogeneity at different scales (Bridge, 2001; Kelly, 2006), the LST aquifer unit extends continuously off the modern coast for over 20 km (Fig. 11, up to 30 km in Fig. 8) and is widespread across the proximal sector (between 0 m and 120 m b.s.l.) of the whole Central Adriatic shelf, with average thickness of about 10 m (Figs. 8 and 11). Spatial distribution, lithology, geometry and lateral continuity (and consequent potential sediment-bodies connectivity) invariably reflect the pattern of a braided fluvial system (Miall, 1977) across the, at that time, subaerially exposed, Adriatic shelf during lowstand sea level conditions. Braided-systems reservoirs are generally characterized by very high sand-to-gross ratios, commonly between 85% and 95% (Atkinson et al., 1990; Bo et al., 2024; Conway and Valvatne, 2003; La Croix et al., 2019). These values are fully consistent with our core and seismic data, and with the latest braided facies model of Miall (2013) and Colombera et al. (2013).

Lowstand fluvial deposits onshore are typical freshwater reservoirs that are exploited for human needs. However, water volumes and salinity in their offshore counterparts are still poorly known with very rare examples based on global scale modelling (Zamrsky et al., 2022), and direct pore water measurements (Sheng et al., 2023). In this study, stratigraphic reconstructions (Figs. 6, 7, 8 and 9) revealed that the LST aquifer beneath the modern western Central Adriatic shelf is sandwiched between two mud-prone (i.e., low-permeability) successions (Figs. 9 and 11): the lower confining unit includes pre-LGM deposits (mainly offshore silty clays), whereas the upper confining unit mostly coincides with latest Pleistocene-Holocene (TST + HST) estuarine to marine mud. The remarkable thickness and lateral continuity of TST and HST (Fig. 9) suggest that transgressive and highstand marine muds should act as an effective permeability barrier against potential seawater intrusion even in the distal sector of the shelf, where both systems tracts gradually thin out (Figs. 9 and 11). This makes the LST a confined aquifer at the scale of the entire western Central Adriatic shelf. Sand bodies, such as isolated distributary channels or transgressive beach barrier, may occur within the upper confining unit, but do not make aquifer systems due to their limited thickness and very scarce lateral continuity (Campo et al., 2020). On the other hand, highstand and shore parallel beach ridges may represent unconfined aquifers, but only in coastal sectors because of their shore-parallel lateral extent (Fig. 11 – Desiderio et al., 2007; Giambastiani et al., 2021). These coastal aquifers are floored by relatively thick estuarine/delta plain (TST+ early HST) muds that generally hinder vertical fluid migration. Locally, TST and HST sands can be thick enough to intercept LST deposits (as shown in Fig. 7b, core S16), thus potentially allowing HST and LST aquifers connection. However, such a possibility is confined only to the coastal sector where LST and HST aquifers may locally overlap, but it is very unlikely on the shelf because of the backstepping configuration of the TST coastal deposits, and because of the very limited offshore continuity of HST sand bodies (Figs. 11, 6 and 7 – Cattaneo et al., 2007). Hydraulic connectivity and potential risk of water contamination surely represent key aspects that needs to be addressed once the LST aquifer is characterized in terms of water quality. Additional data, such as pore-water samples and aquifer modelling should derive from upcoming projects. For sure, high-resolution stratigraphy has shown its effectiveness with the identification of one possible connection site (Fig. 7b, S16). Petrophysical and hydraulic parameters of the potential LST aquifer, such as porosity, permeability, and transmissivity are likely to reflect the generally high-energy characteristics of the braided fluvial environment under lowstand conditions.

Sediment volume assessments of the lowstand aquifer across the western Central Adriatic area (Fig. 8) enable a preliminary estimate of the potential groundwater storage. Based on all the available data and high sand-to-gross ratio, we can reasonably assume that under the

modern shelf, 85% (the lowest value of Bo et al., 2024) of the LST total volume (57.2 km^3) consists of porous unconsolidated sediments (i.e., gravel and sand). Considering an average effective porosity of 28.5% for these lithologies (see Woessner and Poeter, 2020), the LST offshore aquifer might retain about 13.85 km^3 of groundwater. Of course, this is just a preliminary and very gross estimate, with the main goal to draw attention on such an alternative water resource. We are aware of the many uncertainties in terms of aquifer heterogeneity (a common task to groundwater studies) and, most importantly, of water quality. It is very unlikely that OFG can be directly used as potable water, but total dissolved solids concentration values lower than sea water may represent a cost-effective raw source for desalinization, for agricultural and industrial purposes during severe water shortages (Sheng et al., 2023; Zamrsky et al., 2022) or for the numerous water-scarce areas along the Mediterranean coastlines (Bertoni et al., 2020; Lipparini et al., 2023).

The offshore Adriatic LST aquifer was probably recharged meteorically at the time of its formation, between approximately 31.8 to 20 cal kyr BP, when the Adriatic shelf was subaerially exposed (Fig. 2). At present, the recharge of the LST aquifer beneath the modern coastal plain is mainly ascribed to the infiltration of water from the Apennine rivers, whereas recharge by rainfall is important especially in the upstream reaches of rivers (Nanni and Vivalda, 2005), where fluvial gravels crop out (Fig. 11). Considering its stratigraphic continuity, it is very likely that the offshore LST aquifer represents an actively recharging system. This aspect is fundamental in terms of potential exploitation, as only actively recharging systems can be sustainable (Micallef et al., 2021). Under the constant threat of the ongoing climate change, population growth, and consequent increasing need of freshwater, especially in coastal areas (UN-Water, 2020), low-salinity offshore groundwater could represent a strategic resource in the near future. In the northern Adriatic area, proof of low-salinity groundwater stored below lagoonal and shallow-marine settings has been provided by Teatini et al. (2011) and Tosi et al. (2017). Airborne electromagnetic data also suggested the presence of freshwater beneath the Venice Lagoon (Teatini et al., 2011), whereas the cemented beach rocks exploited in patches by the coralligeneous encrusted at their surface, was linked to the influence of less saline fluids related to subsurface freshwater discharge from a sealed water table recharged onland (Tosi et al., 2017). In all these instances, however, the lack of a thick, laterally continuous sealing unit able to prevent sea-water intrusion could have a negative impact in terms of aquifer exploitation and management. Although evaluation of water salinity will be essential to assess its potential as an alternative groundwater resource, the lowstand aquifer of the western Central Adriatic shelf with its confining units (aquitards or aquicludes) is a significantly promising area for upcoming OFG exploration in the Mediterranean Sea. We are aware that for future hydrogeological modelling, additional data will be necessary to shed lights on the internal aquifer heterogeneity, as overbank finer-grained deposits could locally decrease the average high permeability of fluvial sand bodies. Similarly, the vertical fluid migration, documented in different parts of the Adriatic seabed (Capozzi et al., 2012; Colantoni et al., 1979; Conti et al., 2002; Curzi and Veggiani, 1985; Geletti et al., 2008; Hovland and Curzi, 1989; Judd and Hovland, 2007; Rovere et al., 2020; Gordini et al., 2023; Stefanon, 1980), suggests a certain complexity of the two confining units that needs to be further explored for a complete characterization of this aquifer system.

In general, reconstructing facies architecture through integrated, high-resolution sedimentary and seismic facies analysis in a sequence stratigraphic framework can represent a powerful tool for the exploration of OFG lithosomes in the near future.

8. Conclusions

We reconstructed the sequence stratigraphic architecture of the western Central Adriatic system emplaced since the Last Glacial Maximum and evaluated the potential of lowstand coarse-grained fluvial deposits buried beneath transgressive and highstand marine mud as potential offshore freshened groundwater reservoirs. The main results are summarized as follows.

1. On a regional scale, the sequence boundary (SB) is a stratigraphic unconformity that formed in response to the abrupt sea-level fall at the MIS 3/2 transition. Above SB, aggradational fluvial channel-belt gravel-sand bodies and progradational to aggradational delta systems represent the lowstand systems tract (LST). A slightly diachronous transgressive surface (TS) separates LST from an overlying, laterally continuous and mud-dominated succession made up of backstepping, alluvial, estuarine and shallow-marine facies associations, overlain by delta plain deposits and aggradationally to progradationally stacked prodelta clays. The maximum flooding surface (MFS) marks the transition from retrogradational to aggradational-progradational stackings and coincides offshore with a prominent downlap surface and a condensed section.
2. Thickness maps, at the systems tract scale, indicate the lateral continuity and thickness distribution of potential reservoir (LST) and overlying seal unit (TST and HST). The LST covers almost entirely the investigated shelf area (5600 km^2 wide), with an average thickness of about 10 m. The thickest LST depocenters (up to 60 m), north of the Mid-Adriatic Depression (MAD), were assigned to the proximal portion of the Po lowstand shelf-edge delta. In contrast, thinner LST depocenters (< 25 m thick) were fed by Apennines rivers. TST and HST strata display their maximum thickness (80 m) close to the modern coastline.
3. We estimate a total sediment volume of 57.2 km^3 for LST, and ca. 130 km^3 for TST + HST. Based on seismic facies architecture integrated with sediment provenance analysis, on the Central Adriatic shelf, about 52 km^3 of LST deposits were supplied from Apennine sources, whereas 5 km^3 were conveyed through the lowstand Po River system.
4. Sequence stratigraphic analysis along the pathway from river catchments to the sink allowed, for the first time, the identification and mapping of a potential (lowstand) aquifer unit beneath the western Central Adriatic shelf. This offshore aquifer is confined atop by a thick, low-permeability unit (TST + HST muds) that might have hindered salt-water intrusion into the reservoir. The lowstand offshore aquifer represents an actively recharging system that might store about 13.85 km^3 of groundwater, with important implications for possible future sustainable exploitation.
5. Offshore groundwater research is in its infancy and at present substantially lacks an associated stratigraphic methodology aiming at the identification, characterization, and mapping of potential aquifers and aquitard units. The combined sequence stratigraphic and source-to-sink approach tested in this work is likely to represent an effective tool for future exploration of siliciclastic groundwater reservoirs stored in continental shelves worldwide.

Declaration of competing interest

The authors declare the following financial interests/personal relationships which may be considered as potential competing interests:

Alessandro Amorosi reports financial support was provided by Ministry of University and Research.

Data availability

Two well log descriptions Frt001 (Fratello 001) and Cmp001 (Campomarino 001) have been extracted from the ViDEPI (Visibility of petroleum exploration data in Italy) repository and are available at https://www.videpi.com/videpi/pozzi/consultabili.asp.

Acknowledgments

This work was supported by the Italian Ministry of University and Research under the PRIN 2017 program, project number 2017ASZAKJ "The Po-Adriatic Source-to-Sink system (PASS): from modern sedimentary processes to millennial-scale stratigraphic architecture", grant to Alessandro Amorosi. The authors are grateful to the two anonimous reviewers for their very constructive comments, and to Dr. Vito Bracone for providing stratigraphic data on the Biferno coastal plain. We thank Schlumberger for the generous donation of the Petrel software package to the University of Bologna. We are also indebted to Kevin Bohacs and our colleagues at Exxonmobil Upstream Research Company (Houston, TX) that encouraged, supported and intellectually stimulated the collaboration between University of Bologna and ISMAR (CNR).

References

Ainsworth, R.B., 2010. Prediction of stratigraphic compartmentalization in marginal marine reservoirs. Geol. Soc. London Spec. Publ. 347, 199–218. https://doi.org/10.1144/SP347.12.

Aitken, J.F., Flint, S.S., 1996. Variable expressions of interfluvial sequence boundaries in the Breathitt Group (Pennsylvanian), eastern Kentucky, USA. In: Howell, J.A., Aitken, J.F. (Eds.), High Resolution Sequence Stratigraphy: Innovations and Applications. Geological Society of London Special Publication 104, pp. 193–206. https://doi.org/10.1144/GSL.SP.1996.104.01.12.

Allen, J.R., 1965. A review of the origin and characteristics of recent alluvial sediments. Sedimentology 5 (2), 89–191.

Allen, P.A., 2008. From landscapes into geological history. Nature 451, 274–276. https://doi.org/10.1038/nature06586.

Amadori, C., Ghielmi, M., Mancin, N., Toscani, G., 2020. The evolution of a coastal wedge in response to Plio-Pleistocene climate change: the Northern Adriatic case. Mar. Pet. Geol. 122, 104675.

Amorosi, A., Sammartino, I., 2007. Influence of sediment provenance on background values of potentially toxic metals from near-surface sediments of Po coastal plain (Italy). Int. J. Earth Sci. 96, 389–396.

Amorosi, A., Barbieri, M., Castorina, F., Colalongo, M.L., Pasini, G., Vaiani, S.C., 1998. Sedimentology, micropaleontology, and strontium-isotope dating of a lower-middle Pleistocene marine succession ("Argille Azzurre") in the Romagna Apennines, northern Italy. Boll. Della Soc. Geol. Ital. 117, 789–806.

Amorosi, A., Colalongo, M.L., Fusco, F., Pasini, G., Fiorini, F., 1999. Glacio-eustatic control of continental-shallow marine cyclicity from late quaternary deposits of the southeastern Po Plain, northern Italy. Quat. Res. 52, 1–13. https://doi.org/10.1006/qres.1999.2049.

Amorosi, A., Colalongo, M.L., Fiorini, F., Fusco, F., Pasini, G., Vaiani, S.C., Sarti, G., 2004. Palaeogeographic and palaeoclimatic evolution of the Po Plain from 150-ky core records. Glob. Planet. Chang. 40, 55–78. https://doi.org/10.1016/S0921-8181(03)00098-5.

Amorosi, A., Maselli, V., Trincardi, F., 2016a. Onshore to offshore anatomy of a late Quaternary source-to-sink system (Po Plain-Adriatic Sea, Italy). Earth-Sci. Rev. 153, 212–237. https://doi.org/10.1016/j.earscirev.2015.10.010.

Amorosi, A., Bracone, V., Campo, B., D'Amico, C., Rossi, V., Rosskopf, C.M., 2016b. A late Quaternary multiple paleovalley system from the Adriatic coastal plain (Biferno River, Southern Italy). Geomorphology 254, 146–159. https://doi.org/10.1016/j.geomorph.2015.11.023.

Amorosi, A., Bruno, L., Cleveland, D.M., Morelli, A., Hong, W., 2017a. Paleosols and associated channel-belt sand bodies from a continuously subsiding late quaternary system (Po basin, Italy): New insights into continental sequence stratigraphy. Bull. Geol. Soc. Am. 129, 449–463. https://doi.org/10.1130/B31575.1.

Amorosi, A., Bruno, L., Campo, B., Morelli, A., Rossi, V., Scarponi, D., Hong, W., Bohacs, K.M., Drexler, T.M., 2017b. Global sea-level control on local parasequence architecture from the Holocene record of the Po Plain, Italy. Mar. Pet. Geol. 87, 99–111. https://doi.org/10.1016/j.marpetgeo.2017.01.020.

Amorosi, A., Barbieri, G., Bruno, L., Campo, B., Drexler, T.M., Hong, W., Rossi, V., Sammartino, I., Scarponi, D., Vaiani, S.C., 2019. Three-fold nature of coastal progradation during the Holocene eustatic highstand, Po Plain, Italy–close correspondence of stratal character with distribution patterns. Sedimentology 66, 3029–3052.

Amorosi, A., Bruno, L., Campo, B., Costagli, B., Dinelli, E., Hong, W., Sammartino, I., Vaiani, S.C., 2020. Tracing clinothem geometry and sediment pathways in the prograding Holocene Po Delta system through integrated core stratigraphy. Basin Res. 32, 206–215. https://doi.org/10.1111/bre.12360.

Amorosi, A., Sammartino, I., Dinelli, E., Campo, B., Guercia, T., Trincardi, F., Pellegrini, C., 2022. Provenance and sediment dispersal in the Po-Adriatic source-to-sink system unraveled by bulk-sediment geochemistry and its linkage to catchment geology. Earth-Sci. Rev. 234, 104202 https://doi.org/10.1016/j.earscirev.2022.104202.

Amorosi, A., Bruno, L., Caldara, M., Campo, B., Cau, S., De Santis, V., Di Martino, A., Hong, W., Lucci, G., Pellegrini, C., Rossi, V., Sammartino, I., Vaiani, S.C., 2023. Late Quaternary sedimentary record of estuarine incised-valley filling and interfluve flooding: the Manfredonia paleovalley system (southern Italy). Mar. Pet. Geol. 147, 105975 https://doi.org/10.1016/j.marpetgeo.2022.105975.

Anderson, J.B., Rodriguez, A., Abdulah, K., Fillon, R.H., Banfield, L.A., McKLeown, H.A., Wellner, J.S., 2004. Late Quaternary stratigraphic evolution of the Northern Gulf of Mexico margin: asynthesis. In: Anderson, J.B., Fillon, R.H. (Eds.), Late Quaternary Stratigraphic Evolution of the Northern Gulf of Mexico Margin, vol. 79. Society of Economic Paleontologists and Mineralogists (SEPM), pp. 1–23. Special Publication.

Asioli, A., 1996. High resolution foraminifera biostratigraphy in the Central Adriatic basin during the last deglaciation: a contribution to the PALICLAS Project. Mem. Istit. Ital. Idrobiol. 55, 197–218.

Asioli, A., Trincardi, F., Lowe, J.J., Ariztegui, D., Langone, L., Oldfield, F., 2001. Sub-millennial scale climatic oscillations in the central adriatic during the lateglacial: Palaeoceanographic implications. Quat. Sci. Rev. 20, 1201–1221. https://doi.org/10.1016/S0277-3791(00)00147-5.

Atkinson, C.D., McGowen, J.H., Bloch, S., Lundell, L.L., Trumbly, P.N., 1990. Braidplain and deltaic reservoir, Prudhoe Bay field, Alaska. Sandstone Petrol. Reserv. 7–29.

Attias, E., Thomas, D., Sherman, D., Ismail, K., Constable, S., 2020. Marine electrical imaging reveals novel freshwater transport mechanism in Hawai 'i. Sci. Adv. 6, eabd4866.

Attias, E., Constable, S., Sherman, D., Ismail, K., Shuler, C., Dulai, H., 2021. Marine electromagnetic imaging and volumetric estimation of freshwater plumes offshore Hawai'i. Geophys. Res. Lett. 48 e2020GL091249.

Bakken, T.H., Ruden, F., Mangset, L.E., 2012. Submarine groundwater: a new concept for the supply of drinking water. Water Resour. Manag. 26, 1015–1026.

Ballato, P., Strecker, M.R., 2014. Assessing tectonic and climatic causal mechanisms in foreland-basin stratal architecture: insights from the Alborz Mountains, northern Iran. Earth Surf. Process. Landf. 39, 110–125.

Barbieri, G., Rossi, V., Vaiani, S.C., Horton, B.P., 2019. Benthic ostracoda and foraminifera from the North Adriatic Sea (Italy, Mediterranean Sea): a proxy for the depositional characterisation of river-influenced shelves. Mar. Micropaleontol. 153, 101772.

Bard, E., Hamelin, B., Arnold, M., Montaggioni, L., Cabioch, G., Faure, G., Rougerie, F., 1996. Deglacial sea-level record from Tahiti corals and the timing of global Meltwater discharge. Nature 382, 241–244.

Beauboeuf, R.T., Friedman, S.J., 2000. High resolution seismic/sequence stratigraphic framework for the evolution of Pleistocene intra slope basins, western Gulf of Mexico: depositional models and reservoir analogs. In: Gulf Coast Section, SEPM, 20th Annual Research Conference, Deep-Water Reservoirs of the World, Dec. 3–6, pp. 40–60.

Bertoni, C., Lofi, J., Micallef, A., Moe, H., 2020. Seismic reflection methods in offshore groundwater research. Geosciences 10, 299.

Blum, M.D., Aslan, A., 2006. Signatures of climate vs. sea-level change within incised valley-fill successions: Quaternary examples from the Texas GULF Coast. Sediment. Geol. 190, 177–211. https://doi.org/10.1016/j.sedgeo.2006.05.024.

Blum, M.D., Törnqvist, T.E., 2000. Fluvial responses to climate and sea-level change: a review and look forward. Sedimentology 47, 2–48. https://doi.org/10.1046/j.1365-3091.2000.00008.x.

Blum, M.D., Womack, J.H., 2009. Climate change, sea-level change, and fluvial sediment supply to Deepwater systems. In: Kneller, B., Martinsen, O.J., McCaffrey, B. (Eds.), External Controls on Deep Water Depositional Systems: Climate, Sea-Level, and Sediment Flux, vol. 92. SEPM Special Publication, pp. 15–39.

Blum, M.D., Guccione, M.J., Wysocki, D.A., Robnett, P.C., Rutledge, E.M., 2000. Late pleistocene evolution of the lower Mississippi River vally, Southern Missouri to Arkansas. Bull. Geol. Soc. Am. 112, 221–235. https://doi.org/10.1130/0016-7606(2000)112<221:LPEOTL>2.0.CO;2.

Blum, M., Martin, J., Milliken, K., Garvin, M., 2013. Paleovalley systems: Insights from Quaternary analogs and experiments. Earth-Sci. Rev. 116, 128–169. https://doi.org/10.1016/j.earscirev.2012.09.003.

Bo, Z., Hörning, S., Underschultz, J.R., Garnett, A., Hurter, S., 2024. Effects of geological heterogeneity on gas mixing during underground hydrogen storage (UHS) in braided-fluvial reservoirs. Fuel 357, 129949.

Bracone, V., Amorosi, A., Aucelli, P., Ciampo, G., Di Donato, V., Rosskopf, C., 2012. Palaeoenvironmental evolution of the Plio-Pleistocene Molise Periadriatic Basin (Southern Apennines, Italy): Insight from Montesecco Clays. Ital. J. Geosci. 131, 272–275. https://doi.org/10.3301/IJG.2012.20.

Bridge, J.S., 2001. Characterization of fluvial hydrocarbon reservoirs and aquifers: problems and solutions. Latin Am. J. Sedimentol. Basin Anal. 8 (2), 87–114.

Bridge, J.S., 2006. Fluvial facies models: recent developments. In: Posamentier, H., Walker, R.G. (Eds.), Facies Models Revisited, SEPM Special Publication, vol. 84, pp. 85–170.

Brommer, M.B., 2009. Mass-balanced stratigraphy — data model comparison within a closed sedimentary system (Adriatic Sea, Italy). Ph.D Thesis. University of Delft (155 pp.).

Brommer, M.B., Weltje, G.J., Trincardi, F., 2009. Reconstruction of sediment supply from mass accumulation rates in the Northern Adriatic Basin (Italy) over the past 19,000 years. Case Rep. Med. 114, 1–15. https://doi.org/10.1029/2008JF000987.

Bruno, L., Bohacs, K.M., Campo, B., Drexler, T.M., Rossi, V., Sammartino, I., Scarponi, D., Hong, W., Amorosi, A., 2017. Early Holocene transgressive palaeogeography in the Po coastal plain (northern Italy). Sedimentology 64, 1792–1816. https://doi.org/10.1111/sed.12374.

Bruno, L., Campo, B., Di Martino, A., Hong, W., Amorosi, A., 2019. Peat layer accumulation and post-burial deformation during the mid-late Holocene in the Po coastal plain (Northern Italy). Basin Res. 31, 621–639. https://doi.org/10.1111/bre.12339.

Bruno, L., Campo, B., Hajdas, I., Hong, W., Amorosi, A., 2022. Timing and mechanisms of sediment accumulation and pedogenesis: Insights from the Po Plain (northern Italy). Palaeogeogr. Palaeoclimatol. Palaeoecol. 591, 110881 https://doi.org/10.1016/j.palaeo.2022.110881.

Burger, R.L., Fulthorpe, C.S., Austin, J.A., 2001. Late Pleistocene channel incisions in the southern Eel River Basin, northern California: implications for tectonic vs. eustatic in influences on shelf sedimentation patterns, p. 177.
Burns, C.E., Mountney, N.P., Hodgson, D.M., Colombera, L., 2017. Anatomy and dimensions of fluvial crevasse-splay deposits: examples from the cretaceous Castlegate Sandstone and Neslen Formation, Utah, USA. Sediment. Geol. 351, 21–35.
Burrato, P., Ciucci, F., Valensise, G., 2003. An inventory of river anomalies in the Po Plain, Northern Italy: evidence for active blind thrust faulting. Ann. Geophys. 46, 865–882. https://doi.org/10.4401/ag-3459.
Calderoni, G., Della Seta, M., Fredi, P., Lupia Palmieri, E., Nesci, O., Savelli, D., Troiani, F., 2010. Late Quaternary geomorphological evolution of the Adriatic coast reach encompassing the Metauro, Cesano and Misa river mouths (Northern Marche, Italy). Geo Acta Spec. Publ. 3, 109–124.
Campo, B., Amorosi, A., Vaiani, S.C., 2017. Sequence stratigraphy and late Quaternary paleoenvironmental evolution of the Northern Adriatic coastal plain (Italy). Palaeogeogr. Palaeoclimatol. Palaeoecol. 466, 265–278. https://doi.org/10.1016/j.palaeo.2016.11.016.
Campo, B., Amorosi, A., Bohacs, K.M., 2020. Late Quaternary sequence stratigraphy as a tool for groundwater exploration: lessons from the Po River Basin (northern Italy). Am. Assoc. Pet. Geol. Bull. 104, 681–710. https://doi.org/10.1306/06121918116.
Campo, B., Barbieri, G., Di Martino, A., Hong, W., Scarponi, D., Vaiani, S.C., Amorosi, A., 2022. Late Pleistocene to Holocene glacio-eustatic history as recorded in the Pescara paleovalley system (Central Italy, Adriatic basin). Mar. Pet. Geol. 145, 105908 https://doi.org/10.1016/j.marpetgeo.2022.105908.
Cantalamessa, G., Di Celma, C., 2004. Sequence response to syndepositional regional uplift: Insights from high-resolution sequence stratigraphy of late early Pleistocene strata, Periadriatic Basin, Central Italy. Sediment. Geol. 164, 283–309. https://doi.org/10.1016/j.sedgeo.2003.11.003.
Cantalamessa, G., Centamore, E., Chiocchini, U., Colanlongo, M.L., Micarelli, A., Nanni, T., Pasini, G., Potetti, M., Ricci Lucchi, F., 1986. Il Plio-Pleistocene delle Marche. Studi Geol. Camerti 1, 61–81.
Capozzi, R., Guido, F.L., Oppo, D., Gabbianelli, G., 2012. Methane-Derived Authigenic Carbonates (MDAC) in northern-Central Adriatic Sea: Relationships between reservoir and methane seepages. Mar. Geol. 332, 174–188.
Caputo, R., Iordanidou, K., Minarelli, L., Papathanassiou, G., Poli, M.E., Rapti-Caputo, D., Sboras, S., Stefani, M., Zanferrari, A., 2012. Geological evidence of pre-2012 seismic events, Emilia-Romagna, Italy. Ann. Geophys. 55, 743–749.
Carminati, E., Doglioni, C., Scrocca, D., 2003. Apennines subduction-related subsidence of Venice (Italy). Geophys. Res. Lett. 30, 1–4. https://doi.org/10.1029/2003GL017001.
Carruba, S., Casnedi, R., Perotti, C.R., Tornaghi, M., Bolis, G., 2006. Tectonic and sedimentary evolution of the lower Pliocene Periadriatic foredeep in Central Italy. Int. J. Earth Sci. 95, 665–683. https://doi.org/10.1007/s00531-005-0056-4.
Catanzariti, R., Curzi, P.V., Dinelli, E., Vaiani, S.C., 2009. Quaternary subsurface stratigraphy in the Tronto alluvial plain (Italy); palaeoenvironmental evolution and relationships with sediment geochemistry. GeoActa Bol. 8, 33–48.
Cattaneo, A., Steel, R.J., 2003. Transgressive deposits: a review of their variability. Earth-Sci. Rev. 62 (3–4), 187–228.
Cattaneo, A., Trincardi, F., 1999. The late Quaternary transgressive record in the Adriatic epicontinental sea: Basin widening and facies partitioning. In: Bergman, K.M., Snedden, J.W. (Eds.), Isolated Shallow Marine Sand Bodies: Sequence Stratigraphic Analysis and Sedimentological Interpretation, SEPM Special Publication, vol. 64, pp. 127–146.
Cattaneo, A., Correggiari, A., Langone, L., Trincardi, F., 2003. The late-Holocene Gargano subaqueous delta, Adriatic shelf: sediment pathways and supply fluctuations. Mar. Geol. 193, 61–91.
Cattaneo, A., Trincardi, F., Asioli, A., Correggiari, A., 2007. The Western Adriatic shelf clinoform: energy-limited bottomset. Cont. Shelf Res. 27, 506–525. https://doi.org/10.1016/j.csr.2006.11.013.
Catuneanu, O., 2019. Scale in sequence stratigraphy. Mar. Pet. Geol. 106, 128–159. https://doi.org/10.1016/j.marpetgeo.2019.04.026.
Catuneanu, O., Abreu, V., Bhattacharya, J.P., Blum, M.D., Dalrymple, R.W., Eriksson, P. G., Fielding, C.R., Fisher, W.L., Galloway, W.E., Gibling, M.R., Giles, K.A., Holbrook, J.M., Jordan, R., Kendall, C.G.S.C., Macurda, B., Martinsen, O.J., Miall, A. D., Neal, J.E., Nummedal, D., Pomar, L., Posamentier, H.W., Pratt, B.R., Sarg, J.F., Shanley, K.W., Steel, R.J., Strasser, A., Tucker, M.E., Winker, C., 2009. Towards the standardization of sequence stratigraphy. Earth-Sci. Rev. 92, 1–33. https://doi.org/10.1016/j.earscirev.2008.10.003.
Cavallina, C., Bergamasco, A., Cosma, M., Da Lio, C., Donnici, S., Tang, C., Tosi, L., Zaggia, L., 2022. Morpho-Sedimentary Constraints in the Groundwater Dynamics of Low-Lying Coastal Area: the Southern margin of the Venice Lagoon, Italy. Water (Switzerland) 14. https://doi.org/10.3390/w14172717.
Channell, J.E.T., Poli, M.S., Rio, D., Sprovieri, R., Villa, G., 1994. Magnetic stratigraphy and biostratigraphy of Pliocene "argille azzurre"(Northern Apennines, Italy). Palaeogeogr. Palaeoclimatol. Palaeoecol. 110, 83–102.
Ciabatti, M., Curzi, P.V., Ricci Lucchi, F., 1987. Quaternary sedimentation in the Central Adriatic Sea. G. Geol. 49, 113–125.
Clark, P.U., Dyke, A.S., Shakun, J.D., Carlson, A.E., Clark, J., Wohlfarth, B., Mitrovica, J. X., Hostetler, S.W., McCabe, A.M., 2009. The last glacial maximum. Science 325, 710–714. https://doi.org/10.1126/science.1172873.
Colantoni, P., Gallignani, P., Lenaz, R., 1979. Late Pleistocene and Holocene evolution of the North Adriatic continental shelf (Italy). Mar. Geol. 33, M41–M50.
Collinson, J.D., 1996. Alluvial sediments. In: Reading, H.G. (Ed.), Sedimentary Environments: Processes, Facies, Stratigraphy, 3rd ed. Blackwell Science, Oxford, pp. 37–82.
Colombera, L., Mountney, N.P., McCaffrey, W.D., 2013. A quantitative approach to fluvial facies models: Methods and example results. Sedimentology 60 (6), 1526–1558.
Conti, A., Stefanon, A., Zuppi, G.M., 2002. Gas seeps and rock formation in the northern Adriatic Sea. Cont. Shelf Res. 22, 2333–2344.
Conway, A.M., Valvatne, C., 2003. The Murdoch Gas Field, Block 44/22a, UK Southern North Sea. Geol. Soc. Lond. Mem. 20 (1), 789–798.
Correggiari, A., Trincardi, F., Roveri, M., 1992. Regressioni «forzate», regressioni «deposizionali» e fenomeni di instabilità 1n unità progradazionali tardo-quaternarie (Adriatico centrale). G. Geol. 54, 19–36.
Correggiari, A., Roveri, M., Trincardi, F., 1996a. Late pleistocene and holocene evolution of the North Adriatic Sea. Alp. Mediterr. Quat. 9, 697–704.
Correggiari, A., Field, M.E., Trincardi, F., 1996b. Late Quaternary transgressive large dunes on the sediment-starved Adriatic shelf. In: De Batist, M., Jacobs, P. (Eds.), Geology of Siliciclastic Shelf Seas, Geological Society Special Publication, vol. 117, pp. 155–169.
Correggiari, A., Trincardi, F., Langone, L., Roveri, M., 2001. Styles of failure in late holocene highstand prodelta wedges on the adriatic shelf. J. Sediment. Res. 71, 218–236. https://doi.org/10.1306/042800710218.
Correggiari, A., Cattaneo, A., Trincardi, F., 2005a. Depositional patterns in the late Holocene Po delta system. In: Giosan, L., Bhattacharya, J.P. (Eds.), River Deltas–Concepts, Models, and Examples. Special Publications of SEPM, pp. 13–30.
Correggiari, A., Cattaneo, A., Trincardi, F., 2005b. The modern Po Delta system : Lobe switching and asymmetric prodelta growth. Mar. Geol. 223, 49–74. https://doi.org/10.1016/j.margeo.2005.06.039.
Crescenti, U., D'amato, C., 1980. Il Plio-Pleistocene del sottosuolo abruzzese-marchigiano tra Ascoli Piceno e Pescara.
Curzi, P.V., Veggiani, A., 1985. I pockmarks nel mare Adriatico centrale. Acta Nat. l'Ateneo Parm. 21, 79–89.
Curzi, P.V., Tonni, L., Gottardi, G., Mandanici, E., 2017. High resolution sedimentological and geotechnical characterization of the late Quaternary deposits in the Italian central Adriatic coast (Tronto River mouth). Eng. Geol. 220, 219–233. https://doi.org/10.1016/j.enggeo.2017.02.007.
Custodio, E., 2002. Aquifer overexploitation: what does it mean? Hydrogeol. J. 10 (2), 254–277. https://doi.org/10.1007/s10040-002-0188-6.
Dalla Valle, G., Gamberi, F., Trincardi, F., Baglioni, L., Errera, A., Rocchini, P., 2013. Contrasting slope channel styles on a prograding mud-prone margin. Mar. Pet. Geol. 41, 72–82. https://doi.org/10.1016/j.marpetgeo.2012.02.003.
De Santis, V., Caldara, M., 2016. Evolution of an incised valley system in the southern Adriatic Sea (Apulian margin): an onshore–offshore correlation. Geol. J. 51, 263–284.
De Santis, V., Caldara, M., Pennetta, L., 2020a. Transgressive architecture of coastal barrier systems in the ofanto incised valley and its surrounding shelf in response to stepped sea-level rise. Geoscience 10, 1–27. https://doi.org/10.3390/geosciences10120497.
De Santis, V., Caldara, M., Pennetta, L., 2020b. "Continuous" backstepping of Holocene coastal barrier systems into incised valleys: Insights from the Ofanto and Carapelle-Cervaro valleys. Water (Switzerland) 12. https://doi.org/10.3390/w12061799.
Della Seta, M., Del Monte, M., Fredi, P., Miccadei, E., Nesci, O., Pambianchi, G., Piacentini, T., Troiani, F., 2008. Morphotectonic evolution of the Adriatic piedmont of the Apennines: an advancement in the knowledge of the Marche-Abruzzo border area. Geomorphology 102, 119–129. https://doi.org/10.1016/j.geomorph.2007.06.018.
Deramond, J., Souquet, P., Fondecave-Wallez, M.-J., Specht, M., 1993. Relationships between thrust tectonics and sequence stratigraphy surfaces in foredeeps: model and examples from the Pyrenees (Cretaceous-Eocene, France, Spain). Geol. Soc. London Spec. Publ. 71, 193–219.
Desiderio, G., Nanni, T., Rusi, S., 2003. La pianura del fiume Vomano (Abruzzo); idrogeologia, antropizzazione e suoi effetti sul depauperamento della falda. Boll. Della Soc. Geol. Ital. 122, 421–434.
Desiderio, G., Ferracuti, L., Rusi, S., 2007. Structural-stratigraphic setting of middle Adriatic alluvial plains and its control on quantitative and qualitative groundwater circulation. In: Memorie Descrittive Della Carta Geologica d'Italia, pp. 147–162.
Di Martino, A., Sgattoni, G., Di Paola, G., Berti, M., Amorosi, A., 2023. Reconstructing late Quaternary paleovalley systems of Italy through mHVSR: a tool for seismic hazard assessment in modern coastal lowlands. Earth and Space. Science 10 (12) e2023EA003112.
Doglioni, C., 1993. Some remarks on the origin of foredeeps. Tectonophysics 228, 1–20.
Elmi, C., Forti, P., Nesci, O., Savelli, D., 2003. La risposta dei processi geomorfologici alle variazioni ambientali nella pianura padana e veneto friulana, nelle pianure minori e sulle coste nord e centro adriatiche. In: Biancotti, A., Motta, M. (Eds.), La risposta dei processi geomorfologici alle variazioni ambientali, pp. 225–259. MURST Report.
Embry, A.F., Johannessen, E.P., 2017. Two approaches to sequence stratigraphy. In: Stratigraphy & Timescales, vol. 2. Academic Press, pp. 85–118.
Evans, R.L., 2007. Using CSEM techniques to map the shallow section of seafloor: from the coastline to the edges of the continental slope. Geophysics 72, WA105–WA116.
Evans, R.L., Lizarralde, D., 2011. The competing impacts of geology and groundwater on electrical resistivity around Wrightsville Beach, NC. Cont. Shelf Res. 31, 841–848.
Fanucci, F., Moretti, E., Nesci, O., Savelli, D., Veneri, F., 1996. Tipologia dei terrazzi vallivi ed evoluzione del rilievo nel versante adriatico dell'Appennino centro-settentrionale. Il Quaternario 9, 255–258.
Farabollini, P., 1999. Il ruolo delle acque correnti superficiali: esempi dall'area della Montagna dei Fiori (TE). In: Farabollini, P. (Ed.), Workshop Nazionale sulle acque — Il ciclo dell'acqua: problemi e prospettive, Studi Geologici Camerti Volume Speciale, pp. 93–102.

Farrell, K.M., 2001. Geomorphology, facies architecture, and high-resolution, non-marine sequence stratigraphy in avulsion deposits, Cumberland Marshes, Saskatchewan. Sediment. Geol. 139 (2), 93–150.
Ferretti, M., Moretti, E., Savelli, D., Stefanon, A., Tramontana, M., Wezel, D.C., 1986. Late Quaternary alluvial sequences in the North-Western Adriatic Sea from Uniboom profiles. Boll. Oceanol. Teor. Appl. 4, 63–72.
Florineth, D., Schlüchter, C., 1998. Reconstructing the last Glacial Maximum (LGM) ice surface geometry and flowlines in the Central Swiss Alps. Eclogae Geol. Helv. 91, 391–407.
Franzini, M., Leoni, L., Saitta, M., 1972. A simple method to evaluate the matrix effects in X-Ray fluorescence analysis. X-Ray Spectrom. 1, 151–154.
Friedrichs, C.T., Scully, M.E., 2007. Modeling deposition by wave-supported gravity flows on the Po River prodelta: from seasonal floods to prograding clinoforms. Cont. Shelf Res. 27, 322–337. https://doi.org/10.1016/j.csr.2006.11.002.
Frignani, M., Langone, L., Ravaioli, M., Sorgente, D., Alvisi, F., Albertazzi, S., 2005. Fine-sediment mass balance in the western Adriatic continental shelf over a century time scale. Mar. Geol. 222–223, 113–133. https://doi.org/10.1016/j.margeo.2005.06.016.
Galloway, W.E., 1989. Genetic stratigraphic sequences in basin analysis, I. Architecture and genesis of flooding-surface bounded depositional units. Am. Assoc. Pet. Geol. Bull. 73, 125–142.
Galloway, W.E., Garber, J.L., Liu, X., Sloan, B.J., 1993. Sequence stratigraphic and depositional framework of the Cenozoic fill, Central and Northern North Sea Basin. In: Geological Society, London. Petroleum Geology Conference Series. The Geological Society of London, pp. 33–43.
Gamberi, F., Pellegrini, C., Dalla Valle, G., Scarponi, D., Bohacs, K., Trincardi, F., 2020. Compound and hybrid clinothems of the last lowstand Mid-Adriatic deep: Processes, depositional environments, controls and implications for stratigraphic analysis of prograding systems. Basin Res. 32, 363–377. https://doi.org/10.1111/bre.12417.
Garzanti, E., Andò, S., Vezzoli, G., 2009. Grain-size dependence of sediment composition and environmental bias in provenance studies. Earth Planet. Sci. Lett. 277, 422–432.
Gawthorpe, R.L., Fraser, A.J., Collier, R.E.L., 1994. Sequence stratigraphy in active extensional basins: implications for the interpretation of ancient basin-fills. Mar. Pet. Geol. 11, 642–658.
Gawthorpe, R.L., Sharp, I., Underhill, J.R., Gupta, S., 1997. Linked sequence stratigraphic and structural evolution of propagating normal faults. Geology 25, 795–798.
Geach, M.R., Stokes, M., Telfer, M.W., Mather, A.E., Fyfe, R.M., Lewin, S., 2014. The application of geospatial interpolation methods in the reconstruction of Quaternary landform records. Geomorphology 216, 234–246. https://doi.org/10.1016/j.geomorph.2014.03.036.
Geletti, R., Del Ben, A., Busetti, M., Ramella, R., Volpi, V., 2008. Gas seeps linked to salt structures in the Central Adriatic Sea. Basin Res. 20, 473–487.
Geological Map of Italy at 1:50,000 scale, 2024a. Geological Survey of Italy and CARG Project. Sheet: 268. https://www.isprambiente.gov.it/Media/carg/note_illustrative/268_Pesaro.pdf.
Geological Map of Italy at 1:50,000 scale, 2024b. Geological Survey of Italy and CARG Project. Sheet: 281. https://www.isprambiente.gov.it/Media/carg/note_illustrative/281_Senigallia.pdf.
Geological Map of Italy at 1:50,000 scale, 2024c. Geological Survey of Italy and CARG Project. Sheet: 282. https://www.isprambiente.gov.it/Media/carg/note_illustrative/282_Ancona.pdf.
Geological Map of Italy at 1:50,000 scale, 2024d. Geological Survey of Italy and CARG Project. Sheet: 293. https://www.isprambiente.gov.it/Media/carg/note_illustrative/293_Osimo.pdf.
Geological Map of Italy at 1:50,000 scale, 2024e. Geological Survey of Italy and CARG Project. Sheet: 304. https://www.isprambiente.gov.it/Media/carg/note_illustrative/304_Civitanova_Marche.pdf.
Geological Map of Italy at 1:50,000 scale, 2024f. Geological Survey of Italy and CARG Project. Sheet: 339. https://www.isprambiente.gov.it/Media/carg/note_illustrative/339_Teramo.pdf.
Geological Map of Italy at 1:50,000 scale, 2024g. Geological Survey of Italy and CARG Project. Sheet: 360. https://www.isprambiente.gov.it/Media/carg/note_illustrative/360_TorredePasseri.pdf.
Geological Map of Italy at 1:50,000 scale, 2024h. Geological Survey of Italy and CARG Project. Sheet: 361. https://www.isprambiente.gov.it/Media/carg/note_illustrative/361_Chieti.pdf.
Geological Map of Italy at 1:50,000 scale, 2024i. Geological Survey of Italy and CARG Project. Sheet: 372. https://www.isprambiente.gov.it/Media/carg/note_illustrative/372_Vasto.pdf.
Ghazi, S., Mountney, N.P., 2009. Facies and architectural element analysis of a meandering fluvial succession: the Permian Warchha Sandstone, Salt Range, Pakistan. Sediment. Geol. 221 (1–4), 99–126.
Giambastiani, B.M.S., Kidanemariam, A., Dagnew, A., Antonellini, M., 2021. Evolution of salinity and water table level of the phreatic coastal aquifer of the Emilia Romagna region (Italy). Water 13 (3), 372.
Gibling, M.R., Bird, D.J., 1994. Late Carboniferous cyclothems and alluvial paleovalleys in the Sydney Basin, Nova Scotia. Geol. Soc. Am. Bull. 106 (1), 105–117.
Gibling, M.R., Wightman, W.G., 1994. Palaeovalleys and protozoan assemblages in a late Carboniferous cyclothem, Sydney Basin, Nova Scotia. Sedimentology 41 (4), 699–719.
Gibling, M.R., Fielding, C.R., Sinha, R., 2011. Alluvial valleys and alluvial sequences: Towards a geomorphic assessment. In: Davidson, S.K., Leleu, S., North, C.P. (Eds.), From River to Rock Record: The Preservation of Fluvial Sediments and their Subsequent Interpretation, SEPM Society for Sedimentary Geology Special Publication, vol. 97, pp. 423–447.
Giraudi, C., 2017. Climate evolution and forcing during the last 40 ka from the oscillations in Apennine glaciers and high mountain lakes, Italy. J. Quat. Sci. 32, 1085–1098. https://doi.org/10.1002/jqs.2985.
Goodbred, S.L., 2003. Response of the Ganges dispersal system to climate change: a source-to-sink view since the last interstade. Sediment. Geol. 162, 83–104. https://doi.org/10.1016/S0037-0738(03)00217-3.
Gordini, E., Donda, F., Tosi, L., Alessandro, B., Andrea, B., Donnici, S., 2023. The role of methane seepage in the formation of the Northern Adriatic Sea geosites. Mar. Geol. 107081.
Grano, M., Di Giuseppe, R., 2021. I molluschi terrestri e dulciacquicoli (Mollusca : gastropoda, Bivalvia) di Castel di Guido (Lazio, Italia centrale). Boll. Mus. Reg. Sci. Nat. Torino 38, 149–168.
Gustafson, C., Key, K., Evans, R.L., 2019. Aquifer systems extending far offshore on the U. S. Atlantic Margin. Sci. Rep 1–10. https://doi.org/10.1038/s41598-019-44611-7.
Haroon, A., Lippert, K., Mogilatov, V., Tezkan, B., 2018. First application of the marine differential electric dipole for groundwater investigations: a case study from Bat Yam, Israel. Geophysics 83, B59–B76.
Haroon, A., Micallef, A., Jegen, M., Schwalenberg, K., Karstens, J., Berndt, C., Garcia, X., Kühn, M., Rizzo, E., Fusi, N.C., 2021. Electrical resistivity anomalies offshore a carbonate coastline: evidence for freshened groundwater? Geophys. Res. Lett. 48 e2020GL091909.
Harris, C.K., Sherwood, C.R., Signell, R.P., Bever, A.J., Warner, J.C., 2008. Sediment dispersal in the northwestern Adriatic Sea. J. Geophys. Res. Ocean 113.
Hathaway, J.C., Schlee, J.J., Poag, C.W., Valentine, P.C., Weed, E.G.A., Bothner, M.H., Kohout, F.A., Manheim, F.T., Schloam, R., Miller, R.E., 1976. Preliminary Summary of the 1976 Atlantic Margin Coring Project of the US Geological Survey. US Geological Survey.
Hathaway, J.C., Poag, C.W., Valentine, P.C., Manheim, F.T., Kohout, F.A., Bothner, M.H., Miller, R.E., Schultz, D.M., Sangray, D.A., 1979. US Geological Survey Core Drilling on the Atlantic Shelf: Geologic data were obtained at drill-core sites along the eastern US continental shelf and slope. Science 206 (4418), 515–527. https://doi.org/10.1126/science.206.4418.515.
Helland-Hansen, W., Gjelberg, J.G., 1994. Conceptual basis and variability in sequence stratigraphy: a different perspective. Sediment. Geol. 92 (1–2), 31–52.
Helland-Hansen, W., Martinsen, O.J., 1996. Shoreline trajectories and sequences: description of variable depositional-dip scenarios. J. Sediment. Res. 66 (4), 670–688.
Helland-Hansen, W., Sømme, T.O., Martinsen, O.J., Lunt, I., Thurmond, J., 2016. Deciphering earth's natural hourglasses: Perspectives on source-to-sink analysis. J. Sediment. Res. 86, 1008–1033. https://doi.org/10.2110/jsr.2016.56.
Houben, G.J., Stoeckl, L., Mariner, K.E., Choudhury, A.S., 2018. The influence of heterogeneity on coastal groundwater flow - physical and numerical modeling of fringing reefs, dykes and structured conductivity fields. Adv. Water Resour. 113, 155–166. https://doi.org/10.1016/j.advwatres.2017.11.024.
Hovland, M., Curzi, P.V., 1989. Gas seepage and assumed mud diapirism in the Italian Central Adriatic Sea. Mar. Pet. Geol. 6, 161–169.
Hunt, D., Tucker, M.E., 1992. Stranded parasequences and the forced regressive wedge systems tract: deposition during base-level fall. Sediment. Geol. 81, 1–9.
Ivy-Ochs, S., Monegato, G., Reitner, J.M., 2022. The Alps: glacial landforms from the last Glacial Maximum. Eur. Glacial Landsc. 449–460 https://doi.org/10.1016/b978-0-12-823498-3.00030-3.
Jervey, M.T., 1988. Quantitative geological modelling of siliciclastic rock sequences and their seismic expression. In: Wilgus, C.K., Hastings, B.S., Kendall, C.G.S.C., Posamentier, H.W., Ross, C.A., Van Wagoner, J.C. (Eds.), Sea Level Changes — An Integrated Approach, Special Publication, vol. 42. Society of Economic Paleontologists and Mineralogists (SEPM), pp. 47–69.
Judd, A., Hovland, M., 2007. Seabed Fluid Flow. Cambridge University Press, Cambridge (475p).
Kasse, C., Vandenberghe, J., Bohncke, S.J.P., 1995. Climatic change and fluvial dynamics of the Maas during the late Weichselian and early Holocene. Paläoklimaforschung 14.
Kelly, S., 2006. Scaling and hierarchy in braided rivers and their deposits: examples and implications for reservoir modelling. In: Braided Rivers: Process, Deposits, Ecology and Management, 36, pp. 75–106.
Kettner, A.J., Syvitski, J.P.M., 2008. HydroTrend v. 3.0: a climate-driven hydrological transport model that simulates discharge and sediment load leaving a river system. Comput. Geosci. 34, 1170–1183.
Kozarski, S., 1991. Warta, a case study of a lowland river. In: Starkel, L., Gregory, K.J., Thornes, J.B. (Eds.), Temperate Palaeohydrology. Wiley, Chichester, pp. 189–215.
La Croix, A.D., Wang, J., He, J., Hannaford, C., Bianchi, V., Esterle, J., Undershultz, J.R., 2019. Widespread nearshore and shallow marine deposition within the lower Jurassic Precipice Sandstone and Evergreen Formation in the Surat Basin, Australia. Mar. Pet. Geol. 109, 760–790.
Laceby, J.P., Evrard, O., Smith, H.G., Blake, W.H., Olley, J.M., Minella, J.P.G., Owens, P. N., 2017. The challenges and opportunities of addressing particle size effects in sediment source fingerprinting: a review. Earth-Sci. Rev. 169, 85–103.
Lambeck, K., Rouby, H., Purcell, A., Sun, Y., Sambridge, M., 2014. Sea level and global ice volumes from the last Glacial Maximum to the Holocene. Proc. Natl. Acad. Sci. 111, 15296–15303.
Leigh, D.S., Srivastava, P., Brook, G.A., 2004. Late Pleistocene braided rivers of the Atlantic Coastal Plain, USA. Quat. Sci. Rev. 23, 65–84. https://doi.org/10.1016/S0277-3791(03)00221-X.
Leoni, L., Saitta, M., 1976. X-ray fluorescence analysis of 29 trace elements in rock and mineral standards. Rend. Soc. It. Miner. Pet. 32, 497–510.
Leoni, L., Menichini, M., Saitta, M., 1982. Determination of S, Cl and F in silicate rocks by X-Ray fluorescence analyses. X-Ray Spectrom. 11, 156–158.

Lericolais, G., Berne, S., Fenies, H., 2001. Seaward pinch out and internal stratigraphy of the Gironde incised valley on the shelf (Bay of Biscay). Mar. Geol. 175, 183–197.
Li, X., Hu, B.X., Tong, J., 2016. Numerical study on tide-driven submarine groundwater discharge and seawater recirculation in heterogeneous aquifers. Stoch. Env. Res. Risk A. 30, 1741–1755. https://doi.org/10.1007/s00477-015-1200-8.
Lipparini, L., Chiacchieri, D., Bencini, R., Micallef, A., 2023. Extensive freshened groundwater resources emplaced during the Messinian Sea-level drawdown in southern Sicily, Italy. Commun. Earth Environ. 4 (1), 430.
Lisiecki, L.E., Raymo, M.E., 2005. A Pliocene-Pleistocene stack of 57 globally distributed benthic δ18O records. Paleoceanography 20 (1).
Lofi, J., Inwood, J., Proust, J.-N., Monteverde, D.H., Loggia, D., Basile, C., Otsuka, H., Hayashi, T., Stadler, S., Mottl, M.J., 2013. Fresh-water and salt-water distribution in passive margin sediments: Insights from Integrated Ocean Drilling Program Expedition 313 on the New Jersey Margin. Geosphere 9, 1009–1024.
Longhitano, S.G., Della Luna, R., Milone, A.L., Cilumbriello, A., Caffau, M., Spilotro, G., 2016. The 20,000-years-long sedimentary record of the Lesina coastal system (southern Italy): from alluvial, to tidal, to wave process regime change. Holocene 26, 678–698. https://doi.org/10.1177/0959683615618256.
Lucchini, F., Dinelli, E., Mordenti, A., 2003. Geochemical records of palaeoenvironmental changes during late Quaternary in the Adriatic Sea sediments. GeoActa 2, 43–62.
Maliva, R.G., 2016. Aquifer Characterization Techniques, Aquifer Characterization. Springer Hydrogeology, Berlin. https://doi.org/10.2110/pec.04.80.
Maselli, V., Trincardi, F., Cattaneo, A., Ridente, D., Asioli, A., 2010. Subsidence pattern in the central Adriatic and its influence on sediment architecture during the last 400 kyr. J. Geophys. Res. Solid Earth 115, 1–23. https://doi.org/10.1029/2010JB007687.
Maselli, V., Hutton, E.W., Kettner, A.J., Syvitski, J.P.M., Trincardi, F., 2011. High-frequency Sea level and sediment supply fluctuations during termination I: an integrated sequence-stratigraphy and modeling approach from the Adriatic Sea (Central Mediterranean). Mar. Geol. 287, 54–70. https://doi.org/10.1016/j.margeo.2011.06.012.
McCarthy, P.J., Guy Plint, A., 1998. Recognition of interfluve sequence boundaries: integrating paleopedology and sequence stratigraphy. Geology 26 (5), 387–390.
McCarthy, P.J., Faccini, U.F., Plint, A.G., 1999. Evolution of an ancient coastal plain: palaeosols, interfluves and alluvial architecture in a sequence stratigraphic framework, Cenomanian Dunvegan Formation, NE British Columbia, Canada. Sedimentology 46 (5), 861–891.
Meade, R.H., 1972. Transport and deposition of sediments in estuaries. Geol. Soc. Am. Mem. 133, 91–120.
Meade, R.H., 1982. Sources, Sinks, and Storage of River Sediment in the Atlantic Drainage of the United States. J. Geol. 90 (3), 235–252.
Miall, A.D., 1977. A review of the braided-river depositional environment. Earth Sci. Rev. 13 (1), 1–62.
Miall, A.D., 1986. Eustatic sea-level change interpreted from seismic stratigraphy: a critique of the methodology with particular reference to the North Sea Jurassic record. Am. Assoc. Pet. Geol. Bull. 70, 131–137.
Miall, A.D., 1988. Reservoir heterogeneities in fluvial sandstones: lessons from outcrop studies. AAPG bulletin 72 (6), 682–697.
Miall, A.D., 1992a. The Exxon global cycle chart: an event for every occasion? Geology 20, 787–790.
Miall, A.D., 1992b. Alluvial deposits. In: Walker, R.G., James, N.P. (Eds.), Facies Models: Response to Sea Level Change. Geological Association of Canada, Waterloo, Ontario, pp. 119–139.
Miall, A.D., 2013. The Geology of Fluvial Deposits: Sedimentary Facies, Basin Analysis, and Petroleum Geology. Springer.
Micallef, A., Person, M., Haroon, A., Weymer, B.A., Jegen, M., Schwalenberg, K., Faghih, Z., Duan, S., Cohen, D., Mountjoy, J.J., 2020. 3D characterisation and quantification of an offshore freshened groundwater system in the Canterbury Bight. Nat. Commun. 11, 1372.
Micallef, A., Person, M., Berndt, C., Bertoni, C., Cohen, D., Dugan, B., Evans, R., Haroon, A., Hensen, C., Jegen, M., 2021. Offshore freshened groundwater in continental margins. Rev. Geophys. 59 e2020RG000706.
Michael, H.A., Scott, K.C., Koneshloo, M., Yu, X., Khan, M.R., Li, K., 2016. Geologic influence on groundwater salinity drives large seawater circulation through the continental shelf. Geophys. Res. Lett. 43, 10–782.
Milliman, J.D., Syvitski, J.P.M., 1992. Geomorphic/tectonic control of sediment discharge to the ocean: the importance of small mountainous rivers. J. Geol. 100, 525–544.
Mitchum, R.M., 1977. Seismic stratigraphy and global changes of sea level, part 11: Glossary of terms used in seismic stratigraphy. In: Payton, C.E. (Ed.), Seismic Stratigraphy—Applications to Hydrocarbon Exploration. Memoir, vol. 26. American Association of Petroleum Geologists, pp. 205–212.
Mitchum, R.M., Van Wagoner, J.C., 1991. High-frequency sequences and their stacking patterns: sequence-stratigraphic evidence of high-frequency eustatic cycles. Sediment. Geol. 70, 131–160.
Molinari, F.C., Boldrini, G., Severi, P., Dugoni, G., Rapti Caputo, D., Martinelli, G., 2007. Risorse Idriche Sotterranee Della Provincia di Ferrara (in Italian; Transl. Groundwater Resources of the Ferrara Province). DB-MAP printer, Florence, Italy, pp. 1–62.
Monegato, G., Ravazzi, C., Donegana, M., Pini, R., Calderoni, G., Wick, L., 2007. Evidence of a two-fold glacial advance during the last glacial maximum in the Tagliamento end moraine system (eastern Alps). Quat. Res. 68, 284–302. https://doi.org/10.1016/j.yqres.2007.07.002.
Morelli, A., Bruno, L., Cleveland, D.M., Drexler, T.M., Amorosi, A., 2017. Reconstructing last Glacial Maximum and Younger Dryas paleolandscapes through subsurface paleosol stratigraphy: an example from the Po coastal plain, Italy. Geomorphology 295, 790–800. https://doi.org/10.1016/j.geomorph.2017.08.013.
Moscon, G., Correggiari, A., Stefani, C., Fontana, A., Remia, A., 2015. Very-high resolution analysis of a transgressive deposit in the Northern Adriatic Sea (Italy). Alpine Mediterranean Quat. 28 (2), 121–129.
Mountain, G.S., Proust, J.N., McInroy, D., 2009. New Jersey Shallow Shelf: Shallow-Water Drilling of the New Jersey Continental Shelf: global sea Level and Achitecture of Passive Margin Sediments.
Mulder, T., Syvitski, J.P.M., 1996. Climatic and morphologic relationships of rivers: implications of sea-level fluctuations on river loads. J. Geol. 104, 509–523.
Muller, R., Nystuen, J.P., Wright, V.P., 2004. Pedogenic mud aggregates and paleosol development in ancient dryland river systems: criteria for interpreting alluvial mudrock origin and floodplain dynamics. J. Sediment. Res. 74 (4), 537–551.
Müller, H., von Dobeneck, T., Nehmiz, W., Hamer, K., 2011. Near-surface electromagnetic, rock magnetic, and geochemical fingerprinting of submarine freshwater seepage at Eckernförde Bay (SW Baltic Sea). Geo-Marine Lett. 31, 123–140.
Mulligan, A.E., Evans, R.L., Lizarralde, D., 2007. The role of paleochannels in groundwater/seawater exchange. J. Hydrol. 335, 313–329.
Muto, T., Steel, R.J., 1997. Principles of regression and transgression: the nature of the interplay between accommodation and sediment supply. J. Sediment. Res. Sect. B Stratigr. Glob. Stud. 67, 994–1000. https://doi.org/10.1306/d42686a8-2b26-11d7-8648000102c1865d.
Nanni, T., Vivalda, P., 2005. The aquifers of the Umbria-Marche Adriatic region: Relationships between structural setting and groundwater chemistry. Boll. Della Soc. Geol. Ital. 124, 523–542.
Neal, J., Abreu, V., 2009. Sequence stratigraphy hierarchy and the accommodation succession method. Geology 37, 779–782. https://doi.org/10.1130/G25722A.1.
Neal, J.E., Abreu, V., Bohacs, K.M., Feldman, H.R., Pederson, K.H., 2016. Accommodation succession (δA/δS) sequence stratigraphy: Observational method, utility and insights into sequence boundary formation. J. Geol. Soc. Lond. 173, 803–816. https://doi.org/10.1144/jgs2015-165.
Nesci, O., Savelli, D., Mengarelli, D., 1990. I terrazzi vallivi del 1° ordine nei bacini dei fiumi Foglia e Metauro (Appennino Marchigiano). Geogr. Fis. Din. Quat. 13, 63–73.
Nittrouer, C.A., Miserocchi, S., Trincardi, F., 2004. 2004: the PASTA project: investigation of Po and Apennine sediment transport and accumulation. Oceanography 17, 46–57.
Oldfield, F., Asioli, A., Accorsi, C.A., Mercuri, A.M., Juggins, S., Langone, L., Rolph, T., Trincardi, F., Wolff, G., Gibbs, Z., 2003. A high resolution late Holocene palaeo environmental record from the Central Adriatic Sea. Quat. Sci. Rev. 22, 319–342.
Ori, G.G., Roveri, M., Vannoni, F., 1986. Plio-Pleistocene sedimentation in the Apenninic-Adriatic foredeep (Central Adriatic Sea, Italy). In: Allen, P.A., Homewood, P. (Eds.), Foreland Basins, Spec. Publ. Int. Assoc. Sediment, vol. 8, pp. 183–198.
Paldor, A., Katz, O., Aharonov, E., Weinstein, Y., Roditi-Elasar, M., Lazar, A., Lazar, B., 2020. Deep submarine groundwater discharge—evidence from Achziv submarine canyon at the exposure of the Judea group confined aquifer, Eastern Mediterranean. J. Geophys. Res. Ocean 125 e2019JC015435.
Palinkas, C.M., Nittrouer, C.A., Wheatcroft, R.A., Langone, L., 2005. The use of 7Be to identify event and seasonal sedimentation near the Po River delta, Adriatic Sea. In: Marine Geology, pp. 95–112. https://doi.org/10.1016/j.margeo.2005.06.011.
Palmucci, W., Rusi, S., Di Curzio, D., 2016. Mobilisation processes responsible for iron and manganese contamination of groundwater in Central Adriatic Italy. Environ. Sci. Pollut. Res. 23, 11790–11805. https://doi.org/10.1007/s11356-016-6371-4.
Panda, S., Kumar, A., Srivastava, P., Das, S., Jayangondaperumal, R., Prakash, K., 2022. Deciphering the role of late Quaternary sea level fluctuations in controlling the sedimentation in the Brahmaputra Plains. Sediment. Geol. 442, 106289.
Parlagreco, L., Mascioli, F., Miccadei, E., Antonioli, F., Gianolla, D., Devoti, S., Leoni, G., Silenzi, S., 2011. New data on Holocene relative sea level along the Abruzzo coast (central Adriatic, Italy). Quat. Int. 232, 179–186. https://doi.org/10.1016/j.quaint.2010.07.021.
Payenberg, T.H.D., Willis, B.J., Sixsmith, P., Connell, S.D., Powell, A., Milliken, K.T., Posamentier, H.W., Allgoewer, A., Meyers, E., Marsh, T., Sullivan, M.D., Lang, S.C., Fowler, J., Welch, R., Howe, H., Ainsworth, R.B., 2024. Quantification and classification of a giant fluvial-distributive system - the Triassic Mungaroo Formation, NWS, Australia. Earth Sci. Rev. 249, 104676. ISSN 0012-8252. https://doi.org/10.1016/j.earscirev.2024.104676.
Payton, C.E. (Ed.), 1977. AAPG Mem. 26 (516pp).
Pellegrini, C., Maselli, V., Cattaneo, A., Piva, A., Ceregato, A., Trincardi, F., 2015. Anatomy of a compound delta from the post-glacial transgressive record in the Adriatic Sea. Mar. Geol. 362, 43–59.
Pellegrini, C., Maselli, V., Trincardi, F., 2016. Pliocene–Quaternary contourite depositional system along the south-western Adriatic margin: changes in sedimentary stacking pattern and associated bottom currents. Geo-Mar. Lett. 36, 67–79.
Pellegrini, C., Maselli, V., Gamberi, F., Asioli, A., Bohacs, K.M., Drexler, T.M., Trincardi, F., 2017a. How to make a 350-m-thick lowstand systems tract in 17,000 years: the late Pleistocene Po River (Italy) lowstand wedge. Geology 45, 327–330. https://doi.org/10.1130/G38848.1.
Pellegrini, C., Bohacs, K.M., Drexler, T.M., Gamberi, F., Rovere, M., Trincardi, F., Hart, B., Rosen, N.C., West, D., D'Agostino, A., Messina, C., Hoffman, M., Wild, R., 2017b. Identifying the sequence boundary in over- and under-supplied contexts: The case of the late Pleistocene adriatic continental margin. In: Sequence Stratigraphy: The Future Defined, 0. SEPM Society for Sedimentary Geology.
Pellegrini, C., Asioli, A., Bohacs, K.M., Drexler, T.M., Feldman, H.R., Sweet, M.L., Maselli, V., Rovere, M., Gamberi, F., Valle, G.D., Trincardi, F., 2018. The late

Pleistocene Po River lowstand wedge in the Adriatic Sea: Controls on architecture variability and sediment partitioning. Mar. Pet. Geol. 96, 16–50. https://doi.org/10.1016/j.marpetgeo.2018.03.002.
Pellegrini, C., Tesi, T., Schieber, J., Bohacs, K.M., Rovere, M., Asioli, A., Nogarotto, A., Trincardi, F., 2021. Fate of terrigenous organic carbon in muddy clinothems on continental shelves revealed by stratal geometries: Insight from the Adriatic sedimentary archive. Glob. Planet. Chang. 203, 103539 https://doi.org/10.1016/j.gloplacha.2021.103539.
Pellegrini, C., Sammartino, I., Schieber, J., Tesi, T., Paladini de Mendoza, F., Rossi, V., Amorosi, A., 2024. On depositional processes governing along-strike facies variations of fine-grained deposits: Unlocking the Little Ice Age subaqueous clinothems on the Adriatic shelf. Sedimentology 71 (3), 941–973.
Picotti, V., Pazzaglia, F.J., 2008. A new active tectonic model for the construction of the Northern Apennines mountain front near Bologna (Italy). J. Geophys. Res. Solid Earth 113, 1–24. https://doi.org/10.1029/2007JB005307.
Pigorini, B., 1968. Sources and dispersion of recent sediments of the Adriatic Sea. Mar. Geol. 6, 187–229.
Piva, A., Asioli, A., Schneider, R.R., Trincardi, F., Andersen, N., Colmenero-Hidalgo, E., Dennielou, B., Flores, J.A., Vigliotti, L., 2008a. Climatic cycles as expressed in sediments of the PROMESSI borehole PRAD1-2, central Adriatic, for the last 370 ka: 1. Integrated stratigraphy. Geochem. Geophys. Geosyst. 9 https://doi.org/10.1029/2007GC001713.
Piva, A., Asioli, A., Trincardi, F., Schneider, R.R., Vigliotti, L., 2008b. Late-Holocene climate variability in the Adriatic Sea (Central Mediterranean). Holocene 18, 153–167. https://doi.org/10.1177/0959683607085606.
Plint, A.G., McCarthy, P.J., Faccini, U.F., 2001. Nonmarine sequence stratigraphy: updip expression of sequence boundaries and systems tracts in a high-resolution framework, Cenomanian Dunvegan Formation, Alberta foreland basin, Canada. AAPG Bull. 85 (11), 1967–2001.
Posamentier, H.W., Allen, G.P., 1999. Siliciclastic sequence stratigraphy. Concepts Appl. SEPM, Concepts Sedimentol. Paleontol. 7, 210.
Posamentier, H.W., Vail, P.R., 1988. Eustatic controls on clastic deposition II—sequence and systems tract models. In: Wilgus, C.K., Hastings, B.S., Kendal, C.G.C., Posamentier, H.W., Ross, C.A., Van Wagoner, J.C. (Eds.), Sea-Level Changes: An In-Tegrated Approach, Special Publications of SEPM, 42, pp. 125–154.
Posamentier, H.W., Weimer, P., 1993. Siliciclastic sequence stratigraphy and petroleum geology—where to from here? Am. Assoc. Pet. Geol. Bull. 77, 731–742.
Posamentier, H.W., Jervey, M.T., Vail, P.R., 1988. Eustatic controls on clastic deposition I—conceptual framework. In: Wilgus, C.K., Hastings, B.S., Kendal, C.G.C., Posamentier, H.W., Ross, C.A., Van Wagoner, J.C. (Eds.), Sea-Level Changes: An In-Tegrated Approach, Special Publications of SEPM, 42, pp. 109–124.
Post, V.E.A., Groen, J., Kooi, H., Person, M., Ge, S., Edmunds, W.M., 2013. Offshore fresh groundwater reserves as a global phenomenon. Nature 504, 71–78. https://doi.org/10.1038/nature12858.
Puig, P., Ogston, A.S., Guillen, J., Fain, A.M.V., Palanques, A., 2007. Sediment transport processes from the topset to the foreset of a crenulated clinoform (Adriatic Sea). Cont. Shelf Res. 27, 452–474. https://doi.org/10.1016/j.csr.2006.11.005.
Razum, I., Lužar-Oberiter, B., Zaccarini, F., Babić, L., Miko, S., Hasan, O., Ilijanić, N., Beqiraj, E., Pawlowsky-Glahn, V., 2021. New sediment provenance approach based on orthonormal log ratio transformation of geochemical and heavy mineral data: sources of eolian sands from the southeastern Adriatic archipelago. Chem. Geol. 583 https://doi.org/10.1016/j.chemgeo.2021.120451.
Reading, H.G., Richards, M., 1994. Turbidite systems in deep-water basin margins classified by grain size and feeder system. Am. Assoc. Pet. Geol. Bull. 78, 792–822. https://doi.org/10.1306/a25fe3bf-171b-11d7-8645000102c1865d.
Regione Emilia-Romagna, ENI-AGIP, 1998. In: Di Dio, G. (Ed.), Riserve Idriche Sotterranee Della Regione Emilia-Romagna. S.EL.CA., Firenze (120 pp.).
Ricci Lucchi, F., Colalongo, M.L., Cremonini, G., Gasperi, G., Iaccarino, S., Papani, G., Raffi, S., Rio, D., 1982. Evoluzione sedimentaria e paleogeografica nel margine appenninico. In: Cremonini, G., Ricci Lucchi, F. (Eds.), Guida Alla Geologia Del Margine Appenninico-Padano. Soc. Geol. It, pp. 17–46.
Ricci Lucchi, M., Fiorini, F., Colalongo, M.L., Curzi, P.V., 2006. Late-Quaternary paleoenvironmental evolution of Lesina lagoon (southern Italy) from subsurface data. Sediment. Geol. 183, 1–13. https://doi.org/10.1016/j.sedgeo.2005.09.003.
Ridente, D., Trincardi, F., 2002. Eustatic and tectonic control on deposition and lateral variability of Quaternary regressive sequences in the Adriatic basin (Italy). Mar. Geol. 184, 273–293.
Ridente, D., Trincardi, F., 2005. Pleistocene "muddy" forced-regression deposits on the Adriatic shelf: a comparison with prodelta deposits of the late Holocene highstand mud wedge. Mar. Geol. 222, 213–233.
Ridente, D., Trincardi, F., 2006. Active foreland deformation evidenced by shallow folds and faults affecting late Quaternary shelf–slope deposits (Adriatic Sea, Italy). Basin Res. 18, 171–188.
Ridente, D., Foglini, F., Minisini, D., Trincardi, F., Verdicchio, G., 2007. Shelf-edge erosion, sediment failure and inception of Bari Canyon on the Southwestern Adriatic margin (Central Mediterranean). Mar. Geol. 246, 193–207. https://doi.org/10.1016/j.margeo.2007.01.014.
Ridente, D., Trincardi, F., Piva, A., Asioli, A., Cattaneo, A., 2008. Sedimentary response to climate and sea level changes during the past ~400 ka from borehole PRAD1-2 (Adriatic margin). Geochem. Geophys. Geosyst. 9 https://doi.org/10.1029/2007GC001783.
Ridente, D., Trincardi, F., Piva, A., Asioli, A., 2009. The combined effect of sea level and supply during Milankovitch cyclicity: evidence from shallow-marine δ18O records and sequence architecture (Adriatic margin). Geology 37, 1003–1006.
Ronchi, L., Fontana, A., Correggiari, A., Asioli, A., 2018. Late Quaternary incised and infilled landforms in the shelf of the northern Adriatic Sea (Italy). Mar. Geol. 405, 47–67. https://doi.org/10.1016/j.margeo.2018.08.004.
Rossi, V., Horton, B.P., 2009. The application of a subtidal foraminifera-based transfer function to reconstruct Holocene paleobathymetry of the Po Delta, northern Adriatic Sea. J. Foraminiferal Res. 39 (3), 180–190.
Rossi, V., Vaiani, S.C., 2008. Benthic foraminiferal evidence of sediment supply changes and fluvial drainage reorganization in Holocene deposits of the Po Delta, Italy. Marine Micropaleont. 69 (2), 106–118.
Rossi, M., Minervini, M., Ghielmi, M., Rogledi, S., 2015. Messinian and Pliocene erosional surfaces in the Po Plain-Adriatic Basin: Insights from allostratigraphy and sequence stratigraphy in assessing play concepts related to accommodation and gateway turnarounds in tectonically active margins. Mar. Pet. Geol. 66, 192–216.
Rossi, V., Sammartino, I., Pellegrini, C., Barbieri, G., Teodoro, C., Trincardi, F., Amorosi, A., 2024. Coupling palaeobiology and geochemistry from the Holocene of the southern Adriatic Sea (Gulf of Manfredonia, Italy): Shelf facies patterns and eutrophication trends. Palaeogeogr. Palaeoclimatol. Palaeoecol. 639, 112055.
Rovere, M., Pellegrini, C., Chiggiato, J., Campiani, E., Trincardi, F., 2019. Impact of dense bottom water on a continental shelf: an example from the SW Adriatic margin. Mar. Geol. 408, 123–143.
Rovere, M., Mercorella, A., Frapiccini, E., Funari, V., Spagnoli, F., Pellegrini, C., Bonetti, A.S., Veneruso, T., Tassetti, A.N., Dell'Orso, M., 2020. Geochemical and geophysical monitoring of hydrocarbon seepage in the Adriatic Sea. Sensors 20, 1504.
Royden, L., Patacca, E., Scandone, P., 1987. Segmentation and configuration of subducted lithosphere in Italy: an important control on thrust-belt and foredeep-basin evolution. Geology 15, 714–717. https://doi.org/10.1130/0091-7613(1987)15<714:SACOSL>2.0.CO;2.
Russoniello, C.J., Fernandez, C., Bratton, J.F., Banaszak, J.F., Krantz, D.E., Andres, A.S., Konikow, L.F., Michael, H.A., 2013. Geologic effects on groundwater salinity and discharge into an estuary. J. Hydrol. 498, 1–12. https://doi.org/10.1016/j.jhydrol.2013.05.049.
Saucier, R.T., 1994. Geomorphology and Quaternary Geologic History of the Lower Mississippi Valley. Mississippi River Commission, Vicksburg, 205 pp.
Scarponi, D., Kowalewski, M., 2004. Stratigraphic paleoecology: Bathymetric signatures and sequence overprint of mollusk associations from upper Quaternary sequences of the Po Plain, Italy. Geology 32, 989–992. https://doi.org/10.1130/G20808.1.
Scarponi, D., Kaufman, D., Amorosi, A., Kowalewski, M., 2013. Sequence stratigraphy and the resolution of the fossil record. Geology 41, 239–242.
Scarponi, D., Nawrot, R., Azzarone, M., Pellegrini, C., Gamberi, F., Trincardi, F., Kowalewski, M., 2022. Resilient biotic response to long-term climate change in the Adriatic Sea. Glob. Chang. Biol. 28, 4041–4053.
Schlager, W., 1993. Accommodation and supply–a dual control on stratigraphic sequences. In: Cloetingh, S., Sassi, W., Horvath, F., Puigdefabregas, C. (Eds.), Basin Analysis and Dynamics of Sedimentary Basin Evolution. Sedimentary Geology, vol. 86, pp. 111–136.
Schumm, S.A., 1977. The Fluvial System. Wiley-Interscience, New York, 338 p.
Shanley, K.W., McCabe, P.J., 1993. Alluvial architecture in a sequence stratigraphic framework: a case history from the Upper Cretaceous of southern Utah, U.S.A. In: Flint, S., Bryant, I. (Eds.), Quantitative Modeling of Clastic Hydrocarbon Reservoirs and Outcrop Analogues, Special Publication, vol. 15. International Association of Sedimentologists, pp. 21–55.
Sheng, C., Jiao, J.J., Luo, X., Zuo, J., Jia, L., Cao, J., 2023. Offshore freshened groundwater in the Pearl River estuary and shelf as a significant water resource. Nat. Commun. 14 (1), 3781. https://doi.org/10.1038/s41467-023-39507-0.
Sheng, C., Jiao, J.J., Zhang, J., Yao, Y., Luo, X., Yu, S., Ni, Y., Wang, S., Mao, R., Yang, T., Zhan, L., 2024. Evolution of groundwater system in the Pearl River Delta and its adjacent shelf since the late Pleistocene. Sci. Adv. 10 (15) https://doi.org/10.1126/sciadv.adn3924 eadn3924.
Shepherd, J.W., Lang, S.C., Paumard, V., George, A.D., Peyrot, D., 2023. Controls on shelf-margin architecture and sediment partitioning on the Hammerhead shelf margin (Bight Basin, southern Australia): Implications for Gondwanan break-up dynamics between Australia and Antarctica. Earth Sci. Rev. 244, 104538. ISSN 0012-8252. https://doi.org/10.1016/j.earscirev.2023.104538.
Sherwood, C.R., Book, J.W., Harris, C.K., 2015. Sediment dynamics in the Adriatic Sea investigated with coupled models. Oceanography 17, 58 p.
Sømme, T.O., Helland-hansen, W., Martinsen, O.J., Thurmond, J.B., 2009. Relationships between morphological and sedimentological parameters in source-to-sink systems: a basis for predicting semi-quantitative characteristics in subsurface systems. Basin Res. 21, 361–387. https://doi.org/10.1111/j.1365-2117.2009.00397.x.
Stefani, M., Vincenzi, S., 2005. The interplay of eustasy, climate and human activity in the late Quaternary depositional evolution and sedimentary architecture of the Po Delta system, 223, 19–48. https://doi.org/10.1016/j.margeo.2005.06.029.
Stefanon, A., 1980. The acoustic response of some gas-charged sediments in the Northern Adriatic Sea. In: Bottom-Interacting Ocean Acoustics. Springer, pp. 73–84.
Storms, J.E.A., Weltje, G.J., Terra, G.J., Cattaneo, A., Trincardi, F., 2008. Coastal dynamics under conditions of rapid sea-level rise: late Pleistocene to early Holocene evolution of barrier–lagoon systems on the northern Adriatic shelf (Italy). Quat. Sci. Rev. 27, 1107–1123.
Syvitski, J.P.M., Milliman, J.D., 2007. Geology, geography, and humans battle for domi nance over the delivery of fluvial sediment to the coastal ocean. J. Geol. 115, 1–19.
Teatini, P., Tosi, L., Viezzoli, A., Baradello, L., Zecchin, M., Silvestri, S., 2011. Understanding the hydrogeology of the Venice Lagoon subsurface with airborne electromagnetics. J. Hydrol. 411, 342–354. https://doi.org/10.1016/j.jhydrol.2011.10.017.

Thomas, A.T., Reiche, S., Riedel, M., Clauser, C., 2019. The fate of submarine fresh groundwater reservoirs at the New Jersey shelf, USA. Hydrogeol. J. 27 (7), 2673–2694.
Thomas, A.T., Micallef, A., Duan, S., Zou, Z., 2023. Characteristics and controls of an offshore freshened groundwater system in the Shengsi region, East China Sea. Front. Earth Sci. 11, 1198215.
Tosi, L., Zecchin, M., Franchi, F., Bergamasco, A., Da Lio, C., Baradello, L., Mazzoli, C., Montagna, P., Taviani, M., Tagliapietra, D., Carol, E., Franceschini, G., Giovanardi, O., Donnici, S., 2017. Paleochannel and beach-bar palimpsest topography as initial substrate for coralligenous buildups offshore Venice, Italy. Sci. Rep. 7, 1–10. https://doi.org/10.1038/s41598-017-01483-z.
Trincardi, F., Correggiari, A., 2000. Quaternary forced regression deposits in the Adriatic basin and the record of composite sea-level cycles. In: Hunt, D., Gawthorpe, R.L. (Eds.), Sedimentary Response of Forced Regressions, Gological Society of London, Special Publication, vol. 172, pp. 245–269.
Trincardi, F., Correggiari, A., Roveri, M., 1994. Late Quaternary transgressive erosion and deposition in a modern epicontinental shelf: the Adriatic semienclosed basin. Geo-Marine Lett. 14, 41–51. https://doi.org/10.1007/BF01204470.
Trincardi, F., Correggiari, A., Langone, L., 1996. Stratigraphy of the late-Quaternary deposits in the central Adriatic basin and the record of short-term climatic events. Mem. Ist. Ital. Idrobiol. 55, 39–70.
Trincardi, F., Cattaneo, A., Correggiari, A., 2004a. Mediterranean prodelta systems: natural evolution and human impact investigated by EURODELTA. Oceanography 17, 34–45.
Trincardi, F., Cattaneo, A., Correggiari, A., Ridente, D., 2004b. Evidence of soft sediment deformation, fluid escape, sediment failure and regional weak layers within the late Quaternary mud deposits of the Adriatic Sea. Mar. Geol. 213, 91–119.
UN-Water, U.N., 2020. UN-Water Analytical Brief on Unconventional Water Resources. United Nations (UN), Geneva, Switz.
Vacchi, M., Marriner, N., Morhange, C., Spada, G., Fontana, A., Rovere, A., 2016. Earth-Science Reviews Multiproxy assessment of Holocene relative sea-level changes in the western Mediterranean : Sea-level variability and improvements in the de fi nition of the isostatic signal. Earth Sci. Rev. 155, 172–197. https://doi.org/10.1016/j.earscirev.2016.02.002.
Vail, P.R., Mitchum Jr., R.M., Thompson, S.I.I.I., 1977a. Seismic stratigraphy and global changes of sea level, Part 3: relative changes of sea level from coastal onlap. In: Payton, C.E. (Ed.), Seismic Stratigraphy – Applications to Hydrocarbon Exploration, Memoir 26 American Association of Petroleum Geologists, pp. 63–81.
Vail, P.R., Mitchum Jr., R.M., Thompson, S.I.I.I., 1977b. Seismic stratigraphy and global changes of sea level, Part4: global cycles of relative changes of sea level. In: Payton, C.E. (Ed.), Seismic Stratigraphy – Applications to Hydrocarbon Exploration, Memoir 26 American Association of Petroleum Geologists, pp. 83–97.
Vail, P.R., Hardenbol, J., Todd, R.G., 1984. Jurassic unconformities, chronostratigraphy and sea-level changes from seismic stratigraphy and biostratigraphy. AAPG Mem. 36, 129–144.
Van der Zwaan, G.J., Jorissen, F.J., 1991. Biofacial patterns in river-induced shelf anoxia. In: Tyson, R.V., Pearson, T.H. (Eds.), Modern and Ancient Continental Shelf Anoxia. Geo logical Society Special Publication, London, pp. 65–82.
van Geldern, R., Hayashi, T., Böttcher, M.E., Mottl, M.J., Barth, J.A.C., Stadler, S., 2013. Stable isotope geochemistry of pore waters and marine sediments from the New Jersey shelf: methane formation and fluid origin. Geosphere 9, 96–112.
Van Wagoner, J.C., 1995. Overview of sequence stratigraphy of foreland basin deposits: Terminology, summary of papers, and glossary of sequence stratigraphy. In: Van Wagoner, J.C., Bertram, G.T. (Eds.), Sequence Stratigraphy of Foreland Basin Deposits: Outcrop and Subsurface Examples from the Cretaceous of North America. Memoir, vol. 64. American Association of Petroleum Geologists, pp. ix–xxi.
Van Wagoner, J.C., Mitchum, R.M., Posamentier, H.W., Vail, P.R., 1987. An overview of sequence stratigraphy and key definitions. In: Bally, A.W. (Ed.), Atlas of Seismic Stratigraphy, Studies in Geology, vol. 27, vol. 1. American Association of Petroleum Geologists, pp. 11–14.
Van Wagoner, J.C., Posamentier, H.W., Mitchum, R.M., Vail, P.R., Sarg, J.F., Loutit, T.S., Hardenbol, J., 1988. An overview of the fundamentals of sequence stratigraphy and key definitions. In: Wilgus, C.K., Hastings, B.S., Kendall, C.G.C., H.W., P., Ross, C.A., Van Wagoner, J.C. (Eds.), Sea-Level Changes: An Integrated Approach, 42. SEPM Special Publication, pp. 39–45. https://doi.org/10.2110/pec.88.01.0039.
Van Wagoner, J.C., Mitchum, R.M., Campion, K.M., Rahmanian, V.D., 1990. Siliciclastic sequence stratigraphy in well logs, cores, and outcrops: concepts for high-resolution correlation of time and facies. AAPG Methods Explor. 7.
Varma, S., Michael, K., 2012. Impact of multi-purpose aquifer utilisation on a variable-density groundwater flow system in the Gippsland Basin, Australia. Hydrogeol. J. 20, 119.
Vigliotti, L., Verosub, K.L., Cattaneo, A., Trincardi, F., Asioli, A., Piva, A., 2008. Palaeomagnetic and rock magnetic analysis of Holocene deposits from the Adriatic Sea: Detecting and dating short-term fluctuations in sediment supply. Holocene 18, 141–152. https://doi.org/10.1177/0959683607085605.
Vincent, S.J., Hyden, F., Braham, W., 2014. Along-strike variations in the composition of sandstones derived from the uplifting western Greater Caucasus: causes and implications for reservoir quality prediction in the Eastern Black Sea. Geol. Soc. Lond. Spec. Publ. 386, 111–127.
Wang, R., Colombera, L., Mountney, N.P., 2019. Geological controls on the geometry of incised-valley fills: Insights from a global dataset of late-Quaternary examples. Sedimentology 2134–2168. https://doi.org/10.1111/sed.12596.
Weimer, P., Posamentier, H., 1993. Siliciclastic Sequence Stratigraphy: Recent Developments and Applications. American Association of Petroleum Geologists.
Wellner, R.W., Bartek, L.R., 2003. The effect of sea level, climate, and shelf physiography on the development of incised-valley complexes: a modern example from the east China Sea. J. Sediment. Res. 73, 926–940.
Weltje, G.J., 2004. A quantitative approach to capturing the compositional variability of modern sands. Sediment. Geol. 171, 59–77. https://doi.org/10.1016/j.sedgeo.2004.05.010.
Weltje, G.J., Brommer, M.B., 2011. Sediment-budget modelling of multi-sourced basin fills: Application to recent deposits of the western Adriatic mud wedge (Italy). Basin Res. 23, 291–308. https://doi.org/10.1111/j.1365-2117.2010.00484.x.
Woessner, William W., Poeter, Eileen P., 2020. Hydrogeologic Properties of Earth Materials and Principles of Groundwater Flow. The Groundwater Project, Guelph, Ontario, Canada, 205 p (available online at. https://gw-project.org/books/hydrogeologic-properties-of-earth-materials-and-principles-of-groundwater-flow/.
Zaitlin, B.A., Dalrymple, R.W., Boyd, R., 1994. The stratigraphic organization of incised-valley systems associated with relative sea-level change. In: Dalrymple, R.W., Zaitlin, B.A. (Eds.), Incised-Valley Systems: Origin and Sedimentary Sequences, SEPM Special Publication, 51, pp. 45–60.
Zamrsky, D., Karssenberg, M.E., Cohen, K.M., Bierkens, M.F.P., Oude Essink, G.H.P., 2020. Geological heterogeneity of coastal unconsolidated groundwater systems worldwide and its influence on offshore fresh groundwater occurrence. Front. Earth Sci. 7, 1–23.
Zamrsky, D., Essink, G.H.O., Sutanudjaja, E.H., Van Beek, L.P.H., Bierkens, M.F., 2022. Offshore fresh groundwater in coastal unconsolidated sediment systems as a potential fresh water source in the 21st century. Environ. Res. Lett. 17 (1), 014021.
Zamrsky, D., Oude Essink, G.H., Bierkens, M.F., 2024. Global impact of sea level rise on coastal fresh groundwater resources. Earth's. Future 12 (1) e2023EF003581.
Zecchin, M., 2007. The architectural variability of small-scale cycles in shelf and ramp clastic systems: the controlling factors. Earth-Sci. Rev. 84 (1–2), 21–55.
Zecchin, M., Catuneanu, O., 2013. High-resolution sequence stratigraphy of clastic shelves I: units and bounding surfaces. Mar. Pet. Geol. 39, 1–25. https://doi.org/10.1016/j.marpetgeo.2012.08.015.
Zecchin, M., Gordini, E., Ramella, R., 2015. Recognition of a drowned delta in the northern Adriatic Sea, Italy: Stratigraphic characteristics and its significance in the frame of the early Holocene Sea-level rise. Holocene 25, 1027–1038. https://doi.org/10.1177/0959683615575358.
Zecchin, M., Donda, F., Forlin, E., 2017. Genesis of the Northern Adriatic Sea (Northern Italy) since early Pliocene. Mar. Pet. Geol. 79, 108–130. https://doi.org/10.1016/j.marpetgeo.2016.11.009.